

Methods¹

T. Andrén, B.B. Jørgensen, C. Cotterill, S. Green, E. Andrén, J. Ash, T. Bauersachs, B. Cragg, A.-S. Fanget, A. Fehr, W. Granoszewski, J. Groeneveld, D. Hardisty, E. Herrero-Bervera, O. Hyttinen, J.B. Jensen, S. Johnson, M. Kenzler, A. Kotilainen, U. Kotthoff, I.P.G. Marshall, E. Martin, S. Obrochta, S. Passchier, N. Quintana Krupinski, N. Riedinger, C. Slomp, I. Snowball, A. Stepanova, S. Strano, A. Torti, J. Warnock, N. Xiao, and R. Zhang²

Chapter contents

Introduction and coring	1
Lithostratigraphy	10
Biostratigraphy	11
Geochemistry	14
Physical properties	16
Paleomagnetism	24
Microbiology	26
Stratigraphic correlation	30
Downhole logging	32
References	34
Figures	38
Tables	62

Introduction and coring

This chapter documents the primary operational, curatorial, and analytical procedures and methods employed during the offshore and onshore phases of Integrated Ocean Drilling Program (IODP) Expedition 347. This information concerns only shipboard and Onshore Science Party (OSP) methodologies and data as described in the site chapters. Methods for postexpedition research conducted on Expedition 347 samples and data will be described in individual scientific contributions published after the OSP. Detailed drilling and engineering operations are described in “Operations” within each site chapter and “Operational strategy” in the “Expedition 347 summary” chapter (Andrén et al., 2015). The information in this chapter will enable future identification of data and samples for further scientific investigation by interested parties.

Site locations

All Expedition 347 sites (Fig. F1) were positioned using GPS coordinates supplied by the proponents and based on previous site surveys. As a number of holes were proposed at each site for different uses (e.g., paleoenvironment and microbiology), a central hole position was taken from the proponent-supplied coordinates (Hole A), and then additional positions were calculated radiating out from this position at 20 m intervals, with Holes B and C on either side of Hole A, running along the site survey seismic lines, and Holes D and E perpendicular to this orientation, again on either side of Hole A (Fig. F2). The spacing interval of 20 m between holes was chosen to limit drilling disturbance between holes while maintaining a close enough proximity to correlate between them, enabling the formation of a composite recovery and lithologic splice.

Selected positions were relayed to the Hydrographic Surveyor from Geoclean, and the *Greatship Manisha* was settled into position using a dynamic positioning (DP) system. To maintain station accurately within the required tolerance of <1 m for shallow-water sites, the DP system ran for 30–40 min at each location to build a reliable DP model, after which permission was granted to commence operations. Geoclean supplied two transponder systems that were used during coring operations as backup for the DP system should there be a failure in the differential GPS (DGPS) signal because of satellite angles, particularly in the river estuary

¹Andrén, T., Jørgensen, B.B., Cotterill, C., Green, S., Andrén, E., Ash, J., Bauersachs, T., Cragg, B., Fanget, A.-S., Fehr, A., Granoszewski, W., Groeneveld, J., Hardisty, D., Herrero-Bervera, E., Hyttinen, O., Jensen, J.B., Johnson, S., Kenzler, M., Kotilainen, A., Kotthoff, U., Marshall, I.P.G., Martin, E., Obrochta, S., Passchier, S., Quintana Krupinski, N., Riedinger, N., Slomp, C., Snowball, I., Stepanova, A., Strano, S., Torti, A., Warnock, J., Xiao, N., and Zhang, R., 2015. Methods. In Andrén, T., Jørgensen, B.B., Cotterill, C., Green, S., and the Expedition 347 Scientists, *Proc. IODP, 347: College Station, TX (Integrated Ocean Drilling Program)*.

doi:10.2204/iodp.proc.347.102.2015

²Expedition 347 Scientists' addresses.



sites, or malfunction. The primary transponder was fitted to the seabed frame (Fig. F3). The secondary transponder was either deployed on the seabed frame or over the side of the vessel.

Adjustments to the vessel position of <100 m at each site (e.g., when moving or “bumping over” between hole locations) were performed using the existing DP model, as it was considered representative of hydrodynamic conditions over such distances, thereby reducing the waiting time before drilling operations could commence in the new hole.

Drilling platform

For Expedition 347, the maximum required depth of boreholes was 275 meters below seafloor (mbsf) in water depths ranging between 34 and 451 m. Therefore, a multipurpose offshore vessel fitted with a drilling derrick and coring system was selected to carry out the offshore operations. The drilling platform, chosen by Island Drilling and inspected by the European Consortium for Ocean Research Drilling (ECORD) Science Operator (ESO), was the *Greatship Manisha*, a 93 m long offshore vessel with DP (Class 2) capability (Fig. F4). The *Greatship Manisha* had the capacity in terms of provisions and accommodation to support 24 h operations for 45 days. A midterm port call for resupply was therefore required.

Located on the aft deck were 12 ESO containers and an additional container supplied by Island Drilling (Fig. F5) containing the following:

- Two refrigerated “reefer” units,
- Physical properties multisensor core logging laboratory,
- Core curation,
- Geochemistry clean laboratory,
- Microbiology temperature-controlled clean laboratory,
- Science party office,
- ESO office,
- Data management office,
- ESO tools and liner storage,
- ESO drilling coordinators workshop,
- Storage container holding two –80°C freezers for microbiology, and
- Core reception container for initial microbiology sampling (borrowed from Island Drilling).

Coring rig

The vessel was equipped with a large (6 m × 5.3 m) moonpool and a Geoquip GMTR 120 with a heave-compensated system coring rig (Fig. F6). The top

drive had a 120 metric ton capacity, 0–200 rpm with 23,000 ft/lb of torque, and through-bore of 4.125 inches for deployment of in-hole tools. This rig has a combined borehole and water depth capacity of 2000 m when using a standard geotechnical drill string of 7 × 4 drill collars and 5.5 inch drill pipe.

Pipe handling was carried out using a proprietary semiautomated handling system utilizing a pipe handling crane with grab, a remotely operated iron roughneck, and a proprietary catwalk system. This system was capable of handling two pipes at once with minimum manual intervention and hence improved safety.

A 4 m stroke passive heave compensation (semi-active under development) was achieved using nitrogen gas as a compensation buffer with Olmsted valve slingshot protection. The rig was used in association with a 12 metric ton seabed template, fitted with clamps and seabed transponder, to provide the reaction force for in-hole tools.

Wireline coring

Five methods of wireline coring were employed in addition to open-hole drilling using a noncoring assembly. Identifying letters in parentheses after each coring type show the letters used in the operations table in each site chapter to identify the coring method for each core run.

Piston corer system (H)

The piston corer system (PCS) is designed to operate primarily in soft muddy to clayey formations. The PCS operated by advancing the core barrel into the formation through hydraulic pushing. The PCS was set up by fully retracting the core barrel into the core barrel housing, which was then held in place using two shear pins. The pins used were either brass or steel or a combination of the two, depending on the expected strength of the lithology to be cored. The core barrel housing was then lowered into the bottom-hole assembly (BHA) at the base of the drill string. Drill mud/water was pumped into the drill string, pressurizing the closed system and producing a force that overcame the strength of the shear pins, typically in the region of 50–130 bar. When the pins sheared, the corer was forced into the sediment by the pressure of the drill fluid. The number and type of shear pins inserted dictated the pressure at which the core barrel was released and, consequently, the force at which the barrel was pushed into the formation.

During Expedition 347, the PCS was the primary tool, as the lithologies were expected to be clayey material. However, it was also utilized in silty and

sandy formations in an attempt to collect undisturbed cores. After each core was taken, the hole was advanced by drilling to the next sample point. This was carried out either by “advance by recovery” or “advance by barrel stroke.” When advancing by recovery, the depth of the next core run was dictated by the length of core recovered, which was not known until the core was back on deck. To reduce the cycle time, “advance by barrel stroke” was occasionally used, meaning the hole was advanced without knowing the true recovery of the last run. On other occasions, some PCS runs were taken every 3 m regardless of the core length recovered. Piston coring is slower than conventional drilling, as each section has to be cored with the PCS and then drilled out before the next sample can be taken.

Different core catcher combinations were used to optimize core retention with minimal core disturbance. Typically, a flapper catcher was used. However, basket catchers were added if necessary. Although these catchers are stiffer and can cause disturbance in clay cores (e.g., circumference scoring), they are more successful in retaining or assisting to retain very soft clay and sands than a flapper catcher.

Extended coring system (X)

The extended coring system (ECS) is designed to sample unconsolidated and noncohesive formations that are too dense for piston coring but too friable for rotary coring with direct circulation at the bit. A conventional cutting shoe is generally utilized with this system. However, a polycrystalline diamond (PCD) bit can also be used to assist recovery in more granular formations.

The ECS barrel is locked into the BHA and advanced through rotation and flushing in a similar way to diamond rotary coring. The difference is that the end of the core barrel protrudes ahead of the main cutting bit by as far as 12 cm. One of a series of drill bits was used (chosen when considering the lithology encountered or expected), including tungsten, surface set, impregnated diamond, or PCD, all of which minimize flushing at the point where the core enters the core barrel to reduce undercutting and washing away.

Nonrotating core barrel (N)

The nonrotating core barrel (NRCB) is equivalent to a standard diamond rotary core barrel and is designed to core in hard formations. The assembly is a tribarrel construction. The outer barrel locks into and rotates with the BHA, and the inner barrel metal tube hangs from a bearing assembly at the top of the

outer barrel, which removes the rotation of this tube. The final barrel is the plastic liner in which the core is collected and stored.

The NRCB is advanced by rotary coring, with flushing occurring at the point where the core enters the core barrel. Normally, a conventional core spring is used to retain the core, but if the formation is soft or fractured and hence easily washed away, then an additional basket catcher is utilized to assist retention of the material even if the catcher undercuts the core as it passes through the catcher tines. The core cutting bit on the NRCB is retrieved with each core run so the cutting ability can be optimized for each formation encountered.

Push coring assembly (P)

The push coring assembly (PCA) is a simple tube extension which protrudes 1 m (or more if required) beyond the main core bit. The PCA was lowered into the drill string on the wireline, with the drill string raised above the bottom depth of the borehole. When it was in position, the drill string was lowered until either the full stroke of the sample tube was reached or the maximum bit weight was achieved. The drill string was then raised above the length penetrated to allow easier release before recovering the tool to the deck. A similar range of core retention catchers to that used for the PCS and ECS was available for this tool.

Hammer sampler (S)

The hammer sampler (HS) is a rudimentary sampling tool that uses percussive force to drive a tube into the borehole base. The tool has a built-in hammer, which is raised and lowered onto an anvil by lifting and lowering the sample wire manually over a few meters distance. This tool is typically used to acquire a sample if one has not been obtained by conventional methods. It can also be used to clear the main bit if it has become blocked.

The HS was lowered on the wireline to the bottom of the borehole, and the tension was taken on the wire to define the base of the hammer. A mark was made on the wire to identify this fixed point. The rope was then raised to a distance within that of the slide bar on the hammer and lowered by free fall. This action was repeated (typically >25 times) until the fixed point mark had progressed to a point that exceeded the length of the sample tube or a sufficient sample had been acquired to prove the lithology. This method was typically employed when till/diamict lithologies were encountered to acquire spot samples approximately every 3 m.

Noncoring assembly (O)

The noncoring assembly (NCA) uses a small tricone Rock Roller drill bit to plug the hole in the main core bit through which the other sample tools fit. The cones may be either hardened steel or tungsten carbide tips. The tungsten carbide option was used most extensively during this expedition.

The NCA was lowered and picked up on the wireline, allowing advancement without the possibility of cuttings entering the drill string by utilizing washways to move cuttings away from the face of the bit. The recovery to the deck of the NCA allowed it to be examined for trapped cuttings and provided a quick visual estimation of the lithology penetrated, which facilitated subsequent coring tool selection.

Rumohr coring system (L)

In addition to the main drilling system, one member of the science party provided a third-party tool system that could take gravity cores of the surficial sediment to 1 mbsf (Fig. F7). As the system did not include a core catcher, it left the uppermost sediment intact (e.g., for possible varve counting and of the sediment/water interface). This system was deployed over the side of the *Greatship Manisha* using a winch system.

Coring methodology

To ensure efficient drilling and coring, it is essential to apply a steady weight onto the drill bit to prevent swabbing of the hole. Vessel heave can reduce or apply excessive weight onto the drill bit; therefore, the drilling system onboard was heave compensated, with clamps on the seabed template providing a reaction force. The drill string comprised a BHA, a number of drill collars (the number of which varied depending on the expected depth of the borehole), and sufficient American Petroleum Institute (API) drill pipes. This assembly was passed through a cone guide and two sets of clamps located on a seabed frame (SBF) (Fig. F8). The SBF was situated on the seabed, acting as a reentry guide for the string (in the event of having to recover the BHA to the deck) and providing a reaction force for the piston corer.

The main drill bit had an outside diameter of 210 mm (8¼ inches) and a throat of 98 mm. Any tools passing through the bit were required to have an external diameter <95 mm, which corresponds to the internal diameter of the landing ring in the BHA where all inner barrels seat. The various wireline tools were lowered on the wire, with an overshot release tool employed to release the overshot carrying the sampling tool once it was in place.

When taking a piston core sample, on recovery of the overshot to the rooster box, the mud valve was closed and the string pressurized by pumping drilling fluid into the string. When the strength of the pins holding the piston in place was exceeded by the pressure of the drill fluid in the string, they sheared and the core tube fired into the strata. The drill string was then raised to allow the core to break at the base, and the overshot was run again, this time to collect the tool and recover it to the deck. The drillers were able to detect whether there had been a successful “full-stroke” by the pressure gauges on the rig floor.

The core collected was 62 mm in diameter. This is the standard IODP core size, and cores were collected in standard IODP transparent liners. The maximum core run length was 3.3 m. However, the length of a core run was chosen to maximize core recovery and quality while maintaining hole stability, even at the expense of overall penetration speed. When attempting to capture a lithologic interface as defined from seismic profiles, the run lengths were often shortened by raising the corer above the bottom of the borehole by a known height prior to pressuring the drill string.

In some instances, the hole was advanced by open holing—drilling ahead without recovering sediments. This was done in difficult lithologies that could not be recovered using the tools onboard to enable recovery of other lithologies beneath these intervals or when recovery (composite or from an individual hole) of an interval had already reached >90% and the scientific rationale was to try and get deeper within the time constraints. It was also employed when coring multiple holes to ensure that any gaps in recovery from one hole were recovered in another. The advance varied from a small offset of 0.5 m to ensure maximum core overlap between holes in some locations to a more regular spacing of 3 m through the till lithologies to monitor when or whether the lithology was changing.

Seawater was the primary drilling medium utilized until the lithologies encountered required stabilization and increased flushing of drill cuttings. If this occurred on a paleoenvironment hole, then Guar gum, a biodegradable drilling mud, was used. On microbiology holes, however, this medium would have been detrimental to the microbial communities under investigation, and a polymer called GS550 was used as an alternative. Further, a concentrated solution of perfluorocarbon (PFC) was introduced into the seawater or GS550 drilling mud in the microbiology holes to assess potential contamination of the core samples. See “Microbiology” for further details.

As per the risk assessment analysis conducted by ESO and the Natural Environment Research Council during the planning stages of Expedition 347, down-pipe camera/remotely operated vehicle surveys were conducted at Sites M0060, M0064, and M0065 prior to coring operations to assess the seabed for dumped ammunitions and mines from World War II (WWII). A prerequisite for being able to commence operations was to ascertain that the seabed was clear of any obstructions. Coring of all holes at Site M0065 commenced at 2 mbsf with open holing to this depth because of the risk of chemical warfare agents dumped following WWII being recovered. To further mitigate this risk, no surface gravity Rumohr cores were conducted. Coring at Site M0062 commenced at 0.5 mbsf with open holing of the upper 50 cm because of the risk of heavy metals and other contaminants (e.g., DDT pesticide, polycyclic aromatic hydrocarbons [PAHs], hexachlorocyclohexane [HCH], and polychlorinated biphenyls [PCBs]) from nearby abandoned paper mills and industry, as identified by the Swedish Geological Survey (pers. comm., 2012). Surface gravity Rumohr cores were conducted at this site, following a reassessment of the potential risk having cored the main holes. However, the Rumohr corer and the core liners were pressure washed prior to being brought onboard to remove any contamination. In addition, all participants involved in handling these cores wore additional personal protective equipment. These gravity cores were not subsampled onboard and were only split during the OSP once satisfactory precautions were in place.

Downhole logging tools

Downhole logging services were contracted from Weatherford and managed by the European Petrophysics Consortium (EPC). Details and results of the expedition logging program are given in “[Downhole logging](#)” and in each site chapter.

Through-pipe underwater video camera

A through-pipe camera survey was conducted at sites designated as being in potential dumping grounds for WWII munitions as part of the risk assessment mitigation procedures. The British Geological Survey (BGS) supplied an underwater color video camera system and a deployment frame that allowed it to be lowered down inside the API drill pipe. It is based on diver helmet-operated systems, with an umbilical cable relaying direct feed imagery to a monitor located inside the drillers dog house on the drill floor.

The drill pipe was run to just above the seabed (~5 m). The through-pipe camera system was then lowered down inside the pipe. Because of currents remobilizing the surface sediments, it was often necessary

to lower the drill pipe and camera further down while monitoring the live video feed until the sea-floor was clearly visible. Because of the positioning of the three primary holes (A, B, and C) along a transect at 20 m intervals, it was decided to run the pre-drilling camera survey for all holes at once while moving slowly along the transect under DP before returning to commence coring operations at Hole A.

Seabotix remotely operated vehicle

During Expedition 347, the BGS supplied a Seabotix LBV 150 SE Little Benthic Vehicle (LBV) rated to 150 m water depth (Fig. F9). Two color cameras were mounted on the vehicle. The main camera was mounted with a switchable high-intensity LED light array on a tilt mechanism that allowed a 270° range of view. The second camera was a fixed-focus rear-facing unit. The LBV was powered by four thrusters: one vertical, one lateral, and two horizontal. This configuration afforded four-axis maneuverability with a top speed of 3 kt and the ability to work in currents up to 2 kt. The system enabled visual inspection of the drill string and seabed template, in particular at Site M0060 after the drill pipe became stuck and had to be backed off. The LBV allowed real-time analysis of the situation, along with documentation that the situation had been rectified satisfactorily.

Shipboard scientific procedures

Curatorial procedures and sample depth calculations

Expedition numbers for IODP expeditions are sequential, starting with 301. Drilling sites are numbered consecutively. For ESO platforms, numbering starts with Site M0001, with “M” indicating an ESO-operated Mission Specific Platform (MSP). For Expedition 347, the first site was Site M0059. Multiple holes may be drilled at a single site. The first hole drilled is assigned the site number with the suffix “A,” the second hole, the site number and the suffix “B,” and so on. Where shallow gravity cores were taken with the third-party Rumohr coring system, these holes were identified with the suffixes “K,” “L,” and “M” to maintain numbering consistency for the main coring holes.

For Expedition 347, the cored interval normally consisted of the entire drilled section, but in some cases intervals were drilled without coring (e.g., open holing the top of Holes M0062A–M0062C and other intervals between spot cores).

Recovered core is split into sections with a maximum length of 1.5 m and numbered sequentially from the top, starting at 1 (Fig. F10). By convention,

material recovered from the core catcher of a sedimentary core is treated as a separate section labeled “CC” (core catcher) and placed below the last section recovered in the liner. The core catcher is assigned to the top of the cored interval if no other material is recovered. When recovered core is shorter than the cored interval, the top of the core, by convention, is equated to the top of the cored interval to achieve consistency in reporting depth in core.

A soft to semisoft sediment core from less than a few hundred meters below seafloor may expand upon recovery (typically 10%–15%), so the recovered interval may not match the cored interval. In addition, a coring gap can occur between cores (i.e., some cored interval was lost during recovery or was never cut). Thus, a discrepancy may sometimes exist between the drilled meters below seafloor and the curatorial meters below seafloor. For example, the curatorial depth of the base of a core can be deeper than the top of the subsequent core if there has been significant core expansion on recovery to deck. In all of the chapters in this volume, the depths are initially quoted without adjusting for any expansion. However, some chapters also present an adjusted depth, although the science party acknowledge that applying a linear compression factor might not be representative of any nonlinear expansion that might have occurred. Therefore, care should be taken when applying the corrected depths.

Any sample removed from a core is measured in centimeters from the top of the section to the top and bottom of the sample removed. An identification number for a sample comprises the following information: expedition, site, hole, core number, core type, section number, piece number (for hard rock), and interval in centimeters measured from the top of section. For example, a sample identification of “347-M0060A-3H-2, 35–40 cm,” represents a sample removed from the interval 35–40 cm below the top of Section 2, Core 3H (“H” indicates core type; see below), from Hole M0060A during Expedition 347 (Fig. F10). All IODP core identifiers indicate core type. For Expedition 347, the following abbreviations are used:

- H = hydraulic piston corer (equivalent to IODP’s advanced piston corer).
- N = nonrotating core barrel.
- P = push coring assembly.
- S = hammer sampler.
- O = noncoring assembly/open hole.
- X = extended coring system.
- R = rotary coring system.
- L = Rumohr corer.

Descriptions of these tools are presented in “[Wire-line coring](#).”

The depth of a sample in meters below seafloor is calculated by adding the depth of the sample below the section top and the lengths of all higher sections in the core to the core-top datum measured with the drill string.

With regard to numbering of samples taken during the OSP for postcruise research, Expedition 347 is the first expedition within the IODP program to utilize the International Geo Sample Number (IGSN; www.igs.org) alphanumeric system of unique identifiers. Each sample is assigned a unique code, potentially enabling the IODP core repository and investigators to track all samples accurately, even when shared between different laboratories. IGSN is similar to digital object identifiers (DOIs) for articles and data. This method will also provide a central registry for investigators in the future to be able to build on previous work as new techniques and methodologies are developed.

Drilling-induced core deformation

Cores may be disturbed and have extraneous material in them as a result of the coring process. In formations that are unconsolidated, such as loose sands and gravel beds, material from higher intervals may have fallen to the base of the hole or been washed down by drill fluid circulation. This material may then be sampled by the next core run. Therefore, on splitting and description of the cores, the top of each core run was examined for evidence of core disturbance or anomalous material, described as “fall-in.” In addition, it is also possible that on recovery of the piston core barrel, suction can draw in soupy material—this was described as “flow-in.”

Common piston coring-induced deformation includes concave deformation of horizontally laminated sediments, with the laminations appearing to have been pulled downward at the liner edges. In gaseous sediments, recovery of a core to the surface may result in expansion of the core material as the gas comes out of solution. This can significantly disturb the cores, appearing either as small cracks or by driving core segments apart within the liner tube. Pressure within the liner can be reduced by drilling holes in the end caps and/or along the length of the liner. This provides the gas with a means of escape but can also result in some sediment being extruded through the holes with the gas, causing some core disturbance.

IODP depth conventions

IODP utilizes a system of depth scales (measured in meters) that are method specific. The primary scales are as follows:

DSF = drilling depth below seafloor.
 CSF = core depth below seafloor.
 CCSF = core composite depth below seafloor.
 WRF = wireline log depth below seafloor.

During Expedition 347, the cored interval was measured offshore by the drillers in meters below seafloor, equating to drilling depth below seafloor. The depth below seafloor for any core/sample was determined by taking the depth to tagging seafloor with the drill string as the zero core datum and adding on all further advances to the target depth/maximum penetration. Where appropriate, downhole logging data and core measurements were stratigraphically correlated to improve the depth correlation between the wireline log depth below seafloor, drilling depth below seafloor, and core depth below seafloor depth scales. This process is described in more detail in **“Stratigraphic correlation.”**

For all sites except Sites M0060 and M0063, it was possible to formulate a composite splice (see details in “Stratigraphic correlation” in each site chapter). In these instances, postcruise sampling was taken from the splice unless otherwise indicated.

For ease of communication of shipboard results, depths are reported in meters below seafloor (mbsf) unless otherwise stated.

Core handling offshore

As soon as a core was recovered onto deck, it was immediately curated. This involved marking and cutting the cores into sections with a 1.5 m maximum length. Time-sensitive headspace syringe samples were taken for CH₄ analysis immediately following sectioning of the core. Each section was then sealed at the top and bottom by attaching color-coded plastic caps, which were securely taped. Blue caps identify the top of a core section, and white caps indicate the bottom. A yellow cap was placed on section ends to identify where a microbiology whole-round sample had been taken. Core section liners were permanently labeled with an engraving tool. The lengths of the core in each section and the core catcher sample were entered into the Offshore Drilling Information System (Offshore DIS). In some instances where methane-rich sediments continued to de-gas and expand following recovery, holes were drilled into the end caps and along the length of the core sections to allow venting and prevent the end caps from being forced off and core material lost. No core splitting took place during the offshore phase of Expedition 347. All core material was kept in a temperature-controlled refrigerated container offshore and transported back to the IODP Bremen Core Repository (BCR), Center for Marine Environmental Sciences

(MARUM; Germany), at +4°C. On arrival at the BCR, all cores were stored in the main repository, again at +4°C.

In suitable sediments, core catcher samples were taken for later dating using optically stimulated luminescence (OSL). These samples were collected immediately on the drill floor in black plastic layflat sleeving, with the sleeving being held over the end of the core barrel during transference of the sediment. The samples were then double bagged in a dark environment and sealed against any light penetration, thus minimizing the risk of light contamination.

Paleoenvironment cores: offshore sampling and processing

After curation, the cores proceeded through a sequence of processing steps. Geochemists sampled for interstitial water (IW). This was predominantly achieved through the use of Rhizon samplers and syringes. However, 5–10 cm whole rounds were taken for squeezing when the core material became unsuitable for using Rhizon samplers.

The core catcher or subsample of core catcher material was given to the sedimentologists and biostratigraphers for initial description after being photographed by the core curator. Shipboard sedimentologists also took the opportunity to assess the main core sections through the clear plastic liner, in particular to identify lithologic boundaries and any evidence of varved sequences. The microbiologists documented the degree of core disturbance in core sections from the first paleoenvironment hole drilled to inform their later subsampling strategy at designated microbiology holes (Sites M0059, M0060, M0063, and M0065).

Core sections were allowed to equilibrate to “container” temperature before they were run through the slow-track multisensor core logger (MSCL) at a resolution of either 1 or 2 cm spacing, depending on the lithology and scientific requirements. This enabled stratigraphic correlation between different holes at the same site using magnetic susceptibility measurements, ensuring maximum stratigraphic overlap between holes. The cores were then transferred to a 4°C temperature-controlled reefer.

Microbiology cores: offshore sampling and processing

Following the initial cutting of cores into sections on the drill floor, syringe samples were immediately taken from the bottom of Section 1 and the top of Section 2 when required for time-sensitive measurements such as headspace samples, PFC contamina-

tion, and DNA testing. The cores were then curated as previously described, with the exception of permanent engraving.

Following initial curation, the core sections were then taken immediately to the Fast-track MSCL, where they were run through magnetic susceptibility loops at 2 cm resolution without allowing any time for temperature equilibration to minimize microbiological degradation prior to sampling, fixing, and storage. These data were then used to stratigraphically correlate the microbiology cores with the paleo-environment cores, which facilitated real-time drilling decisions. The cores were then taken into a core reception container where they were subsampled for further microbiology and IW analyses, which consisted of taking a combination of syringe samples and whole rounds (see “[Microbiology](#)”). After subsampling, the remaining cores were returned to curation for final labeling and permanent engraving.

The cores were then sampled for additional IW, using Rhizon syringes where necessary to acquire the required volume of pore water, and allowed to reach container temperature. Finally, core sections >15 cm in length were run through the slow-track MSCL to acquire the full suite of petrophysical information and then transferred to a 4°C temperature-controlled reefer.

Samples taken offshore for IW were analyzed for salinity, pH, alkalinity, ammonium, sulfide, and methane while offshore to aid microbiological sampling at geochemical boundaries/transitions. See “[Geochemistry](#)” for further details.

Offshore core flow is summarized in [Figure F11](#).

Core handling at the Onshore Science Party

The OSP was held at the BCR from 22 January to 20 February 2014. Before splitting, all cores were measured for thermal conductivity and natural gamma radiation (NGR). See “[Physical properties](#)” for further details.

After removal from refrigerated storage, cores were split lengthways into working and archive halves. Cores were split from top to bottom. Therefore, investigators should be aware that younger material could have been transported downward on the split face of each core. The core splitters have horizontal and vertical wire cutters, steel plates to keep soupy material in place during splitting, and a diamond saw for more indurated material at their disposal. However, most cores were able to be split using wire cutters.

The archive half of the core was taken immediately for high-resolution digital line scanning (see SLAB-

CORESCAN in “[Supplementary material](#)”). The core was then described by the sedimentologists, aided by thin sections and smear slides (see “[Lithostratigraphy](#)” for further details). Following description, the archive halves were wrapped and put back into the core repository reefer.

The working half of the core was first taken for color reflectance measurements. See “[Physical properties](#)” for further detail. Following this, and on completion of core description, the working halves were sampled. The first samples taken were for IODP minimum measurements, encompassing biostratigraphic analyses, paleomagnetism analysis on discrete cubes, physical property measurements, and total organic carbon measurements. See “[Physical properties](#),” “[Paleomagnetism](#),” “[Biostratigraphy](#),” and “[Lithostratigraphy](#)” for further details. Following these measurements, sampling for postcruise research was undertaken. The working halves were then wrapped and put back into the core repository reefer. Each sample taken was logged into the Expedition Drilling Information System (Expedition DIS).

Samples taken from the cores offshore for IW were analyzed for cations (major and trace elements) and anions (chlorinity, bromide, sulfate, and phosphate) during the OSP. See “[Geochemistry](#)” for further details.

Onshore core flow is summarized in [Figure F12](#).

Data handling, database structure, and Access

Data management during the offshore and onshore phases of Expedition 347 had two stages. The first stage was the capture of metadata and data during the offshore and onshore parts of the expedition. Central to this was the Expedition DIS, which stored information about drilling, core curation, sampling, and primary measurements. The second stage was the longer term postexpedition archiving of Expedition 347 data sets, core material, and samples. This function was performed by the World Data Center for Marine Environmental Sciences (PANGAEA) and the BCR.

The Expedition DIS is a flexible and scalable database system originally developed for the International Continental Drilling Program (ICDP) and adapted for ESO. The underlying data model for the Expedition DIS is compatible with those of the other IODP implementing organizations and ICDP. For the specific expedition platform configuration and workflow requirements of Expedition 347, the Expedition DIS data model, data import pumps, and user interfaces were adapted to form the Baltic Sea Expedition DIS. This also included some new functionality, such as setting up predefined series for quicker entry of

microbiology samples and IW subsamples and tools for the handling of Fast-track MSCL data.

The Expedition DIS was implemented in SQLServer-2008 R2 installed on a central server with Microsoft-based client PCs connecting to the system through a Microsoft Access 2010 user interface. It was the first time the new version of the DIS was used for an MSP expedition, though much of the user interfaces such as input forms remain similar to the previous version. The work on DIS development is carried out by Smartcube.

Offshore, the Expedition DIS was used to capture metadata related to core and sample curation, store core catcher photographs and downhole logging data, and print section, sample, and subsample labels. In addition, the database also stored primary measurements data:

- MSCL data (both standard MSCL and Fast-track),
- Visual core descriptions of core catcher material,
- IW analyses, and
- Smear slide descriptions.

Expedition scientists and ESO staff also generated a variety of spreadsheet files, text documents, and graphics containing operations and scientific data, geological descriptions, and interpretations. Therefore, in addition to the structured metadata and data stored in the Expedition DIS, all data files were stored in a structured file system on a shared file server. Backups of the Expedition DIS and the file server were made continuously and also replicated on the backup server. The EPC was responsible for the capture and processing of MSCL and downhole logging data.

During the offshore phase, the Corewall Correlator application was used to view and correlate MSCL data (particularly magnetic susceptibility data) from different holes and against downhole logging data.

On completion of the offshore phase of the expedition, the Expedition DIS database and the file system were transferred to the BCR to continue data capture during the OSP. Onshore, additional data types were captured in the Expedition DIS: core close-up images, high-resolution line-scan images, color reflectance data, thin section data, NGR data, smear slide data, and full visual core descriptions of the split cores. All other data, including spreadsheets and preliminary results, were loaded onto a shared file server. The Expedition DIS was backed up daily, and the file server was backed up twice daily. During the onshore phase, line-scan images and MSCL, NGR, and downhole logging data were loaded into the Corewall Corelyzer and Correlator applications for visualization and core correlation purposes.

After the expedition, the sampling and core curation data were exported from the Expedition DIS to Curation DIS, the long-term BCR core curation system.

In the second stage, all Expedition 347 data were transferred to the PANGAEA information system. PANGAEA is a member of the International Council of Scientific Unions World Data Center system. It has a flexible data model that reflects the information processing steps in earth science fields and can handle any related analytical data (Diepenbroek et al., 1999, 2002). It is used for processing, long-term storage, and publication of georeferenced data related to earth sciences. PANGAEA's data management functions include quality checking, data publication, and metadata dissemination that follows international standards.

The data captured in the Baltic Sea Expedition DIS and the data stored in the shared file server were transferred to PANGAEA following initial validation procedures. The data transfer process was completed by the time of publication of the Expedition reports section of this volume. Until the end of the moratorium period, data access was restricted to the expedition scientists through unique usernames and passwords. However, following the moratorium, all data except the downhole wireline data will be published online (www.PANGAEA.de). PANGAEA will continue to acquire, archive, and publish new results derived from Expedition 347 samples and data sets. Downhole wireline data are archived at brg.ideo.columbia.edu/logdb with a link from PANGAEA.

IODP MSP data are downloadable from the MSP data portal (iodp.wdc-mare.org).

Core, section, and sample curation using the Baltic Sea Expedition DIS

Expedition 347 followed IODP protocols and naming conventions (see “[Curatorial procedures and sample depth calculations](#)”). The Expedition DIS captured the curation metadata and printed the appropriate labels, also to IODP standards. The curation metadata comprise

- Expedition information,
- Site information (latitude, longitude, water depth, start date, and end date),
- Hole information (hole naming by letter, latitude, longitude, water depth, start date, and end date),
- Core information (core number, core type, top depth, bottom depth, number of sections, core catcher availability, curator on shift, time and date for core on deck, and any additional remarks),
- Section data (section number and length, curated length, and curated top depth),

- Sample information (repository, request number, code observer, expedition, site, hole, core, section, half, sample top and sample bottom, and sample volume),
- Calculated core recovery percentage (on the basis of drilled or cored length versus curated recovery), and
- Calculated section recovery (on the basis of section length versus curated recovery).

Because of expanding sediments, recovery often exceeded 100%. No corrections were made within the Expedition DIS for this, with top and bottom depths of sections (in meters below seafloor) calculated on the basis of the core-top depth. However, the operations summary table (see T1 in the “Expedition 347 summary” chapter [Andrén et al., 2015]) shows adjusted recovery percentages for holes with >100% suggested recovery.

Lithostratigraphy

This section provides a summary of the procedures for the description and documentation of the sedimentology of cores recovered during Expedition 347. It outlines the methodology of the visual core description and our system for sediment classification, as well as the data entry procedure upon manual completion of visual core description (VCD) sheets. Information presented here is a result of observations made by members of the OSP sedimentology team.

Shipboard descriptions from core catcher samples and preliminary observations were incorporated in these descriptions.

Onshore methodology

Visual core description

Visual description of the recovered cores was conducted by members of the sedimentology team. This description was performed on the archive halves of the split cores at the BCR.

Individual core sections measuring a maximum of 1.5 m in length were placed into core trays for visual inspection. Descriptions were initially made by hand on VCD template sheets. These featured a high-resolution line-scan image of each core section, with a series of columns for manual entry of graphics to denote lithology and illustrate aspects such as grain size variations and sedimentological features (Figs. F13, F14, F15; see handwritten VCD scans in HAND-VCD in “Supplementary material”). Grain size divisions for clay, silt, sand (very fine, fine, medium, coarse, and very coarse), granules, and pebbles were defined in accordance with Wentworth (1922) (Fig.

F16), and we employed subdivisions of this to allow for a more robust classification with reference to Shepard (1954) (i.e., “silty sand”) (Fig. F17). Divisions were assessed through visual comparison using a hand lens and grain size card.

Color was noted with reference to the Munsell color chart (Munsell Color Company, Inc., 1988) to assign an estimated value; however, the core was also fed through an automated color reflectance procedure (see “Physical properties”), which provides a quantification of color based on the Munsell index.

Composition was estimated using a combination of hand lenses and microscopy observations of smear slides. This allowed for semiquantified estimates of mineral and bioclastic composition to produce a sediment classification.

Bioturbation intensity (1–6) was determined using the ichnofabric index from Bann et al. (2008) (e.g., 1 = bioturbation absent, 3 = moderate bioturbation, and 6 = total biogenic homogenization of sediment).

The number of gravel clasts (>2 mm) was counted for each 10 cm section of core in gravel-bearing sediments. Lithology, shape, and surface features were recorded on the VCD sheets for clasts with diameter >2 cm.

Core disturbance

Evidence of drilling-related disturbance was captured on the VCD sheets (Fig. F13). Drilling disturbance of relatively soft or firm sediments (i.e., where inter-grain motion was possible) was classified into four categories:

1. Slightly disturbed: bedding contacts are slightly bent.
2. Moderately disturbed: bedding contacts are extremely bowed.
3. Extremely disturbed: bedding is completely deformed and may show diapiric or minor flow structures.
4. Soupy: sediments are water saturated and show no traces of original bedding or structure.

In addition to these main categories for soft and lithified sediments, several other terms were used to characterize drilling disturbance:

- Washed gravel: fine material is suspected to be lost during drilling, with only washed coarse material remaining. This may have resulted from problems in the drilling and recovery of coarse-grained lithologies.
- Flow-in: soupy, displaced sediment pulled into the core liner during retrieval.
- Fall-in: downhole contamination resulting from loose materials falling from the drill hole walls.

- Sand/gravel contamination along core liner: isolated pieces of coarse contamination occurring alongside the core liner away from the core top.

Smear slides

Smear slide observations were utilized in the identification of fine-grained sediments (clay, silt, and very fine sand) and sediment matrix. Smear slides were prepared by mixing sediment and distilled water on a glass slide. Distilled water was evaporated on a hot plate, and the dried sample was mounted in Norland optical adhesive 61 using ultraviolet light. Relative abundances of silt and clay, accessory minerals, and biogenic components were estimated for each smear slide using a polarizing microscope (Marsaglia et al., 2013). Data were entered into the DIS using a Smear Slide Input Form template previously created during the offshore phase of the expedition.

Percentage compositions of sand, silt, and clay were estimated semiquantitatively using a standard visual composition chart by Terry and Chilingar (1955); however, finer grain sizes may be underestimated using this method (Bahn et al., 2008).

Preliminary petrography of the sediments was also performed on the smear slides. Microfossil and mineral identification in smear slides during the description process were noted to help direct sampling strategies.

Data entry and the Digital Information System

Visual core descriptions were entered into the DIS using a template for Visual Section Unit Description. Results of smear slide analyses were entered using the Smear Slide Input Form. VCD forms were scanned and linked to the Section Unit Description in DIS.

Offshore methodology

During the offshore phase, the lithologic characterization of sediments was based on visual analysis of core catcher material. For visual grain size classification, we used the approach of Wentworth (1922) (see “[Visual core description](#)”). The Munsell color chart (Munsell Color Company, Inc., 1988) was used to define in situ/wet sediment color. Because of possible core catcher disturbance, a classification of bioturbation intensity was not always possible and was only noted where the sediment was clearly bioturbated. Smear slides from the core catcher material were prepared in the same manner as described in “[Smear slides](#)” (see SMEARSLIDSCANS in “[Supplementary material](#)”). Onboard analyses of smear slides were carried out using a polarization microscope, with special focus on determining grain size, mineral

composition, texture, and microfossils. Results were documented within the DIS. It should be noted that the possibility of artificial mixing of core catcher sediment is quite high, and the results should therefore be treated with some caution. All offshore core catcher descriptions were directly entered into the DIS without using any handwritten VCDs.

In addition to the description of core catcher material, entire liner sections were also studied to detect sedimentological features not always visible in the core catcher material, such as major hiatuses and glacial varves.

Sediment classification

The sediment classification scheme used during Expedition 347 is descriptive and defines lithology on the basis of composition and texture. The scheme has been used previously in the Ocean Drilling Program.

Nomenclature criteria for fine-grained sediments that do not contain gravel are defined by the relative proportions of sand, silt, and clay-sized material, based on the ternary classification scheme of Shepard (1954) (Fig. [F17](#)). Generic or interpretive terms such as pelagic and turbidite do not appear in this classification and were avoided because the aim was to provide a purely descriptive account of the sediments. Based on the classification scheme employed, the term “clay,” for example, is used for both clay minerals and other siliciclastic material <4 μm in size. The term “mud” describes a subequal mixture of silt and clay. For sediments with a gravel component, a modified version of the classification scheme of Moncrieff (1989) was used (Fig. [F18](#)).

Examples of principal names of fine-grained sediments are clay, silty clay, silt, sandy silt, or sand. For lithified sediments, the suffix “-stone” is added to the principal names of sand, silt, or mud. Where quartz is not the dominant mineral, a modifier is used to denote the dominant mineral phase (e.g., glauconite sand). Biogenic components are not described in textural terms at this stage; instead, they are given more detailed observations using microscopy of smear sections. In terms of visual core description, sediments with visible bioclastic components as the dominant phase are classified with a similar modifier as mentioned above (i.e., sediment with 55% sand-size foraminifers and 45% siliciclastic clay is called foraminifer clay).

Biostratigraphy

Table [T1](#) provides the master species list for Expedition 347.

Diatoms

During the OSP, selected core intervals were subsampled via toothpick scrape into individual clean glass beakers. Subsamples were then treated with 1–2 mL of 30% H₂O₂ to remove organic material and allowed to react for several hours. The resulting sediment slurry was pipetted onto clean glass coverslips and allowed to dry on a hot plate. Coverslips were permanently affixed to clean glass slides with Naphrax mountant.

Each slide was viewed under light microscopy at a magnification of 400× or 1000× for ~1 h to qualitatively characterize the diatom assemblage. Diatoms were identified primarily according to Snoeijs et al. (1993–1998), with additional identifications from Witkowski (2000), Cleve-Euler (1951), Fryxell and Hasle (1972, 1980), Hasle (1978a, 1978b), Hasle and Lange (1992), Hustedt (1930), Krammer and Lange-Bertalot (1986, 1988, 1991a, 1991b), Muylaert and Sabbe (1996), Mölder and Tynni (1967, 1968, 1969, 1970, 1971, 1972, 1973), Sabbe and Vyverman (1995), Snoeijs (1992), Tomas (1997), and Tynni (1975, 1976, 1978, 1980). Salinity-based affinities of diatoms follow Snoeijs et al. (1993–1998). Silicoflagellates were identified according to Tomas (1997). Chrysophyte cysts were divided into morphotypes by reference to the structure of the cyst walls.

Foraminifers

Variations in benthic foraminiferal assemblages in the Baltic Sea Basin reflect changes in salinity, temperature, oxygen concentration, and water depth that may be representative of glacial–interglacial climatic events (Knudsen, 1994). The presence/absence data and assemblage composition of benthic foraminifers therefore have the potential to be used as a chronologic constraint (Kristensen et al., 2000). Planktonic foraminifers are not found in the modern Baltic Sea because of its low salinity and shallow water depths and are only rarely found in the Kattegat. There was no evidence of planktonic foraminifers in this expedition's cores, except as occasional redeposited pre-Quaternary specimens. Identification of benthic foraminifers was based on standard reference literature for the Baltic Sea Basin (e.g., Feyling-Hanssen et al., 1971; Feyling-Hanssen, 1972; Austin, 1991; Seidenkrantz, 1993; Alve and Murray, 1999; Murray and Alve, 2011; Pillet et al., 2013).

Offshore, samples for identification of foraminifers and other microfossils were taken from every core catcher sample in both paleoenvironmental and microbiology holes (sediment volumes were generally ~5–20 cm³, or in some cases as much as 30 cm³). Additional onshore ~20 cm³ samples were taken mid-

way between core catchers to improve the resolution and refine biostratigraphic control, resulting in an overall sample resolution of ~1.5 m.

Sandy intervals that yielded samples barren of microfossils were sampled less frequently. Longer intervals between samples also occurred where core catchers were not available, particularly in microbiology holes.

The raw samples were directly washed over a 63 µm sieve with tap water (where necessary, an ultrasonic cleaner or a soft brush was used to disaggregate sediments while rinsing) and rinsed with deionized water. Care was taken to ensure that the sediment used for washing represented all types of material found in the core catcher. However, when sediment smeared from another interval during the drilling process was clearly visible, this “contaminated” sediment was excluded whenever possible.

While offshore, an initial inspection for foraminifers and other microfossils was performed on the remaining (>63 µm) wet sample before a second inspection was conducted on the dry sediment. During the OSP, the samples were oven dried in filter paper at 40–50°C and were inspected for foraminifers and other microfossils.

Foraminifers were picked from the >63 µm size fraction and identified to species or genus level. In samples with low numbers of foraminifers or limited sample volume, all foraminifers were picked for identification. In high foraminiferal abundance samples, a minimum of ~50 individuals was picked. Visible signs of test dissolution or broken tests were recorded. Redeposited foraminifers, both pre-Quaternary and occasionally also Eemian, commonly occurred in specific intervals at the more westerly located sites (M0059 and M0060) and were noted and excluded from in situ species assemblage and abundance results. Pre-Quaternary foraminifers were distinguished by their often recrystallized or frosty tests (Rasmussen et al., 2005); in the case of Cretaceous foraminifers and nearly all planktonic foraminifers, these were identifiable as pre-Quaternary species. The presence of redeposited Eemian foraminifers could be determined when the faunal assemblage contained both relatively warm and cold water species (Seidenkrantz, 1993).

Abundance of foraminifers and species/genera diversity was recorded at all sites. At sites with foraminifers of more than one species or genus, a count was made of the number of species/genera present in each sample to generate a foraminiferal “diversity” profile. Samples with greater species or genus diversity were interpreted as indicating more saline or more oxic conditions.

Benthic foraminiferal abundance was defined as follows and shown in plots as a 0–5 value:

- 0 = B (barren; 0 specimens).
- 1 = V (very rare; <5 specimens).
- 2 = R (rare; 5–10 specimens).
- 3 = F (few; 10–100 specimens).
- 4 = C (common; 101–500 specimens).
- 5 = A (abundant; >500 specimens).

Benthic foraminiferal diversity was defined as follows:

- B = barren (0 species).
- L = low (1–3 species).
- M = medium (4–6 species).
- H = high (7–10 species).
- V = very high (>10 species).

This diversity classification applied during the OSP is a more rapid approximation of published statistically based species assemblage technique. Postcruise investigation will likely adopt published quantification methods.

In addition to foraminifers, while offshore, ostracods and bivalves were picked from the >63 µm sediment fraction for identification when present, and their abundance was recorded. Other microfossils such as diatoms, pollen, and organic matter (plant, animal, or charcoal) were recorded when present and identified where possible.

Approximately 490 samples for foraminifers were prepared from core catchers during the offshore phase of Expedition 347. The total number of samples prepared during the offshore and onshore phases of the expedition is reported in each site chapter.

Ostracods

The Baltic Sea is a relatively well studied area in terms of its ostracod fauna. Although there is no established biostratigraphy based on ostracods for the Baltic Sea, numerous publications are available on the ecology of the Baltic Sea species (e.g., Rosenfeld, 1977; Borck and Frenzel, 2006; Frenzel et al., 2005, 2010; Veihberg et al., 2008). Salinity is the main factor determining ostracod distribution in the Baltic Sea (Frenzel et al., 2010), making ostracods very useful for paleosalinity reconstructions. Analysis of population-age structure can be used to evaluate the autochthoneity of the assemblage, which is crucial when studying shallow-water environments (Whalley, 1983).

During the offshore phase, ostracods were picked during examination of core catcher samples (typical sample interval = ~3.3 m) of variable volume ranging from 5 to 30 cm³. Additional onshore ~20 cm³ sam-

ples were taken halfway between core catchers to improve the sample resolution. The resultant sample resolution is therefore ~1.5 m. Sandy intervals that yielded samples barren of microfossils were sampled less frequently.

All samples were washed over a 63 µm mesh sieve. Subsequently, the samples were oven dried in paper filters at 40°–50°C. Ostracods were picked from the entire sample residues, identified, and counted. Although ostracod abundance was relatively low (<10 specimens in most samples), preservation was good in most samples. Redeposited valves were recorded in several sandy intervals. The number of juvenile specimens was also recorded.

For preliminary paleosalinity reconstruction, ostracods were divided into the following categories: freshwater, very shallow water oligohaline, and shallow-water brackish-marine species and marine species typical of the North Atlantic shelves. For the onshore data plots, the number of valves per sediment volume was plotted against meters below seafloor as an estimation of abundance. The following abundance categories were distinguished and are shown in tables:

- A = abundant (>50 specimens).
- C = common (20–50 specimens).
- F = few (5–20 specimens).
- R = rare (1–5 specimens).
- B = barren (no specimens found).

Palynology

Palynomorphs

Twenty core catcher samples of 5–10 mL volume were processed for palynological analysis during the preonshore phase. The following approach was adopted:

1. Treatment with 40% HCl (1 day), involving dissolving a tablet containing ~18,500 *Lycopodium* spores;
2. Decanting (3 times);
3. Treatment with 50% HF (1 day);
4. Decanting (4 times); and
5. Sieving through a 10 µm mesh.

The samples were then mounted on slides in glycerine jelly.

During the OSP, 3–10 mL of sediment was processed per sample (depending on sediment type). The following approach was used for the majority of samples:

1. Treatment with 10% HCl (3–12 h, depending on strength of reaction), involving dissolving two tablets containing ~18,500 *Lycopodium* spores;
2. Neutralizing with 10% KOH;

3. Centrifuging twice (3000 rpm, 5–10 min) and decanting;
4. Treatment with 40% HF (over 1–2 nights);
5. Neutralizing with 40% KOH;
6. Centrifuging twice (3000 rpm, 5–10 min) and decanting; and
7. Mounting on glycerine jelly and/or pure glycerine.

Terrestrial palynomorphs

Slides were examined for terrestrial palynomorphs under 200×, 400×, and 1000× magnification and partly with use of phase contrast. Pollen grains, plant spores, freshwater algae (particularly *Botryococcus* and *Pediastrum*), and fungal spores (morphotypes only) and arthropod remains (particularly chironomid remains) were assessed.

The aim was to count as many as 75–150 pollen grains per sample to ensure statistical relevance to a reasonable degree, even if bisaccate pollen were over-represented. The pollen guides of Beug (2004) and the Faegri and Iversen (1989) pollen key were used for pollen identification.

Marine palynomorphs

Although the palynological focus was on terrestrial palynomorphs, marine palynomorphs (organic-walled dinoflagellate cysts and foraminiferal test linings) were also analyzed (at approximately half the resolution, or 35–75 counts/sample) compared to the pollen analysis, using the same slides as for pollen analysis to achieve a direct land-sea correlation and to differentiate fully marine, brackish, and lacustrine environments. Dinoflagellate cysts (dinocysts) were generally identified to genus or species level. The dinoflagellate atlas of Marret and Zonneveld (2003) and publications on Baltic Sea dinocysts (e.g., Nehring, 1997) were used for dinoflagellate cyst identification. Foraminiferal test linings were divided in two groups (planispiral and trochospiral), and fragments with several chambers were counted as one third foraminifer. The ratio of dinocysts plus foraminiferal test linings versus nonsaccate pollen grains was used as an estimate for the site-shoreline distance.

Geochemistry

Offshore interstitial water sampling and analysis

Pore water sampling

Cores were sampled for pore water immediately on recovery, using either Rhizon samplers or squeezers. Rhizon samplers (CSS-F 5 cm; Rhizosphere Research Products, Netherlands) are narrow elongated cylin-

dric filters (0.2 μm pore size; 5 cm long; 130 μL volume) with a stiff plastic core (Seeberg-Elverfeldt et al., 2005; Dickens et al., 2007). Before use, each Rhizon was soaked for several hours in ultrapure water (Elga Purelab Classic UV), which was subsequently ejected under pressure with a syringe and discarded prior to sampling. A 3.8 mm hole was drilled through the plastic core liner using a spacer on the drill bit to avoid penetrating the core itself. A Rhizon sampler with the same diameter as the hole was then inserted into the core. Negative pressure was applied by attaching a 20 mL all-plastic pulled-back syringe to the Rhizon sampler, in which the pore water was collected. The sediment cores remained capped throughout this process to maintain an environment as similar to the original sediments as possible.

When Rhizon sampling took place before core logging (i.e., paleoenvironmental holes), Rhizon samplers remained in the cores for 2–3 h. When Rhizon samples were taken after Fast-track core logging (i.e., microbiology holes), the Rhizons remained in the core for as long as 9 h. Usually, two Rhizons were used per core section, spaced 10 cm apart to obtain sufficient pore water from a single interval while minimizing overlap.

Whole-round sections 10 cm in length obtained from the microbiology cores were squeezed in a Teflon-lined titanium squeezer of piston-cylinder design (described in detail at www.marum.de/en/Acquisition.html). Whole rounds were nearly always cut from the bottom of the first core section (unless both sections were sampled), as this material was most likely to be undisturbed. Before the whole-round samples were prepared for squeezing, a pre-prepared, rinsed Rhizon was inserted to obtain the first 1–2 mL of pore water to fulfill a sample request for postcruise research. Whole rounds were scraped clean on all surfaces to remove drilling mud and material from the outer surface that may have been smeared down the core liner. They were then cut to <54 mm diameter to fit into the squeezer. Once in the squeezer, sediment was contained when under pressure (up to 10 tons/inch², equivalent to 137,900 kPa, applied by a hydraulic press) by a circular titanium screen at the base of the cylinder overlain by nylon mesh and a paper filter (Whatman 1; 55 mm), through which the water was pushed to an online filter (Sartorius; 0.2 μm; 25 mm; nylon) and through that into a 20 mL all-plastic syringe. All parts of the squeezer that come in contact with either the sediment or pore water are made of polytetrafluoroethylene (PTFE), titanium (grade 2), or polyamide plastic (Delrin).

We collected pore water reference samples, including seawater from each site, tap water, artificial seawater,

and the different mud types and additives used while drilling. These samples were treated like pore water samples, analyzed, and split to cover the IODP required measurements.

After sampling, all syringes were placed in a glove bag under nitrogen, and the extracted pore water was transferred to a 20 mL polypropylene vial. When multiple Rhizon samples were taken from one core section, pore water samples were combined in a single vial. Oxygen was monitored in the glove bag using a Dräger Pac 5500 oxygen sensor and was typically <1 vol% (Sites M0059–M0062). At Site M0063, however, it was not possible to maintain such low oxygen concentrations, possibly as a result of degradation of the closure mechanism on the glove bag. For those samples and for all following sites, one of the Rhizon syringes was transferred directly to a cation vial. The sample was subsequently split into six fractions: a pore water sample for total sulfide (add 1 mL of sample to a vial prefilled with 0.4 mL 5% Zn acetate), cations and trace elements (1–3 mL of sample acidified with 1% concentrated trace metal grade HNO₃ per sample), pH/alkalinity (0.5 mL), ammonium (0.2–0.5 mL), salinity (0.5 mL), and anions (1–3 mL).

Pore water analysis

Pore waters from all holes were analyzed on board for pH, alkalinity, ammonium, and salinity. In addition, sulfide was analyzed on the first paleoenvironmental hole of every site where a microbiology hole was cored (Sites M0059, M0060, M0063, and M0065). Pore water pH was measured using an ion-specific electrode (Mettler Toledo) with a 2-point calibration on 0.2–0.5 mL of pore water. The same sample was then utilized for the measurement of alkalinity by single-point titration to pH 3.95 with 0.01, 0.05, or 0.2 M HCl according to standard procedures (Grasshoff et al., 1983). Ammonium was measured by conductivity after separation as NH₃ through a PTFE membrane in a flow-through system. In the latter technique, modified after Hall and Aller (1992), ammonia is stripped from a 100 µL sample by an alkaline carrier solution (0.2 M Na citrate in 10 mM NaOH), passed through a 200 mm × 5 mm PTFE membrane, and redissolved as NH₄⁺ in an acidic solution (1 mM HCl). Ammonium ions were then measured as the resulting conductivity signal in the acidic carrier in a microflow-through cell. All samples collected for pH, alkalinity, and salinity analyses were stored at 4°C, and measurements were conducted within 24 h or, for ammonium, within 24–48 h of sample collection.

Total sulfide was measured spectrophotometrically applying the methylene blue method of Cline (1969)

using a DR 6900 Hach Lange (Berlin, Germany) spectrophotometer. Total sulfide is referred to as H₂S throughout the text for simplicity, though H₂S was not quantified. Salinity was determined by optical refraction (Krüss Optromic digital refractometer DR 6300), calibrated with International Association for the Physical Sciences of the Oceans (IAPSO) seawater standards by OSIL having salinities of 10, 30, 35, and 38.

Subsamples for cations, trace elements, and anions were stored at 4°C for further onshore analysis at the University of Bremen (Germany) via inductively coupled plasma–optical emission spectrometry (ICP-OES; Al, B, Ba, Ca, Fe, K, Mg, Mn, Na, P, S, Si, Sr, Ti, Li, Mo, Rb, V, and Zr) and ion chromatography (Cl, Br, and SO₄) measurements.

Methane sampling and analysis

Methane samples were taken from all cores when the core material was intact and thus suitable for sampling. Methane concentrations were determined for each core of the first paleoenvironmental hole on the microbiology sites (Sites M0059, M0060, M0063, and M0065) for chemical zonation, following standard protocols for headspace sampling and analysis. A 5 cm³ sediment sample was collected with a cut-off disposable syringe from the freshly exposed end of every section within the uppermost 20 m of each hole. Deeper than this, the sampling frequency was reduced and one sample was taken from the bottom of the first section within each core. The sample was extruded into a 20 mL glass vial filled with 8 mL of 1 M NaOH solution, immediately crimp-sealed with a gas-tight septum, and stored upside down at room temperature prior to analysis. After the sample was shaken and left for gas equilibration, 250 µL of headspace volume was manually injected using a gas-tight glass syringe into an Agilent A7890 gas chromatograph (GC) equipped with a PLOT 5A column (30 m × 0.53 mm, inner diameter = 50 µm) and coupled to a flame ionization detector (FID). Helium was used as carrier gas with a constant flow of 5 mL/min. The oven was held isothermal at 30°C for 3 min. Quantification of methane was achieved by comparison of its chromatographic response with an external three-point calibration curve using 0.01%, 0.1%, and 1% methane standards.

The concentration of methane in interstitial water was derived from the headspace concentration by the following equation (Shipboard Scientific Party, 2003), where methane that remains undetected because dissolution in the aqueous phase is minimal (e.g., Duan et al., 1992), is not accounted for:

$$\text{CH}_4 = [\chi M \times P_{\text{atm}} \times \text{VH}] / [R \times T \times \phi \times \text{VS}],$$

where

- VH = volume of sample vial headspace,
 VS = volume of whole sediment sample,
 χ_M = molar fraction of methane in headspace gas
 (obtained from gas chromatograph analysis),
 P_{atm} = pressure in vial headspace (assumed to be the
 measured atmospheric pressure when the vials
 were sealed),
 R = universal gas constant,
 T = temperature of vial headspace in degrees Kel-
 vin, and
 ϕ = sediment porosity (determined from mois-
 ture and density measurements on nearby
 samples).

Onshore science party chemical analyses

Pore water analysis

A total of 689 filtered (0.2 μm) and acidified (10 μL of concentrated HNO_3/mL) pore water samples were analyzed for cations and trace metals using analytical equipment at the University of Bremen. All samples were diluted 10-fold with 1% HNO_3 and analyzed for Al, B, Ba, Ca, Fe, K, Mg, Mn, Na, P, S, Si, Sr, and Ti using a Varian Vista Pro CCD ICP-OES equipped with a sea-spray nebulizer and a cyclon spray chamber. Trace elements (Al, Ba, Fe, Li, Mn, Mo, P, Rb, Ti, V, Zn, and Zr) were analyzed on a second set of 10-fold diluted samples using an Agilent Technologies 700 Series ICP-OES equipped with a K-style conical nebulizer. Standardization was performed against multielement solutions prepared from commercial standards with either a 1% HNO_3 matrix adjusted to a NaCl concentration similar to the matrix in the samples (for trace element samples with salinity >5) or 1% HNO_3 only (all other samples). Calibration standards for major elements and trace elements were prepared using IAPSO seawater and National Institute of Standards and Technology Certified Reference Material (NIST CRM). Measurement precision was $\pm 3\%$ for major elements and $\pm 5\%$ for trace elements.

Trace element analyses for Al and Zn were either below the detection limit or showed contamination and therefore are not reported for all sites. Rubidium, Mo, Ti, V, and Zr had concentrations above the detection limit, and results were consistent between holes for some of the sites. Table T2 indicates which sites had acceptable data (denoted by “Y”). These data are listed in the tables in each site chapter. For elements analyzed for both major and trace elements, reported values came from the major element analyses, with the exception of Ti.

A total of 711 filtered and unacidified pore water samples were analyzed for anions (chloride, bro-

mide, and sulfate) using a Metrohm 882 compact ion chromatograph at the University of Bremen. A 40-fold dilution of IAPSO seawater and standards prepared from commercial single anion standards were used for calibration. Measurement precisions were $\pm 0.6\%$ for Cl, $\pm 3.5\%$ for Br, and $\pm 1.6\%$ for S (1σ).

Bulk geochemical analysis of sediments

Approximately 10 cm^3 of sediment was freeze-dried and ground to a fine powder using an agate mortar. Total carbon (TC), total organic carbon (TOC), and total sulfur (TS) were measured using a LECO CS-300 carbon-sulfur analyzer. Approximately 65 mg of the homogenized sample was weighed in a ceramic cup and heated in a furnace. The evolved CO_2 and SO_2 were then measured with a nondispersive infrared detector to provide a measure of the sedimentary TC and TS content. To determine the TOC content, sediments (~65 mg) were decalcified using 12.5% HCl to remove carbonate species and analyzed as described above. Total inorganic carbon (TIC) was determined by subtracting TOC from TC. All data are reported in weight percent (wt%) dry sample with an analytical precision $<3\%$ absolute based on replicate sample analysis.

Physical properties

The primary objective of the petrophysical program was to collect high-resolution physical properties data that will enable

- Characterization of lithostratigraphic units and formation properties,
- Facilitation of hole-to-hole correlation,
- Retrieval and construction of complete composite stratigraphic sections together with lithologic and sedimentological descriptions for each hole, and
- Provision of data for the construction of synthetic seismograms and investigation of the characteristics of major seismic reflectors.

Offshore, the physical properties program involved collecting high-resolution, nondestructive measurements on whole-round cores using a Geotek MSCL. The standard MSCL is equipped with four sensors that sequentially measure gamma density, transverse compressional wave (P -wave) velocity, noncontact electrical resistivity (NCR), and magnetic susceptibility. Note that “gamma density” refers to the bulk density of the core as derived from the collimation of gamma rays through the core (see “[Gamma density](#)”).

The second MSCL system used offshore was a rapid magnetic susceptibility MSCL system “Fast-track”

utilizing two offset Bartington loop sensors. This facilitated timely stratigraphic correlation and provided a means to correlate the microbiology holes to the paleoceanographic holes at the same site. The Fast-track MSCL provided the only opportunity to obtain a complete record of petrophysical measurements from the microbiology cores recovered at specific sites, as the cores were rapidly subsampled offshore to prevent microbial degradation.

Onshore, the physical properties program included natural gamma ray (NGR) measurements (measured on whole-round cores prior to the OSP), digital line scan imaging, and color reflectance (measured on split cores during the OSP). Lower resolution measurements of thermal conductivity were also performed on unsplit (whole-round) cores using a full-space needle probe prior to the OSP. During the OSP, separate subsamples for discrete *P*-wave velocity and moisture and density (MAD) analyses were acquired at an approximate resolution of one per core section (about every 1.5 m) from the working halves of the split core. *P*-wave velocities were typically not performed on shallow core sections because of the lack of sediment consolidation. If possible, *P*-wave velocities were measured on samples taken from the same depth interval as the MAD measurements (i.e., from adjacent stratigraphic levels).

Offshore petrophysical measurements: standard MSCL

The MSCL is equipped with four primary sensors mounted on an automated track that sequentially measure gamma density, *P*-wave velocity, NCR, and magnetic susceptibility. Two additional secondary sensors allow these primary measurements to be corrected for core diameter and temperature. Automated measurements were taken on whole-round core sections after they had equilibrated to ambient room temperature with the MSCL set up in horizontal mode. Core sections shorter than 15 cm were not included in the logging process. Core catcher (CC) intervals were measured if they were longer than 15 cm.

The quality and validity of the MSCL data are a function of both core quality and sensor precision. Optimal measurements for all sensors require a completely filled core liner and fully fluid-saturated cores for *P*-wave velocity and gamma density measurements. In sections where the core liner is not filled or the core is insufficiently saturated, the measurement quality is compromised. In terms of sensor precision, gamma density and MS sensors are affected by the duration of each point measurement. *P*-wave velocity, NCR, and MS are affected by room and core temperature. To attain optimal resolution of data

during Expedition 347, a measurement sampling interval of 2 cm was chosen for all sensors, based on the amount of core and time available. A decision was made to change the measurement sampling interval to 1 cm at Sites M0061 and M0062 (Ångermanälven River estuary) to characterize the varved sediments recovered at a higher resolution.

A full calibration of the MSCL sensors was conducted at the start of the expedition, every time the system was rebooted (for example, after power failure or after transit), and when calibration checks revealed unacceptable departures from the full calibration values (Table T3). Checks on the full calibration were then performed approximately once every 6 h to consistently monitor the machine and sensor performance. The calibration check involved logging three calibration reference pieces (a magnetic susceptibility standard, a core liner filled with distilled water, and a core liner filled with 17.5 g/L salinity fluid [NaCl]) and comparing the results to the values derived during the full calibration. This allowed the performance of the four primary sensors to be assessed quickly and consistently; if the calibration check values departed from the acceptable range, a full calibration was performed (Table T3).

Measurement principles

Gamma density

Gamma density is measured by determining the attenuation of gamma rays (mainly by Compton scattering) that pass through the cores and is used to estimate bulk density. The degree of attenuation is proportional to the electron density in the gamma path (Rider, 2006). Gamma attenuation coefficients vary as a function of atomic number, but as most rock-forming minerals have similar and low atomic numbers, the correlation between gamma density and bulk density is generally very good. A small (370 MBq) ^{137}Cs source (half-life = 30.2 y) was used to produce a collimated gamma beam with primary photon energies of 0.662 MeV. Two collimators are available (2.5 and 5 mm). The 5 mm diameter collimator was used throughout MSCL measurement operations during Expedition 347. The standard sampling interval was set at 2 cm (except at Sites M0061 and M0062, where a 1 cm interval was used) with count time set to 10 s (the same as the magnetic susceptibility sensor). The resolution with this setup is 0.5 cm.

Calibration of the system for Expedition 347 was completed using a stepped water/aluminum density standard (provided by Geotek). Initial full calibration was performed using a standard core liner (~0.3 m length) containing a stepped aluminum calibration piece centered inside the liner, which was filled with

distilled water (“wet calibration”). Gamma counts were taken for 60 s through each of the five aluminum steps of known thicknesses (6, 5, 4, 3, and 2 cm). In addition, the gamma count of the liner filled with only distilled water was recorded. Regular (every 6 h) calibration checks were conducted during logging using the distilled water calibration piece and compared to the full calibration values. All data were handled using the processing parameters from these wet calibrations. Dry calibrations (air/aluminum) were also conducted and are available should reprocessing be required.

P-wave velocity

Transverse *P*-wave velocity was measured using two *P*-wave transducers aligned perpendicular to the core axis with *P*-waves passing through the core horizontally (in whole-core set up). A compressional wave pulse centered on a frequency of 230 kHz was transmitted through the core. The *P*-wave transducers also function as displacement transducers, monitoring the small variations of the outside diameter of the liner over which the traveltime was measured. These variations are ultimately used in processing the gamma density, *P*-wave velocity, and magnetic susceptibility data sets. Standard measurement spacing was set at 2 cm (except at Sites M0061 and M0062, where a 1 cm interval was used), as for all other sensors.

Initial calibration was performed using a core liner filled with distilled water (~0.3 m in length), measured at a known temperature. The calibration was repeated as necessary when checks revealed a departure from the acceptable initial calibration value. Calibration checks were made by logging the distilled water-filled calibration piece at regular intervals during the core logging process (one calibration check every 6 h).

P-wave measurement is critically affected by the quality of the core. Poor data results occur where undersized core causes separation between the core material and core liner. Also, if the cores are gaseous or insufficiently water saturated, then an optimal propagation of *P*-waves will not be achieved through the core. During Expedition 347, whenever the core had obvious insufficient water saturation and/or contact with the liner was poor, the quality of the *P*-wave data was considered to be unreliable and a note was appended to the comments column in the MSCL spreadsheet.

Noncontact electrical resistivity

Electrical resistivity of sediment cores was measured using the NCR sensor. The measurement is based on

a technique using two sets of coils, allowing for comparison of readings from the core (one set of coils with readings taken in air (second set of coils). The transmitter coil induces a high-frequency magnetic field in the core, which induces electrical currents in the core that are proportional to the core's conductivity (inversely proportional to resistivity). The very small magnetic fields regenerated by these electrical currents are measured by a receiver coil and normalized with the separate set of identical coils operating in air. The spatial resolution of this measurement is ~2 cm. The measurement interval selected was 2 cm (except at Sites M0061 and M0062, where a 1 cm interval was used), the same as for the other sensors.

Initial calibration was performed using six standard core liner sections (~0.3 m in length) containing water of known but varying salinity. Five standards were made up to concentrations (NaCl) of 35, 17.5, 8.75, 3.5, 1.75, and 0.35 g/L. The sixth standard was filled with distilled water. Calibration checks were undertaken every 6 h and consisted of logging a standard piece of core liner filled with 17.5 g/L saline fluid. The calibration procedure was repeated as necessary whenever calibration checks indicated an unacceptable difference from the initial calibration values.

Resistivity measurements indicate the amount and kind of pore fluid in the core sediment. Because these values are integrated over a depth of several centimeters, measurements taken near the ends of a core section are automatically removed. Furthermore, any trends in values toward these deleted values should be used with caution.

Magnetic susceptibility

Whole-core magnetic susceptibility was measured on the MSCL using a Bartington MS2 meter coupled to a MS2C sensor coil. The loop sensor has an internal diameter of 80 mm, corresponding to a coil diameter of 88 mm. The loop used for Expedition 347 was a standard loop operating at a frequency of 565 Hz, which means no correction factor need be applied to the data. The MS2 system operates on two fixed sensitivity levels $\times 0.1$ and $\times 1$, corresponding to 10 s and 1 s sampling integration periods, respectively. For Expedition 347, all cores were measured using the 10 s ($\times 0.1$) setting. Magnetic susceptibility measurements were made at a sampling interval of 2 cm (except at Sites M0061 and M0062, where a 1 cm interval was used). The sensor automatically zeroes and takes a free air reading at the start and end of each run to account for instrument drift by subtraction of a linear interpolation between readings. Magnetic susceptibility data were recorded as corrected volume-specific units ($\times 10^{-5}$ SI).

The accuracy of the magnetic susceptibility sensor was checked using a calibration standard (made of impregnated resin) with a bulk susceptibility of 754×10^{-5} SI (598×10^{-6} cgs). This calibration piece was centered within a core liner, and calibration checks were carried out approximately every 6 h to check reliability of the sensor.

Quality assurance and quality control

Two quality assurance/quality control (QA/QC) checks were carried out, one during the offshore phase of the expedition and one before the OSP. During the offshore phase, QA/QC involved core quality description, use of hard copy and electronic MSCL log sheets and calibration sheets, repeat MSCL logging of calibration standards (calibration checks) every 6 h, and repeat logging of selected cores as described below. Postoffshore systematic cross-checks of electronic calibration, data files, and processed data were made. The final data set was made available during the onshore phase both as raw and processed data.

In addition to sensor calibrations and calibration checks to ensure the accuracy and consistency of the sensors, a QA/QC measurement plan was in place during the offshore phase of the expedition. The reproducibility of the MSCL data was assessed by repeat logging a selection of core sections from each hole. Attempts were made to log core sections from roughly every 50 m in depth to avoid any bias. Typically, sections that were completely filled with sediment were selected to ensure accurate and representative measurements could be obtained from all sensors. A limited number of QA/QC cores were selected to monitor and document the influence of temperature change on the measurements achieved. In this case, each of the selected core sections were first logged “cold” and then relogged every 2 h until they were temperature equilibrated. The temperature of the sediment was measured with a thermometer inserted into the bottom of each of the chosen core sections.

In general, reproducibility was good. Repeat measurements were highly reproducible for gamma density and magnetic susceptibility, but there was often a variation in the NCR values and, occasionally, *P*-wave velocity. NCR variations sometimes existed between the measurements of individual core sections and particularly at the end of Sections 2 and 3. However, the 6 h calibration checks showed that all sensors were performing perfectly and were well within the acceptable limits of the full calibration parameters. In light of this, the first resistivity sensor was exchanged for the spare one to test a different sensor response. Results from both sensors were equivalent.

It was therefore concluded that, as NCR measurements are extremely sensitive and can be adversely affected by temperature, repeat logging after chilling in the reefer could not yield identical results to the original data.

MSCL logsheets

Throughout the expedition, information was recorded on both hard copy and electronic MSCL logsheets in an attempt to ensure all information that affects the quality of the result was retained. QA/QC included

- Observation of core liner fill, fluid content, and cracks in the core;
- Top depths cross-checked with final DIS depths;
- Notes for sections where there were apparently sensor issues;
- Notes for those sections measured at a 1 cm sampling interval (instead of the standard 2 cm); and
- Notes on the presence of metal in any section noted and cross-checked with the DIS.

Deletion of values around core endcaps

Offshore, operators deleted from the processed files all data around endcaps that were clearly affected by these caps. As the amount of data affected varies for each sensor and the effect is gradational away from the end of the core, different analyzers may choose to delete various amounts of data. Therefore data were checked before the OSP for errors and consistency.

The “raw data” have no deleted values. For the “processed data,” endcaps and bad data points (e.g., from metal in the liner or cracks) were removed.

Fast-track MSCL

The Fast-track MSCL comprised two offset 90 mm magnetic susceptibility loops, each taking a measurement every 4 cm; in combination the offset loops rapidly provided data at 2 cm intervals. The Fast-track MSCL was employed during Expedition 347 to provide a rapid logging record of the microbiology cores immediately after they were curated, as the sediments needed to be sampled by the microbiologists as soon as possible after retrieval from the borehole. The Fast-track MSCL therefore provided the only opportunity to obtain a complete composite record of petrophysical measurements on the microbiology cores and greatly facilitated stratigraphic correlation between the cores recovered from individual holes at each site. This aided stratigraphic correlation, enhanced the coring strategy, and helped to op-

imize recovery both at each site and across all the sites in general.

Magnetic susceptibility

Whole-core magnetic susceptibility was measured on the Fast-track MSCL using two Bartington MS2 meters each coupled to a MS2C sensor coil. Both loop sensors had an internal diameter of 90 mm. The loops used for Expedition 347 were nonstandard loops operating at frequencies of 513 and 621 Hz, which require correction factors of 0.908 (513 Hz) and 1.099 (621 Hz) to be applied to the data. The MS2 system operates on a fixed sensitivity level of 5 s sampling integration periods. For Expedition 347, all cores were measured at a sampling interval of 4 cm, but with two sensors working offset, this resulted in a sampling resolution of 2 cm. The sensor automatically zeroes and takes a free air reading at the start and end of each run to account for instrument drift by subtraction of a linear interpolation between readings. Magnetic susceptibility data were recorded as corrected volume specific units ($\times 10^{-5}$ SI).

The accuracy of the magnetic susceptibility sensors was checked using two calibration standards (made of impregnated resin) with bulk susceptibilities of 185×10^{-5} SI (147×10^{-6} cgs) and 767×10^{-5} SI (610×10^{-6} cgs), respectively. These calibration pieces were centered within a core liner, and calibration checks were carried out approximately every 6 h to check the reliability and consistency of the sensors.

Quality assurance and quality control

QA/QC checks were carried out during the offshore phase. QA/QC involved core quality description, use of hard copy and electronic Fast-track MSCL logsheets and calibration sheets, and regular calibration checks. This consisted of the repeat logging of both calibration standards every 6 h to monitor sensor precision and accuracy. The final data set was made available during the offshore phase as raw data.

Onshore petrophysical measurements

The OSP was held at the BCR from 22 January to 20 February 2014; preonshore measurements were performed between the end of November 2013 and the start of the OSP. Onshore petrophysical methods are described in the order in which they were performed. NGR and thermal conductivity were measured on whole-round cores in advance of the OSP (preonshore). Line scanning and color reflectance measurements were conducted on split-core sections, immediately after splitting, to record accurate colors prior to core desiccation and oxidation. Digital images of archive halves were made with a digital

imaging system. Discrete color reflectance measurements of working halves were made with an MSCL system. *P*-wave and MAD measurements were conducted on discrete samples taken from the working-half cores. A helium gas pycnometer was used to measure the matrix volume of discrete samples at an approximate resolution of one sample per core section. Discrete *P*-wave velocity measurements were performed on semiconsolidated and consolidated samples with a Geotek DPW sensor.

Natural gamma radiation

NGR emissions of sediments are a function of the random and discrete decay of radioactive isotopes, predominantly those of ^{238}U , ^{232}Th , and ^{40}K and their radioactive daughter products (for example, ^{208}Tl , ^{228}Ac , and ^{214}Bi). These decays are measured through scintillation detectors housed in a shielded collector. For Expedition 347, a bismuth germanate (BGO) crystal was used as scintillation material. Total counts per second were measured by integration of all emission counts over the gamma ray energy range between 0 and 3 MeV. Measuring total counts gives a reasonable precision with relatively low counting times (minutes per sample) and is well suited for correlation with core and downhole wireline logging measurements. No corrections were made to NGR data from Expedition 347 to account for volume effects related to sediment incompletely filling the core liner.

Measurements were carried out at 4° – 6°C in the refrigerated core repository at the MARUM–Center for Marine Environmental Sciences at the University of Bremen to ensure there was minimal drift in measurement over time. After the equipment became temperature equilibrated, a source of ^{133}Ba and a source of ^{60}Co were used for energy calibration of the spectrum. A zero reading of background NGR counts was taken before measurements began, and a calibrated clean sandstone background was also obtained. To obtain the clean sandstone background a small section of liner (~ 50 cm) was filled with clean, wet sand and the NGR spectra was acquired. This calibrated clean sandstone background allows for the ambient levels of background gamma radiation to be subtracted from the measurement, a method that was used during Expedition 347 preonshore NGR measurements. To track potential drift of the spectra a daily check was performed on standard U and K samples to ensure the K spectra peak was within the correct energy window. These data were recorded at the same time each day and are available on request.

NGR measurements began 6 weeks prior to the start of the OSP and were completed before the OSP began on 22 January 2014. A Geotek XYZ frame system

was employed that allowed up to six core sections to be logged during a single run. The gamma ray detector has a measurement window of 7.5 cm, and the sampling interval was set at 9 cm to maximize the resolution of measurements in the time available while minimizing resampling of intervals. The count time at each sampling point was set at 2 min. This sampling interval and count time provided the highest resolution and best data quality possible within the time available to complete the core logging. For the shorter sections (<30 cm), measuring points were individually selected so that a greater density of data points could be acquired, and cores <15 cm in length were not measured. Where cracks >1 cm were present, the interval around the crack was omitted, and the top 5 cm and bottom 5 cm of each core section was discarded to minimize the error associated with the endcaps.

Thermal conductivity

Thermal conductivity was measured with the TeKa TK04 system using the needle-probe method in full-space configuration for soft sediments (Von Herzen and Maxwell, 1959). The needle probe contains a heater wire and calibrated thermistor. It is assumed to be a perfect conductor because it is significantly more conductive than the sediments measured. Cores were measured at 4°–6°C in the refrigerated core repository at the MARUM–Center for Marine Environmental Sciences at the University of Bremen. Thermal conductivity of unsplit cores from Expedition 347 was measured by inserting the needle probe into the sediment through a small hole drilled into the core liner parallel to the working half/archive half surface (splitting surface) to ensure minimum disturbance to either split-core section. Generally, thermal conductivity (k) is calculated from the following:

$$k(t) = (q/4\pi) \times \{[\ln(t_2) - \ln(t_1)]/[T(t_2) - T(t_1)]\},$$

where

- T = temperature (K),
- q = heating power (W/m), and
- t_1, t_2 = time interval (normally 80 s duration) along the heating curve(s).

The optimal choice of t_1 and t_2 is difficult to determine; commonly, thermal conductivity is calculated from the maximum interval (t_1 and t_2) along the heating curve where $k(t)$ is constant. In the early stages of heating, the source temperature is affected by the contact resistance between the source and the full space, and in later stages it is affected by the finite length of the heating source (assumed infinite in theory). The special approximation method (SAM)

employed by the TK04 software is used to develop a best fit to the heating curve for all of the time intervals where

$$20 \leq t_1 \leq 40,$$

$$45 \leq t_2 \leq 80,$$

and

$$t_2 - t_1 > 25.$$

A good measurement results in a match of several hundred time intervals along the heating curve. The best solution (output thermal conductivity) is that which most closely corresponds to the theoretical curve. Numerous measuring cycles were automatically performed at each sampling location.

Thermal conductivity measurements were taken from one location within each core and sampled at a frequency of one per core, preferably from Section 2, where available, for selected holes at each site. If core quality was not appropriate, the nearest section to it was selected. Measurements were taken in soft sediments, into which the TK04 needles could be inserted without risk of damage.

The quality of thermal conductivity measurements was monitored as measurements were taken. Multiple measurements (up to 10 per thermal conductivity run) were taken at the selected depth within each core. Data quality was evaluated by the operator, with spurious or poor data owing to boundary effects and reflections (especially where there was not good contact between the core and the probe [due to cracking]) being removed prior to calculation of a mean thermal conductivity and standard deviation. Where possible, a minimum of four good quality measurements were chosen to calculate the mean thermal conductivity and a variance of less than $\pm 5\%$ was sought. Sometimes the SAM employed by the TK04 software could not calculate a best fit to the heating curve because of boundary effects or a lack of contact between needle and sediment.

Digital imaging

Digital linescan images of the split cores were obtained during the OSP using the Avaatech Superslit X-ray fluorescence (XRF) core scanner. The XRF scanner has an option for linescan camera and linear light source. The line scanner produces high-resolution color images and also outputs accurate color data in red-green-blue (RGB) and Commission Internationale d'Eclairage (CIE) "L" (lightness), "a" (green to red chromacity), and "b" (blue to yellow chromacity) units ($L^*a^*b^*$) because of individual charge-cou-

pled device (CCD) pixel calibration. The Linescan Program uses the Stemmer Common Vision Blox (CVB) platform to acquire and process color images.

The camera system contains a 3-CCD camera using 3×2048 pixels with beam-splitter and a manually controlled Pentax 50 mm lens. The image resolution is ~ 150 pixel/cm ($70 \mu\text{m}/\text{cm}$) in crosscore and downcore directions. With an exposure time of 5 ms, a scan speed of 125 mm/s was achieved. Added to this is initialization time and camera repositioning after a scan. The image coverage is ~ 13.5 cm crosscore and in the downcore direction a maximum of 153 cm.

Every split core was imaged with a color/gray chart beside it, and this scan is available as the original file. Three output files were generated for each core section: a high-resolution bitmap file (.BMP), a compressed image file (.JPEG) (see SLABCORESCAN in “[Supplementary material](#)”), and a numeric text file (.TXT). Numeric data are in RGB units. The linescan system was calibrated every 24 h with black and white calibration. All split cores were measured using aperture setting $f/5.6+$ (a fixed value between 5.6 and 8). Additional apertures were used when necessary but were always run in addition to the standard aperture used on all cores. Consistency of equipment settings was chosen over custom settings to ensure uniformity of the data set. Software features necessitated the length of line scan images at a couple of centimeters longer than the curated core length. Bitmap picture files were modified to match the length of the cores after the image was taken. Where a whole-round sample had been removed from the core, a foam placer was inserted in its place. For Expedition 347, blue pieces of foam labeled “MBio” were used to fill voids created by the large number of microbiology samples that were taken during the offshore phase of Expedition 347 (see “[Microbiology](#)”) from the microbiology holes (e.g., M0059C and M0060B). The operator verified that the full core section had been imaged during the scan before the data were accepted.

Diffuse color reflectance spectrophotometry

Working halves of all split cores were measured during the OSP at a 4 cm sampling interval using a Minolta spectrophotometer (model CM-2600d) installed on a Geotek split-core MSCL system. Badly disturbed core sections or core sections shorter than 5 cm were not measured. Core sections with significantly high fluid content were omitted because of the risk of sensor damage. On this integrated MSCL system, the spectrophotometer moves vertically, interlocked with the *P*-wave equipment. For Expedition 347, color reflectance measurements were carried out separately, with all other MSCL sensors

switched off. White calibration of the spectrophotometer was carried out once per day, and a calibration for zero was performed once per day on starting up the machine. Vertical adjustment of spectrophotometer and pusher adjustment to the reference point were performed before every run. The split calibration piece (stepped aluminum) for gamma density was used as the reference height of the spectrophotometer. Prior to measurement, the core surface was covered with clear plastic wrap to maintain a clean spectrometer window.

Spectrophotometric analysis produced three types of data:

- L^* , a^* , and b^* values, where L^* is a total reflectance index ranging from 0% to 100%, a^* is green (–) to red (+) chromaticity, and b^* is blue (–) to yellow (+) chromaticity;
- Munsell color values; and
- Intensity values for 31 contiguous 10 nm wide bands across the 400–700 nm interval of the visible light spectrum.

Measurement quality is affected by the degree and uniformity of sediment fill in the split liner, by cracks or other core disturbance, and by the smoothness of the clear plastic wrap over the core surface (e.g., no air bubbles). Comments for every section (e.g., cracks, holes and voids in sediment, and quality of the sediment surface) were appended to the spectrophotometer data to allow for better retrospective evaluation of data quality. When utilizing the spectrophotometric measurements, it is recommended that detailed examination of core photos/images and disturbance descriptions/tables be undertaken to filter out unreliable or spurious data.

P-wave velocity from discrete samples

P-wave velocity was derived from the traveltime of seismic waves passing through a sample of known thickness. *P*-wave velocity varies with the lithology, porosity, and bulk density of the material; the state of stress, such as lithostatic pressure; and the fabric or degree of fracturing. In marine sediments and rocks, *P*-velocity values are also controlled by the degree of consolidation and lithification, by fracturing, and by occurrence and abundance of free gas and gas hydrates. *P*-wave velocity is used together with density measurements to calculate acoustic impedance or reflection coefficients, which can be used to estimate the depth of reflectors observed in seismic profiles and to construct synthetic seismic profiles.

P-wave analyses were performed with a Geotek *P*-wave logger for discrete samples (PWL-D), which consists of a mechanical section containing the transducers (between which the sample to be mea-

sured is placed), an electronic panel, and a laptop. Acoustic coupling is through solid neoprene surfaces (pads on the transducers) and is improved by applying downward pressure on the sample between transducers and by wetting the neoprene with distilled water. A laser distance transducer measures the thickness of the sample. The PWL-D system can measure velocities on cubic or cylindrical, consolidated, semiconsolidated or lithified core specimens. Unconsolidated samples are not suitable for measurement with the PWL-D because they tend to crumble or squash when placed between the transducers. The system allows measurements to be taken in the x -, y -, and z - directions of the core to study P -wave velocity anisotropy. To know the orientation, the cubes taken were marked on the surface with an arrow pointing to the top of the core.

The basic velocity equation is

$$v = d/t,$$

where

d = distance traveled through the material (m) and
 t = traveltime (s).

The PWL-D was calibrated several times a day using a standard of known length and P -wave velocity provided by Geotek. At the start of each set of samples measured, a calibration check was performed using the same standard. To monitor instrument drift, the velocity of the calibration piece was also recorded at the end of each measuring session.

Time delays subtracted to correct traveltime are delays related to the latency of transducers and electronics (t_{delay}) and delays related to the peak detection procedure (t_{pulse}). Delays were determined during calibration with zero distance. For routine measurements on discrete samples with the PWL-D system, the equation for the velocity is

$$v_{\text{sample}} = (10000 \times d_{\text{sample}})/(TOT - PTO),$$

where

v_{sample} = velocity through sample (m/s),
 d_{sample} = measured thickness of the sample (mm),
 TOT = measured total traveltime (μs), and
 PTO = delay correction (μs).

A pulse is sent to the transmitter sensor, which generates an ultrasonic compressional pulse at ~230 kHz that propagates through the sample and is received by the receiver sensor. The received signal is processed through an analog to digital converter before appearing in the software display. The signal is digitized at a sampling frequency of 12.5 MHz.

In the software, a threshold detector determines the first positive or negative excursion on the received pulse and can be adjusted by the operator. The pulse timing is achieved by measuring the time to the first zero crossing after the threshold has been exceeded. In this way, the traveltime measured is approximately one-half of the wavelengths after the start of the pulse but is measured without any errors caused by signal amplitude. A delay can be used to define the point at which the software should start its threshold detection. The delay should be set before the start of the signal.

Sample quality strongly affects the ability to acquire P -wave velocity data. It was important during Expedition 347 to prepare the sample correctly to get good contact between the transducers. Preparation involved cutting the sample to ensure there were two flat, parallel surfaces to aid good acoustic coupling with the transducers, wetting the pads of the transducers, and applying downward pressure. P -wave velocity is also sensitive to temperature (Leroy, 1969) and increases with increasing temperature. Temperature was recorded during every measurement and was so uniform that no temperature corrections were applied.

P -wave velocity was measured on discrete samples taken from the working halves of split cores, at an average of one per section in semiconsolidated or consolidated sediments and adjacent to the MAD samples. Relatively shallow sections were typically not measured because of the lack of the requisite consolidation.

P -wave measurements were performed three times in each direction (x -, y -, and z -directions), and an average was calculated for each direction. The data files are in comma-separated value (CSV) format, containing a header with the core and sample identifier followed by measured data and calculated velocity. The waveform is recorded in two columns containing the time base and voltage changes.

Moisture and density

Moisture and density (MAD) properties (bulk density, dry density, grain density, water content, porosity, and void ratio) were derived from measurement of the wet and dry masses of core samples and their dry volumes. Discrete samples (~6 cm³) were acquired at an approximate resolution of one per core section from the working halves of split cores at vertically adjacent stratigraphic levels to the P -wave subsamples.

These wet samples were transferred into previously weighed 10 mL glass beakers and weighed to a precision of 0.001 g using an electronic balance to deter-

mine the wet mass (M_{wet}). Samples were next dried in a convection oven at $60^\circ \pm 5^\circ\text{C}$ for a period of 24 h followed by cooling to room temperature in a desiccator for at least 2 h. Dry sediments were successively weighed to determine dry mass (M_{dry}).

The volume of dried sample was immediately analyzed using a Quantachrome pentapycnometer (helium-displacement pycnometer) with a precision of 0.02 cm^3 . This equipment allowed the simultaneous analysis of four samples and one standard (calibration spheres). Volume measurements were repeated a maximum of five times or until the last three measurements exhibited $<0.01\%$ standard deviation for Site M0059, with a purge time of 1 min. After this, to speed up the pycnometer process and as no difference could be observed between using 3 and 5 measurements, volume measurements were only repeated 3 times with a purge time of 1 min for the following sites. Volume measurements were averaged per sample (V_{dry}). Calibration spheres were successively cycled between different pycnometer cells for each run to check for accuracy, instrument drift, and systematic error.

The mass of the evaporated water (M_{water}) is given by

$$M_{\text{water}} = M_{\text{wet}} - M_{\text{dry}}$$

The volume of pore water (V_{pw}) is given by

$$V_{\text{pw}} = M_{\text{pw}}/\rho_w$$

where

$$\begin{aligned} M_{\text{pw}} &= \text{mass of the pore water and} \\ \rho_w &= \text{pore water density (1.024 g/cm}^3\text{)}. \end{aligned}$$

Salt precipitated in sample pores during the drying process is included in M_{dry} and V_{dry} values, resulting in the following approximations:

- The mass of pore water (M_{pw}) is given by the mass of the evaporated water ($M_{\text{water}} = M_{\text{pw}}$);
- The mass of solids, including salt (M_{solid}), is given by the dried mass of the sample ($M_{\text{dry}} = M_{\text{solid}}$); and
- The volume of solids, including salt (V_{solid}), is given by the measured dry volume from the pycnometer ($V_{\text{dry}} = V_{\text{solid}}$).

The mass of the evaporated water (V_{wet}) is given by

$$V_{\text{wet}} = V_{\text{solid}} + V_{\text{pw}}$$

For all sediment samples, water content (w) is expressed as the ratio of the mass of pore water to the wet sediment (total) mass:

$$w = M_{\text{pw}}/M_{\text{wet}}$$

Wet bulk density (w), dry bulk density (d), sediment grain density (g), and porosity (ϕ) are calculated from the previous equations (density is given in g/cm^3):

$$w = M_{\text{wet}}/V_{\text{wet}}$$

$$d = M_{\text{solid}}/V_{\text{wet}}$$

$$g = M_{\text{solid}}/V_{\text{solid}}$$

and

$$\phi = V_{\text{pw}}/V_{\text{wet}}$$

Expedition 347 samples were selected from undisturbed intervals. However, it was not possible to ensure that all were completely uncontaminated by fluid introduced during the core collection, splitting, and sampling process.

Paleomagnetism

The main objectives of the OSP paleomagnetic work were to (1) establish a magnetic susceptibility profile at each site based on discrete samples of known volume and mass; (2) establish, if possible, site-specific paleomagnetic secular variation (PSV) profiles that could be compared for relative dating purposes to regional Holocene master curves based on multiple lake varve chronologies (Snowball et al., 2007) and a late glacial master curve (Lougheed, 2013; Lougheed, et al., in press); and (3) detect geomagnetic field excursions that took place during the latest glacial cycle (reviewed by Laj and Channel, 2007; Singer, 2014). Some background information about the parameters measured and the reason for establishing them is provided below.

Fundamental magnetic properties, magnetic susceptibility, and natural remanent magnetization

Depending on their composition, materials can display one or more of three fundamental responses to the application of an external magnetic field. The weakest response, which is inherent to all materials, is actually negative (i.e., the field induced in the sample has a polarity that opposes that of the applied field). This property is known as “diamagnetism” and is the only response exhibited by, for example, water, organic compounds, most plastics, and some minerals, such as pure quartz and calcite. Collectively, these are called “diamagnets.” A stronger, positive linear response (“paramagnetism”) is exhibited by minerals that are “paramagnetic,” and mineral examples include many members of the iron ox-

ide phase system (e.g., lepidocrocite), the iron sulfide phase system (e.g., pyrite and marcasite), ferromagnesian minerals (e.g., biotite and pyroxene), and iron carbonates (e.g., siderite). Another example of a paramagnet is the hydrated iron phosphate mineral vivianite, which is commonly found as an authigenic phase in organic-rich, reduced freshwater lake sediments.

Pure iron is “ferromagnetic,” and ferromagnetism is the strongest type of positive response to an applied magnetic field. Similar ionic ordering gives rise to “ferrimagnetism” and “antiferromagnetism,” which are important to paleomagnetism because of the capability of “ferromagnets” (e.g., pure iron) and “ferrimagnetic” and “canted anti-ferromagnets” to retain a memory of a magnetic field that they were once exposed to. This memory is called “magnetic remanence.” Natural minerals that behave as “ferrimagnets” at temperatures and pressures normally experienced close to the Earth’s surface include magnetite, titanomagnetite, maghemite, monoclinic pyrrhotite, and greigite.

Magnetic susceptibility is a parameter that defines how easily a material can be magnetized. Geologists routinely measure this parameter at room temperature and pressure, although temperature-dependent measurements may detect changes in crystallographic structure, which causes magnetic transitions and can be diagnostic of specific minerals (e.g., the Verwey transition in magnetite). Magnetic susceptibility is a dimensionless ratio between the intensity of magnetization (M) induced in a sample by an externally applied field (H) of known intensity (i.e., M/H); this ratio can span many orders of magnitude, both positive and negative. If the magnetic susceptibility is expressed on a volumetric basis the volume magnetic susceptibility (κ) is obtained. Magnetic susceptibility may also be expressed per unit mass, as χ , and the SI units are cubic meters per kilogram (m^3/kg).

Mineral ferrimagnets have susceptibilities that are many orders of magnitude higher than paramagnets and diamagnets. Thus, even if naturally occurring ferrimagnetic minerals account for only a few parts per thousand of a sample, they can dominate the magnetic susceptibility and determine the ability of it to acquire and carry a natural remanent magnetization (NRM).

In natural sediments, NRM is commonly acquired in two fundamental ways. One way is through the acquisition of a (post-)depositional remanent magnetization (pDRM). pDRMs require that mineral grains fall out of a calm fluid suspension and that the Earth’s ambient magnetic field exerts a torque on them and they align along the direction of the field. They are subsequently buried by nonmagnetic grains

and are locked into position close to or just below the sediment/water interface and at a depth that can be dependent on the degree of consolidation and bioturbation. pDRMs are frequently carried by primary ferrimagnetic and antiferromagnetic iron oxides that originate from continental erosion. A second way is through the precipitation of secondary authigenic and diagenetic minerals that are capable of acquiring magnetic remanence when the crystals grow and pass through the superparamagnetic to single-domain grain size threshold. This threshold is mineral specific but is often exceeded in the submicrometer grain size window.

A large range of lithologies was encountered during the offshore phase of the expedition. Processes that lead to the production and transport of clastic magnetic minerals to sedimentary basins in the Baltic Sea include the glacial erosion of the Fennoscandian Shield, which is a varied provenance consisting of predominantly igneous and metamorphic rocks, postglacial weathering, pedogenesis, and isostatic land uplift (the present rate at Sites M0061 and M0062 is ~ 1 cm/y). Primary productivity and the subsequent degradation of organic matter can cause the reductive dissolution of clastic iron oxides and the diagenesis/authigenesis of iron sulfides, and these processes can decrease the concentration of magnetic minerals or enhance them, respectively. For example, Sohlenius (1996) shows that authigenic greigite formed through the downward diffusion of sulfide from relatively organic rich sediments deposited during the Littorina Sea stage of the Baltic Sea into underlying clays that characterize the Anclyus Lake (Sohlenius, 1996). Reinholdsson et al. (2013) subsequently discovered that laminated sapropels, which formed during the Littorina Sea stage, were magnetically enhanced because of the presence of magnetosomal greigite, which are single-domain grains produced by magnetotactic bacteria (MTB) in the water column, just under the anoxic–oxic transition zone (AOTZ).

Paleomagnetic sampling and measurements

OSP samples for magnetic susceptibility and measurement of the direction and strength of the NRM were obtained using standard plastic IODP paleomagnetic cubic boxes (external dimensions of $2\text{ cm} \times 2\text{ cm} \times 2\text{ cm}$ and an internal volume of 7.6 cm^3). At Site M0066, additional minicubes were also utilized, measuring $1\text{ cm} \times 1\text{ cm} \times 1\text{ cm}$. The sampling interval (resolution) was restricted by the OSP duration and other sampling programs. With the exception of Sites M0059, M0060, and M0063, the samples were taken from the sections that contributed to the com-

posite splices for each site and at intervals of ~0.5 m, with small adjustments made for voids and sediment disturbances. At Site M0059 samples were taken from all core sections that included a sampling point. Samples within each core section were oriented with respect to each other. At Site M0060, there was only one paleoenvironmental hole drilled and so samples were taken from these cores. At Site M0063, the formation of a composite splice was not possible because of the expanding nature of the gaseous sediments and lack of significant MSCL tie points (see “**Stratigraphic correlation**”). Therefore, the OSP sampling scheme was targeted toward the holes where the majority of shipboard and post-cruise samples were taken to better aid later research. Additional higher resolution sampling, up to every 5 cm, was performed in areas of specific interest.

Magnetic susceptibility measurements and wet density

Magnetic susceptibility was measured using a KLY 2 (AGICO) Kappabridge that operates at a frequency of 920 Hz and a magnetic induction of 0.4 mT (equivalent to a field intensity of 300 A/m), with a noise level of 2×10^{-10} m³/kg. The Kappabridge was calibrated using a standard with a bulk susceptibility of 1165×10^{-6} SI, and this procedure was repeated every morning before measurements began and after approximately every 50 samples.

The wet weight of the samples was established with a DISPE TP-200 electronic balance with a precision of 1×10^{-5} kg. The weight of the paleomagnetic sample cubes and their diamagnetic contribution to magnetic susceptibility was established by measuring five empty cubes. The sample measurements were then corrected according to the respective averages. The volumetric samples and masses were used to make an additional estimate of bulk density that could be cross-checked with the continuous MSCL data.

NRM measurements and alternating field demagnetization

The NRM direction and intensity of discrete samples were measured using the 2G-Enterprises horizontal pass-through super-conducting rock magnetometer (SRM 755–4000) that was made available for the OSP by the University of Bremen. The standard IODP sample cubes used during the OSP were measured in batches of eight or less using the pass-through conveyor.

A series of at least 16 pilot samples was selected from each site to cover the full range of magnetic susceptibility. After measurement of NRM, the samples were sequentially demagnetized by alternating fields (AF)

at the following steps: 5, 10, 15, 20, 30, 40, 50, 60, and 80 mT. The magnetic remanence measured between each step. Orthogonal plots and visualization of the demagnetization spectra were produced in PuffinPlot (Lurcock and Wilson, 2012).

Microbiology

All sampling for microbiology was completed during the offshore phase of Expedition 347. At four sites (M0059, M0060, M0063, and M0065), at least one separate hole was drilled to sample for microbiology, biogeochemistry, geochemistry, and detailed interstitial water chemistry. Cores from these holes were subsampled in a specialized microbiology containerized laboratory within 1–2 h of recovery onto the deck. Only cores taken by piston corer were used for microbiology, as other types of coring retrieved sediment were too disturbed and contaminated with drilling fluid.

As soon as a core arrived on deck, it was curated into 1.5 m sections (Sections 1 and 2 with a short Section 3 if recovery was >91%). Sediment samples were immediately taken from the freshly exposed lower end of Section 1 using cut-off syringes; two 5 cm³ syringe samples were taken from every core for methane analyses conducted. Three 5 cm³ syringe samples were taken for PFC contamination tests from all cores shallower than 30 mbsf and every second core deeper than 30 mbsf. The positions of the three PFC samples at the exposed core end were (A) in the center (“interior”), (B) halfway between the center and the periphery (“halfway”), and (C) at the periphery, against the inner wall of the core liner (“exterior”). Three 5 cm³ samples were also taken, on a limited number of occasions, with sterilized cut-off syringes in the same A-B-C pattern for later DNA analyses of potentially contaminating microorganisms.

The core sections were then taken immediately to core curation for labeling and entering into the DIS. From there, the sections were run through the Fast-track MSCL without waiting for equilibration to room temperature (as per the usual procedure). As soon as logging was complete (<25 min), each section was transferred to the core reception container where subsampling for microbiology and biogeochemistry took place.

Subsampling was undertaken using cut-off syringes, scooping out using a sterile spatula, or by taking whole-round core segments, predominantly of 5 or 10 cm lengths. The short core segments remaining following microbiology sampling from this hole were capped. If they were longer than 15 cm, they were allowed to equilibrate and run through the

normal slow-track MSCL. All remaining core was then stored together with the other core sections in the refrigerated container at +4°C.

Perfluorocarbon contamination tracer

PFC tracer was injected into the stream of drilling fluid during the coring of each microbiology hole to serve as a tracer for sediment core contamination with microbes from drilling fluid. Similar methodologies have been applied during previous ocean drilling expeditions (Smith et al., 2000a, 2000b; Lever, 2006). The PFC tracer used was perfluoromethylcyclohexane (C₇F₁₄) (Smith et al., 2000b). The PFC was pumped undiluted directly into the main stream of drilling fluid (seawater or drilling mud) at a rate of 0.1 mL/min (0.18 g/min) using a high-performance liquid chromatography (HPLC) pump (Alltech Model 301). The target concentration of PFC in the drilling fluid was 1 mg PFC/L, which is the maximum solubility of perfluoromethylcyclohexane in water (Smith et al., 2000b).

The three 5 cm³ syringe samples taken for PFC analyses from the freshly exposed lower end of Section 1 were immediately extruded into 20 mL headspace vials, prefilled with 5 mL Milli-Q water, and capped with a butyl rubber septum and an aluminum crimp seal. The vials were kept upside down at +4°C until later analysis in the shore-based laboratory within 1–2 weeks. A 10 mL liquid sample was also taken in a headspace vial for PFC analysis of seawater (D) collected from the top end of each whole piston core immediately after the core arrived on the cutting table (“liner fluid”). Finally, a sample was also taken of the drilling fluid (E) being used directly at the drill derrick, which was immediately subsampled into a 20 mL headspace vial. “D” and “E” provided controls for the detailed PFC analysis.

Analyses of PFC samples were performed at the Center for Geomicrobiology at Aarhus University in Denmark. All measurements were carried out using a gas chromatograph with an electron capture detector (Agilent 7820A GC), following the technical specifications described previously (Smith et al., 2000b) and subsequently used during other ocean drilling expeditions (e.g., Smith et al., 2000a; Lever et al., 2006). However, to ensure full PFC recovery from sediments, all headspace vials containing samples were preincubated for ≥2 h at 80°C. During this time, headspace vials were rotated horizontally using a rotisserie in a hybridization oven (Problot 12 hybridization system, Labnet International, USA). Preliminary tests conducted during IODP Expedition 337 and at the Center for Geomicrobiology at Aarhus University had shown this modified preincubation

technique to be necessary for full PFC extraction into headspace (M.A. Lever, pers. comm., 2013).

Microbiology sampling

Sites M0059, M0060, and M0065 had shallow water depths of <100 m. Because of the relatively shallow water and the time required for processing the samples, it was necessary to moderate the pace of piston coring in the uppermost part of the hole where sampling density was greatest. This worked effectively and helped minimize time between the core arriving on deck and being sampled. Between 20 and 30 mbsf, the microbiology sampling became faster as fewer samples were requested, and the normal rate of coring was resumed.

To manage the large and complex sampling program, a detailed sampling scheme was produced for each new site. This scheme was not only available in tabular form but was also prepared graphically for each core run with a corresponding estimated depth interval. As coring proceeded and the core run lengths were modified to account for any sediment expansion, the real depths sampled increasingly deviated from the predicted depths, yet the depth indication remained instructive as a guideline for execution of the sampling program. The graphical sampling scheme included two pages for each core number, one page for the initial syringe sampling scheme (e.g., Fig. F19), and one page for the cutting of whole-round cores (WRCs; e.g., Fig. F20). To improve the overview and avoid mistakes, an easily recognizable color coding scheme was used for each individual sample request and their sample requirements (Fig. F21). The sampling schematics were displayed where cutting and sample distribution took place and also in the cooled microbiology container where further sample preparation and bagging was done.

The sections from the microbiology hole were taken to the core reception container immediately after MSCL logging for further sampling and data entry of samples. All persons handling the samples wore nitrile gloves to minimize contamination of microbiology or biomarker samples. The endcaps on core sections were removed, and subsamples were taken using cut-off sterile syringes from the exposed core ends according to the sampling scheme. The condition of each section was assessed in case there were disturbed parts of the core, which were then avoided when sampling. This assessment was also guided by previous analysis of the occurrence of cracks, bubbles, or free liquid surrounding the core in the paleoenvironment cores recovered from the hole drilled immediately prior to the microbiological hole. These

observations were useful for the later evaluation of potential contamination of core samples. Syringe samples were taken from both the bottom of Section 1 and the top and bottom of Section 2. No samples were taken from the top of Section 1, which had been exposed to drilling fluid, or from the short (~30 cm) Section 3/core catcher material.

After initial syringe sampling, core sections were cut into consecutive short whole-round segments with a hacksaw according to the sampling plan. A black line was first made with a marker pen around the core liner where the cut was to be made, using as a guide a 5 cm short piece of split core liner that could be clipped around the core section being worked on. During sawing, care was taken to cut only the liner where possible, while rotating the core to minimize contamination of the central part through smearing by the hacksaw blade. A sterilized wire was then used to cut the WRCs, which were subsequently sealed with standard endcaps. Concurrent with the subsampling, the data for each sample was entered into the DIS.

Immediately after sampling in the core reception container, the syringe samples and WRCs were carried to the microbiology container, where further treatment was carried out. The microbiology container was kept at +12°C to avoid the ambient temperature rising to a level that could adversely affect heat-sensitive cells. The in situ temperature of the cored sediments varied from the annual mean water temperature of approximately +9°C at the south-western sites to about +5°C in the Landsort Deep. The ambient air temperatures ranged mostly from +4°C to about +12°C and thus largely resembled the in situ temperature of cored sediments.

Counting of microbial cells

Total counts of microbial cells were carried out as the only offshore standard IODP microbiology analysis. Further counts were done during the onshore sampling party. Remaining counts will be done after the OSP at the Kochi Core Repository (Japan) and Cardiff University (Wales, UK); however, these will be conducted as postcruise research.

Direct counts were carried out on fluorescently labeled cells using three different methods: (1) acridine orange direct counts and fluorescence microscopy, (2) SYBR green DNA stain and flow cytometry, or (3) SYBR green DNA stain and fluorescence microscopy.

Acridine orange direct counts (AODC)

Samples were taken with a sterile 5 cm³ cut-off plastic syringe from the core end. A 1 cm³ plug was ex-

truded into a sterile serum vial containing 9 mL of 2% (v/v) filter-sterilized (0.2 µm) formaldehyde in 2% (w/v) NaCl. The vial was capped, crimped, and shaken vigorously using a vortex mixer to disperse the sediment plug.

Numbers of total prokaryotic cells and dividing or divided cells were determined using acridine orange as a fluorochrome dye with epifluorescence microscopy (Fry, 1988). Fixed samples were mixed thoroughly, and a 5–20 µL subsample was added to 10 mL of 2% (v/v) filter-sterilized (0.1 µm) formaldehyde in 2% NaCl. Acridine orange (50 µL of a 1 g/L filter-sterilized [0.1 µM] stock solution) was added, and the sample was incubated for 3 min. Stained cells and sediment were filtered down on a 0.2 µm black polycarbonate membrane (Osmonics, USA). Excess dye was flushed from the membrane by rinsing with a further 10 mL aliquot of 2% (v/v) filter-sterilized formaldehyde in 2% NaCl, and the membrane was mounted for microscopic analysis in a minimum of paraffin oil under a coverslip. Mounted membranes were viewed under incident illumination with an Olympus BX53 microscope fitted with a 100 W mercury vapor lamp, a wide-band interference filter set for blue excitation, a 100× (numerical aperture = 1.3) Plan Neofluar objective lens, and 10× oculars. Prokaryote-shaped fluorescing objects were enumerated, with the numbers of cells on particles doubled in the final calculation to account for masking by sediment grains.

The detection limit for prokaryotic cells by this procedure is ~1 × 10⁵ cells/cm³ (Cragg, 1994).

The percentage of cells involved in division has been suggested as an indication of growth, although the assessment of dividing cells has never had a standardized approach in the literature. Dividing cells were defined operationally as those having clear invagination. A divided cell is operationally defined as a visually separated pair of cells of identical morphology. The percentage of cells involved in division is then calculated as follows:

$$\text{Percentage of dividing cells} = \frac{[\text{number of dividing cells} + 2 (\text{number of divided cell pairs}) \times 100]}{\text{total number of prokaryotic cells}}$$

Cell counts by flow cytometry

A 1 cm³ sample of sediment was taken from every 1.5 m core section by a cut-off syringe with sterilized tip and immediately mixed with 9 mL of fixation solution (4% formaldehyde in 2.5% NaCl). This 10% slurry was dispersed by vortex mixer and then stored at +4°C. A 40 µL sample of the slurry was diluted 1250 times in pH 8.0 tris-EDTA (TE) buffer. The diluted slurry was sonicated for 10 min to separate sed-

iment particles and cells. The sample was then filtered through a 40 μm cell strainer (BD Falcon) to remove large particles. An aliquot of 2 μL of SYBR green I (Invitrogen) fluorescent stain was mixed with 50 μL of the diluted sample and incubated at room temperature for 10 min. A total of 950 μL of TE buffer was added to the stained sample. The final sample volume was thus 1002 μL , with a total final dilution of 1:25,000.

For cell counting on board the *Greatship Manisha* we used an Accuri C6 flow cytometer that is designed for fieldwork and may be operated on a research vessel. We customized the excitation filters of the Accuri C6 to 530/30 and 530/43 nm to detect SYBR green. A formaldehyde-fixed *Escherichia coli* suspension was used as a standard to calibrate the instrument. A 100 μL aliquot of each sample was used to analyze cell abundance. Because of ship motion, the volumetric pump system of the Accuri C6 was not accurate. We therefore estimated the sample volume by two independent methods: (1) by calculating the volume based on the *E. coli* calibration sample and (2) by calculating the volume based on a known number of added fluorescent beads that passed through the flow cell together with the sample.

Microscopic counts using SYBR green

The flow-cytometric counts were compared with direct cell counts of the same samples in the fluorescence microscope. Membrane-based counting was carried out at JAMSTEC in Kochi, Japan.

The slurry was first diluted with 2.5% NaCl and sonicated for 40 min using an ultrasonic homogenizer (Bioruptor UCW-310, Cosmo Bio Co., Tokyo, Japan). The sample was treated with 1% HF for 20 min at room temperature after sonication. A 50 μL aliquot from the HF treated sample was filtered through a 0.22 μm pore size black polycarbonate membrane. About 5 mL of filtered (0.22 μm) 2.5% NaCl solution was placed into the filter tower prior to the addition of the supernatant to ensure even distribution of cells on the filter. The membrane was then washed with 5 mL of TE buffer, and roughly 2×10^8 fluorescent microsphere beads (Fluoresbrite Bright Blue Carboxylate Microsphere [BB beads], 0.5 μm , Polysciences, PA, USA) were added for use in focus adjustment (Morono et al., 2009). A quarter of the membrane was cut and stained with SYBR green at room temperature in the dark for 10 min followed by washing with 50 mM tris-EDTA (TE) buffer. The membrane was sealed on a glass slide for microscopic cell counting. Microscopic fluorescence image acquisition (at 525/36 nm [center wavelength/bandwidth] and 605/52 nm \times 490 nm excitation) was performed automatically using a fluorescence microscope sys-

tem equipped with an automatic slide shifter (Morono and Inagaki, 2010). The resulting images were analyzed using the macro of Metamorph software (Molecular Devices, Sunnyvale, CA, USA) to discriminatively enumerate microbial cells on the membrane.

Onshore microbiology analyses

Apart from the total cell counts, all other analyses of the microbiology samples were conducted onshore as postcruise research. To give an overview of the large microbiological and biogeochemical research program on this expedition, we provide the following overview of samples. Requests are arranged according to type of analysis.

Individual samples were treated differently on board the ship. Many were kept at -80°C and transferred as frozen samples to the requesting laboratories. Some frozen syringe samples that depended on having intact cells upon thawing were frozen on board the ship in a Cells Alive System (CAS) freezer (cas-fresh.trustpass.alibaba.com) provided by JAMSTEC. The CAS freezer exposes the samples to a high-frequency alternating magnetic field that allows the sample to be cooled to -10°C without freezing (Iwasaka et al., 2011). When the magnetic field is switched off, the samples rapidly freeze without formation of destructive ice crystals. Samples were subsequently transferred to -80°C storage.

Samples containing live bacteria for later experiments were kept at $+4^\circ\text{C}$ in the ESO refrigerated container until they could be transferred to onshore laboratories. Most of those samples were sensitive to oxygen and needed to be kept in an anoxic atmosphere. They were therefore placed in gas-tight plastic bags and flushed with di-nitrogen gas before the bags were sealed with a heat sealer. The plastic bags available as supplied by ESO were made from multilaminated aluminum tube foil consisting of orthophthalaldehyde/polyethylene/aluminum/polyethylene layers with thicknesses of 15/15/12/75 μm (Gruber-Folien GmbH & Co, Straubing, Germany). Other varieties of gas-tight bags were supplied by individual laboratories requesting samples. Some bags were also supplied with an oxygen scrubber (Oxoid AnaeroGen) which develops CO_2 , but no H_2 , when taking up O_2 from the air.

Because of the nature of mission-specific platforms, laboratory space was not available to undertake experiments with live microorganisms offshore. To avoid deterioration of these samples due to prolonged storage on board the ship, the samples were offloaded from the vessel and sent to the respective laboratories as soon as possible after each microbiol-

ogy hole had been cored. For further information on this process, see the “Operations” section in each site chapter. Frozen microbiology samples were offloaded halfway through the expedition during a port call to Nynäshamn on the Swedish Baltic Sea coast and at the end of the Expedition in Kiel, Germany. Distribution of both cooled and frozen samples to the requesting laboratories was organized jointly by ESO and the Center for Geomicrobiology at Aarhus University.

Samples taken for onshore research encompassed the following areas:

- Total cell enumeration;
- Phylogenetic and functional genetic diversity;
 - Extraction of DNA for metagenomic analysis, functional genes of predominant metabolism, genes diagnostic of low-energy subsistence, and metagenomic data to support single-cell genomes;
 - Intracellular vs. extracellular DNA extraction to distinguish living vs. ancient DNA, as well as real-time polymerase chain reaction (qPCR) of marker genes of the two DNA pools, including 16S rRNA genes of bacteria and archaea and 18S rRNA genes of animals and plants;
 - Bacterial and archaeal 16S rRNA and eukaryotic 18S rRNA genes, as well as quantification of specific bacterial groups (including JS1) using qPCR;
 - Sorting of single cells, amplification and sequencing of single-cell genomes; focus on archaea; qPCR of functional genes; and catalyzed reporter deposition–fluorescence in situ hybridization (CARD-FISH) of specific groups;
 - Metatranscriptomics and identification of active microbial communities by RNA, as well as focus on S and Fe metabolism;
 - Cultivation of fermenters and iron/manganese/sulfate reducers, qPCR of functional genes (*dsr*, *apr*, *mcrA*, and *cbbl*) and of 16S rRNA genes of specific groups (including JS1 and Chloroflexi, Geobacteraceae, Archaea, and Bacteria), and CARD-FISH of Bacteria and Archaea; and
 - Endospores of thermophilic bacteria, quantification by most probable number (MPN) technique, and cultivation of eukaryotic spores.
- Virus;
 - Viral abundance, viral diversity by PCR/pulsed-field gel electrophoresis (PFGE) or by metagenomics, and viral production/lysogeny; and
 - Prophages in bacterial isolates and potential viral production in sediment by ³H-thymidine incorporation.
- Microbial activity in live samples;
 - Sulfate reduction rate experiments using ³⁵SO₄²⁻, modeling of rates, and calculation of cell-specific rates;
 - ¹⁴C-tracer experiments with methane oxidation, acetogenesis, and methanogenesis from diverse substrates; cultivation and DNA extraction; and stable isotope probing (SIP); and
 - Combined analyses of microbial activity and diversity with focus on sapropels and varved clays.
- Methanogenic degradation of complex organic molecules; cultivation; and SIP and δ¹³C isotope signatures;
- Biomarkers of microbial activity;
 - Analyses of living microbial biomass, microbial necromass, and bacterial endospores from bacterial signature molecules (total amino acids, D/L-amino acids, muramic acid, and dipicolinic acid); and intact polar lipids.
- Microbial substrates; and
 - Analyses of low molecular weight organic acids (volatile fatty acids [VFA]).
- Contamination tests;
 - Measurement of PFC contamination tracer at sediment depths used for microbiology and analyses done in Aarhus and results distributed to laboratories receiving microbiology samples.

Stratigraphic correlation

The objectives of Expedition 347 include examination of the sedimentary record at high resolution. Thus, recovery of a stratigraphically complete/composite geological record is important. Stratigraphic correlation consisted of the following:

1. Ensuring the maximum core recovery for each site by monitoring core overlap and identifying recovery gaps in each hole that must be targeted in an adjacent hole,
2. Seismic-core (sedimentary facies) correlation, and
3. Generating composite depth scales and splice records for each site to aid postcruise sampling at the OSP and postcruise research.

Ensuring optimal core recovery

Core recovery from a single hole is insufficient to generate a complete geological record because even with nominal 100% core recovery there are recovery gaps between adjacent cores. To obtain a complete sedimentary record, multiple adjacent holes were cored, offset in depth by 0.5–1.5 m between cores

from different holes. The continuity of recovery was assessed by generating composite sections that aligned prominent features in physical property data from adjacent holes. With the data gained from the Fast-track MSCL (see “[Physical properties](#)”), it was possible to adjust the coring strategy before moving to a new hole. This ensured that intervals missing in previous cores could be recovered from an adjacent hole to optimize recovery, using an offset coring strategy with the offset amount advised by the stratigraphic correlators.

Seismic-core correlation

Correlation between seismic profiles and cores utilized a number of different aspects:

- Measured acoustic/sound velocity vs. sediment type,
- Acquired depth and stratigraphic observations tested by comparison with major core surfaces visible as peaks in the geophysical data,
- Downhole logs (mainly total gamma ray and velocity) (see “[Downhole logging](#)”), and
- MSCL logs (density and magnetic susceptibility) (see “[Physical properties](#)”).

Data integration required interpretation of sedimentary units and then correlation to observed physical property boundaries.

MSCL data provide indicators of lithologic variation. Bulk density in water-saturated sediments is related to porosity and is partially controlled by grain size. Acoustic velocity is controlled by porosity and density, and magnetic susceptibility may reflect changes in lithology—for example, the proportion of organic/biogenic components relative to lithogenic components. Downhole logging data (see “[Downhole logging](#)”) proved useful in filling core gaps due to limited recovery in unconsolidated sandy intervals or where spot-coring strategy was necessary.

Composite

Core depths are recorded in meters below seafloor from the upper part of the first core in each hole. Consecutive depth measurements were determined by the length of each core run. To align similar features, which record physical (geological) properties between different holes (or even different sites), MSCL physical property measurements were correlated to create a composite depth (mcd) scale. This was achieved by loading the MSCL data files from the Expedition DIS into the stratigraphic correlation software (Correlator v1.693; developed at Lamont-Doherty Earth Observatory) and shifting cores relative to each other using prominent signals as tie

points. During this step, the total length on the meters composite depth scale was typically longer than the original meters below seafloor scale. With Correlator software, data sets from adjacent holes could be correlated simultaneously. A tie point, which gives the preferred correlation, is selected between data from different cores (e.g., from the first core in the first hole drilled and a core in a second hole). All the data from the second hole (that will be correlated with the chosen core) below the correlation point are vertically shifted to align the tie points between the holes. After choosing an appropriate tie point and adjusting the depths, the shifted section becomes the next “reference” section and a tie is made to a core from the first hole. Working downhole in an iterative fashion, each core is vertically shifted. Where there is no overlap, consecutive cores are appended. The tie points are recorded in an output (“affine”) table in units of meters composite depth. Confidence of correlation/composite was estimated for each tie point by the Stratigraphic Correlator using a value/number from 1 to 4:

- 1 = poor.
- 2 = fair.
- 3 = relatively good.
- 4 = good.

Fast-track MSCL measurements run immediately on cold cores at low resolution provided essential information on correlating the microbiology holes with the paleoenvironmental holes, as most of the cores/sections were later subsampled (whole rounds) for microbiology studies prior to being run through the normal MSCL slow track, reducing the number and length of core sections for detailed correlation and splicing.

Splicing

The next step in the stratigraphic correlation workflow was splicing. Splice records were generated by selecting sections from adjacent holes to avoid core gaps or disturbed sediment, resulting in a continuous (single) composite record. The splice is typically ~10%–15% longer relative to the original raw data, mainly because of expansion of sediment cores and the linear transformation of the composited features. The splice table defines tie points between core sections in meters composite depth. Confidence of splicing was also estimated using values from 1 to 4:

- 1 = poor.
- 2 = fair.
- 3 = relatively good.
- 4 = good.

The splicing formed the basis for onshore sediment sampling for postcruise research.

Downhole logging

Offshore downhole logging operations for IODP Expedition 347 were provided by Weatherford Wireline Service and managed by the EPC. The EPC is primarily responsible for the planning, acquisition, QA/QC, and science support related to petrophysical measurements on MSPs. Petrophysical data collection in relation to this consortium includes downhole measurements (i.e., borehole logging) and physical properties (e.g., magnetic susceptibility, acoustic properties, resistivity, and density) measured on cores (continuous and discrete; see “**Physical properties**”).

The set of downhole geophysical instruments utilized during Expedition 347 was chosen based on the scientific objectives, the coring technique, and the anticipated borehole conditions at the six sites.

Weatherford’s Compact logging tools were used (Table T4). The suite of downhole geophysical methods was chosen to obtain high-resolution electrical images of the borehole wall, measure borehole size, and measure or derive petrophysical or geochemical properties of the formations such as porosity, electrical resistivity, acoustic velocity, and natural gamma radiation. No nuclear tools were deployed during Expedition 347.

The Weatherford Compact suite comprised the following tools:

- The gamma ray tool (MCG) that measures the natural gamma radiation.
- The spectral gamma ray tool (SGS), which allows for the identification of individual elements that emit gamma rays (e.g., potassium, uranium, and thorium).
- The sonic sonde (MSS) that measures formation compressional slowness (inverse velocity).
- The array induction tool (MAI), which measures electrical conductivity of the formation. The output of this tool comprises three logs of induction electrical conductivity at shallow, medium, and deep investigation depths.
- The microimager (CMI), which is a memory capable resistivity microimaging tool. The eight arms in two planes of the CMI provide four independent radii measurements, which can be used to record borehole size and identify near-borehole stress regimes.

Operations

The logging team consisted of one engineer and one operator from Weatherford, supervised and assisted by the Petrophysics Staff Scientist.

A total of nine boreholes (Holes M0059B, M0059E, M0060B, M0062D, M0063A, M0064A, M0064D, M0065A, and M0065C) were prepared for downhole logging measurements. Measurements were performed in open borehole conditions (no casing). Despite challenging borehole conditions (nonconsolidated formations, risk of collapse, etc.), the recovery and overall quality of the downhole logging data is good. The gamma ray tool was used at the top of every tool string as a communication tool and for correlation between different runs. The induction tool was usually run first, followed by the other tool strings. The choice of tool strings was based on borehole conditions and drilled depth, and because of borehole conditions, it was not possible to log with all tools in every borehole (Table T5).

Each tool was logged on a tool string with the MCG always on top. A logging run commenced with zeroing the tool to a fixed point (drillers zero) corresponding to the top of the drill pipe. Each logging run was recorded and stored digitally. During acquisition, data flow was monitored for quality and security in real time using tool-specific acquisition boxes (Weatherford Well Manager Software). Tools were raised at speeds that ranged from a minimum of 5 m/min to a maximum of 10 m/min depending on the tool string used and the resolution chosen. Recordings were taken both downhole and uphole. Because of the real-time data display, it was possible to stop uphole recovery once the drill pipe was entered. At the end of logging, the Well Manager Software was used for visualization, QA/QC, processing, interpretation, and plotting of the data. Only uphole logs were used to process data.

Logging tool descriptions and acquisition parameters

Technical schemes on individual tools are shown in Figure F22. Additional information can be found on the Weatherford Web site (www.weatherford.com). Detailed information on their geological applications is available in Schlumberger (1989), Serra (1984, 1986) and Rider (2002).

Natural gamma probe

The MCG tool is a sensitive gamma ray detector consisting of a scintillation counter and a photomultiplier. When gamma rays pass through the sodium iodide crystal they cause a flash. These flashes are collected by the photomultiplier and stored in the attached condenser over a set period of time. The energy accumulated during this time is the detector value at that depth. The MCG tool was calibrated to API gamma ray units (gAPI), a unit defined by the American Petroleum Institute for gamma ray log

measurements. The vertical resolution of the MCG tool is 305 mm. The downhole measurement interval was 0.1 m as standard and 0.025 m for high resolution.

Spectral natural gamma probe

Unlike other instruments that record total gamma ray emissions, the SGS tool allows identification of certain individual elements that emit gamma rays. Naturally occurring radioactive elements such as K, U, and Th emit gamma rays with a characteristic energy. K decays into two stable isotopes (Ar and Ca), and a characteristic energy of 1.46 MeV is released. U and Th decay into unstable daughter elements that produce characteristic energy at 1.76 and 2.62 MeV, respectively.

The most prominent gamma rays in the U series originate from decay of ^{214}Bi and in the Th series from decay of ^{208}Tl . It is thus possible to compute the quantity (concentration) of parent ^{238}U and ^{232}Th in the decay series by counting gamma rays from ^{214}Bi and ^{208}Tl , respectively. The SGS detector for gamma rays is a sodium iodide (NaI) scintillation crystal optically coupled to a photomultiplier. The instrument was master-calibrated by the manufacturer prior to the expedition. As the probe moves up the borehole, gamma rays are sorted according to their emitted energy spectrum and the number of counts in each of the three preselected energy intervals is recorded. These intervals are centered on the peak values of ^{40}K , ^{214}Bi , and ^{208}Tl . Tool output comprises Th and U in ppm and K in percent of total gamma ray counts in API. The vertical resolution of the used tool is ~305 mm. The downhole measurement interval was 0.1 m standard or 0.025 m for high resolution.

Induction resistivity probe

The MAI tool measures electrical conductivity of the geological formation. Variations in electrical conductivity correspond primarily to variations in lithology (composition and texture), formation porosity, saturation, and interstitial fluid properties (salinity). An oscillator sends an alternating current of constant amplitude and frequency through an emitting coil. This current generates an alternating electromagnetic field that induces Foucault currents in the formation. These Foucault currents are proportional to the formation conductivity and generate their own electromagnetic fields. When passing through a receiving coil (solenoid), these secondary magnetic fields induce electromotive forces that are proportional to the flow running through the coil. The output of the MAI tool comprises three conductivity logs at varying intervals of investigation: shallow,

medium, and deep induction (ranging from 0.3 to 1.2 m). Measured conductivity can then be converted into electrical resistivity. The MAI tool has a vertical resolution of 0.610 m. The downhole measurement interval was 0.1 m standard and 0.025 m for high resolution.

Full waveform sonic probe

The MSS tool measures formation compressional slowness (inverse velocity) and when bulk density and elastic properties are known (from core measurements) an estimate of porosity can be derived from sonic measurements.

This downhole instrument is composed of an acoustic transmitter and receivers. The transmitter emits an acoustic signal that propagates through the borehole fluid to the rock or sediment interface, where some of the energy is critically refracted along the borehole wall. As a result of wavefront spreading (Huygens principle), some of the refracted energy is transmitted back into the borehole adjacent to a receiver. Each receiver picks up the signal, amplifies it, and digitizes it. Recorded waveforms are then examined, and compressional (*P*-) wave arrival times are manually or automatically selected (picked). Arrival times are the transit times of the acoustic energy, and by measuring the acoustic transit time, knowing the distance between the two receivers, the velocity of the fluid, and the borehole diameter, the sonic velocity of the rock or sediment can be calculated. Consequently, the interval velocity value is calculated at each sampling point. The MSS tool measures formation compressional waves at five spacings with 0.3 and 0.6 m vertical resolution. Unlike traditional 3 to 5 ft (0.9 to 1.5 m) sonic tools, the MSS tool uses a single-sided array with depth-derived cave compensation and tilt correction for improved response in poor borehole conditions. The downhole measurement interval was 0.1 m standard resolution or 0.025 m high resolution.

Microimager

The CMI tool is a memory capable resistivity micro-imaging tool that can be deployed with or without a wireline. The design and conveyance flexibility of the tool facilitate access into highly deviated wells and past bad hole conditions without compromising borehole coverage. The CMI tool has eight arms in two planes (Fig. F22). The upper four arms have pads that contain 20 buttons in two rows. The upper caliper arms are cross-linked, helping to centralize the tool and provide two borehole diameter measurements. The bottom four pads have 24 buttons in two rows. The lower four caliper arms are independently articulated to maintain good borehole contact,

which is crucial for high-image quality. They also provide four independent radii measurements, which can be used to identify near-borehole stress regimes. The vertical resolution is 5.1 mm and the depth of investigation is 25.4 mm.

Data processing

Logging data were processed using the Well Manager Software package (Weatherford) offshore and Interactive Petrophysics (Senergy) onshore.

Depth adjustments

The main processing task involved evaluating the depth of each logging run and referencing the data to the rig floor and seafloor. While deploying all the tools separately in the same section, a fixed zero depth position (loggers zero) was maintained at the top of the drill pipe. Typical reasons for depth corrections include ship heave and tide. Using Interactive Petrophysics (Senergy), the original logs were depth adjusted to the seafloor (in meters wireline log depth below seafloor [m WSF]) using the drillers depth to seafloor. Slight discrepancies (<0.5 m) may exist between the seafloor depths seen in the downhole logs (gamma ray) and those determined by the drillers as clay was present on the seabed frame.

When necessary, logs have been matched manually by the log analyst to a reference log using distinctive peaks. In such cases, gamma ray logs are taken as reference logs (continuous). Generally the depth discrepancies between logs are <1.5 m.

Invalid data

Invalid log values have been replaced by a null value of -999.25. The cause of the removed invalid log values can include the following:

- Log data in pipe and
- The effect when approaching the metallic pipe in open-hole condition.

Environmental corrections

Environmental corrections are designed to remove any effect from the borehole (size, roughness, temperature, and tool standoff) or the drilling fluids that may partially mask or disrupt the log response from the formation. Here, no postacquisition corrections of this type were applied.

Log merges

Where applicable for the processed logs, overlapping log runs have been merged to give one continuous log. In the overlapping regions, data have been

checked by the log analyst to make sure distinctive peaks and troughs correlate.

Quality control

Data quality is assessed in terms of reasonable values for the logged formation, repeatability between different passes of the same tool, and correspondence between logs affected by the same formation property. Considering the challenging borehole conditions, the overall quality of the downhole logging data is very good.

Data delivery

The downhole data are available in the USIO online log database. Processed standard data are available in ASCII and LAS format. Processed depths are referred to as wireline depth below seafloor scales. CMI image files are also available in PDF format (and scales).

References

- Alve, E., and Murray, J.W., 1999. Marginal marine environments of the Skagerrak and Kattegat: a baseline study of living (stained) benthic foraminiferal ecology. *Palaeogeogr., Palaeoclimatol., Palaeoecol.*, 146(1–4):171–193. [doi:10.1016/S0031-0182\(98\)00131-X](https://doi.org/10.1016/S0031-0182(98)00131-X)
- Andrén, T., Jørgensen, B.B., Cotterill, C., Green, S., Andrén, E., Ash, J., Bauersachs, T., Cragg, B., Fanget, A.-S., Fehr, A., Granoszewski, W., Groeneveld, J., Hardisty, D., Herrero-Bervera, E., Hyttinen, O., Jensen, J.B., Johnson, S., Kenzler, M., Kotilainen, A., Kotthoff, U., Marshall, I.P.G., Martin, E., Obrochta, S., Passchier, S., Quintana Krupinski, N., Riedinger, N., Slomp, C., Snowball, I., Stanpanova, A., Strano, S., Torti, A., Warnock, J., Xiao, N., and Zhang, R., 2015. Expedition 347 summary. *In* Andrén, T., Jørgensen, B.B., Cotterill, C., Green, S., and the Expedition 347 Scientists, *Proc. IODP, 347*: College Station, TX (Integrated Ocean Drilling Program). [doi:10.2204/iodp.proc.347.101.2015](https://doi.org/10.2204/iodp.proc.347.101.2015)
- Austin, W.E.N., 1991. Late Quaternary benthic foraminiferal stratigraphy of the western U.K. continental shelf [Ph.D. dissert.]. School of Ocean Sciences, Bangor Univ., Wales.
- Bann, K.L., Fielding, C.R., MacEachern, J.A., and Tye, S.C., 2008. Sedimentology and ichnology of mixed wave- and storm-dominated deltaic deposits: examples from the Permian of Australia. *In* Hampson, G.J., Dalrymple, R., and Burgess, P. (Eds.), *Advances in Shelf and Shoreline Stratigraphy*. Spec Publ.—SEPM (Soc. Sediment. Geol.). http://www.searchanddiscovery.com/documents/2006/06088houston_abs/abstracts/bann02.htm
- Beug, H.-J., 2004. *Leitfaden der Pollenbestimmung für Mitteleuropa und angrenzende Gebiete*: München (Verlag Friedrich Pfeil).
- Borck, D., and Frenzel, P., 2006. Micro-habitats of brackish water ostracods from Poel Island, southern Baltic Sea

- coast. *Senckenbergiana Marit.*, 36(2):99–107. doi:10.1007/BF03043723
- Cleve-Euler, A., 1951. Die Diatomeen von Schweden und Finland. *K. Sven. Vetenskapsakad. Handl., Fjärde Serien*, 2.
- Cline, J.D., 1969. Spectrophotometric determination of hydrogen sulfide in natural waters. *Limnol. Oceanogr.*, 14(3):454–458. doi:10.4319/lo.1969.14.3.0454
- Cragg, B.A., 1994. Bacterial properties in deep sediment layers from the Lau Basin (Site 834). In Hawkins, J., Parson, L., Allan, J., et al., *Proc. ODP, Sci. Results*, 135: College Station, TX (Ocean Drilling Program), 147–150. doi:10.2973/odp.proc.sr.135.106.1994
- Dickens, G.R., Koelling, M., Smith, D.C., Schneiders, L., and the IODP Expedition 302 Scientists, 2007. Rhizon sampling of pore waters on scientific drilling expeditions: an example from the IODP Expedition 302, Arctic Coring Expedition (ACEX). *Sci. Drill.*, 4:22–25. doi:10.2204/iodp.sd.4.08.2007
- Diepenbroek, M., Grobe, H., Reinke, M., Schlitzer, R., and Sieger, R., 1999. Data management of proxy parameters with PANGAEA. In Fischer, G., and Wefer, G. (Eds.), *Use of Proxies in Paleoceanography: Examples from the South Atlantic*: Heidelberg, Germany (Springer-Verlag), 715–727. doi:10013/epic.11224
- Diepenbroek, M., Grobe, H., Reinke, M., Schindler, U., Schlitzer, R., Sieger, R., and Wefer, G., 2002. PANGAEA—an information system for environmental sciences. *Comp. Geosci.*, 28(10):1201–1210. doi:10.1016/S0098-3004(02)00039-0
- Dittert, N., Corrin, L., Diepenbroek, M., Grobe, H., Heinze, C., and Ragueneau, O., 2002. Management of (pale-) oceanographic data sets using the PANGAEA information system: the SINOPS example. *Comput. Geosci.*, 28(7):789–798. doi:10.1016/S0098-3004(01)00112-1
- Duan, Z., Møller, N., Greenberg, J., and Weare, J.H., 1992. The prediction of methane solubility in natural waters to high ionic strength from 0° to 250°C and from 0 to 1600 bar. *Geochim. Cosmochim. Acta*, 56(4):1451–1460. doi:10.1016/0016-7037(92)90215-5
- Faegri, K., and Iversen, J., 1989. *Textbook of Pollen Analysis* (4th ed.): Chichester (Wiley).
- Feyling-Hanssen, R.W., 1972. The foraminifer *Elphidium excavatum* (Terquem) and its variant forms. *Micropaleontology*, 18(3):337–354. doi:10.2307/1485012
- Feyling-Hanssen, R.W., Jørgensen, J.A., Knudsen, K.L., and Andersen, A.L., 1971. Late Quaternary foraminifera from Vendsyssel, Denmark and Sandnes, Norway. *Bull. Geol. Soc. Den.*, 21:67–317. http://2dggf.dk/xpdf/bull21-02-03-67-71.pdf
- Frenzel, P., Henkel, D., Siccha, M., and Tschendel, L., 2005. Do ostracod associations reflect macrophyte communities? A case study from the brackish water of the southern Baltic Sea coast. *Aquat. Sci.*, 67(2):142–155. doi:10.1007/s00027-004-0756-z
- Frenzel, P., Keyser, D., and Viehberg, F.A., 2010. An illustrated key and (palaeo)ecological primer for postglacial to Recent Ostracoda (Crustacea) of the Baltic Sea. *Boreas*, 39(3):567–575. doi:10.1111/j.1502-3885.2009.00135.x
- Fry, J.C., 1988. Determination of biomass. In Austin, B. (Ed.), *Methods in Aquatic Bacteriology*: Chichester (Wiley), 27–72.
- Fryxell, G.A., and Hasle, G.R., 1972. *Thalassiosira eccentrica* (Ehrenb.) Cleve, *T. symmetrica* sp. nov., and some related centric diatoms. *J. Phycol.*, 8(4):297–317. doi:10.1111/j.1529-8817.1972.tb04044.x
- Fryxell, G.A., and Hasle, G.R., 1980. The marine diatom *Thalassiosira oestrupii*: structure, taxonomy and distribution. *Am. J. Bot.*, 67(5):804–814. doi:10.2307/2442672
- Grasshoff, K., Ehrhardt, M., and Kemling, K. (Eds.), 1983. *Methods of Seawater Analysis* (2nd ed.): Weinheim, F.R.G. (Verlag Chemie).
- Hall, P.O.J., and Aller, R.C., 1992. Rapid, small-volume, flow injection analysis for ΣCO_2 and NH_4^+ in marine and freshwaters. *Limnol. Oceanogr.*, 37(5):1113–1119. doi:10.4319/lo.1992.37.5.1113
- Hasle, G.R., 1978a. Some freshwater and brackish water species of the diatom genus *Thalassiosira* Cleve. *Phycologia*, 17(3):263–292. doi:10.2216/i0031-8884-17-3-263.1
- Hasle, G.R., 1978b. Some *Thalassiosira* species with one central process (Bacillariophyceae). *Norw. J. Bot.*, 25:77–110. http://www.obs-vlfr.fr/LOV/aquaparadox/html/PFD/Taxonomic%20Monographs/Hasle1978.pdf
- Hasle, G.R., and Lange, C.B., 1992. Morphology and distribution of *Coscinodiscus* species from the Oslofjord, Norway, and the Skagerrak, North Atlantic. *Diatom Res.*, 7(1):37–68. doi:10.1080/0269249X.1992.9705196
- Hustedt, F., 1930. Die Kieselalgen Deutschlands, Österreichs und der Schweiz: unter Berücksichtigung der übrigen Länder Europas sowie der angrenzenden Meeresgebiete (Vol. 1 and 2). In Rabenhorst, L. (Ed.), *Kryptogamen-Flora von Deutschland, Österreich und der Schweiz*: Leipzig (Akad. Verlag).
- Iwasaka, M., Onishi, M., Kurita, S., and Owada, N., 2011. Effects of pulsed magnetic fields on the light scattering property of the freezing process of aqueous solutions. *J. Appl. Phys.*, 109(7):07E320. doi:10.1063/1.3556776
- Knudsen, K.L. 1994. The marine Quaternary in Denmark: a review of new evidence from glacial–interglacial studies. *Bull. Geol. Soc. Den.*, 41(2):203–218. http://2dggf.dk/xpdf/bull41-02-203-218.pdf
- Krammer, K., and Lange-Bertalot, H., 1986. Bacillariophyceae, Part 1. Naviculaceae. In Ettl, H., Gerloff, J., Heynig, H., and Mollenhauer, D. (Eds.), *Süßwasserflora von Mitteleuropa* (Vol. 2/1): Stuttgart, Germany (Gustav Fischer Verlag).
- Krammer, K., and Lange-Bertalot, H., 1988. Bacillariophyceae, Part 2. Bacillariaceae, Epithemiaceae, Surirellaceae. In Ettl, H., Gerloff, J., Heynig, H., and Mollenhauer, D. (Eds.), *Süßwasserflora von Mitteleuropa* (Vol. 2/2): Stuttgart, Germany (Gustav Fischer Verlag).
- Krammer, K., and Lange-Bertalot, H., 1991a. Bacillariophyceae, Part 3. Centrales, Fragilariaceae, Eunotiaceae. In Ettl, H., Gerloff, J., Heynig, H., and Mollenhauer, D. (Eds.), *Süßwasserflora von Mitteleuropa* (Vol. 2/3): Stuttgart, Germany (Gustav Fischer Verlag).
- Krammer, K., and Lange-Bertalot, H., 1991b. Bacillariophyceae, Part 4. Achnantaceae. In Ettl, H., Gärtner, J.G.,

- Gerloff, J., Heynig, H., and Mollenhauer, D. (Eds.), *Süßwasserflora von Mitteleuropa* (Vol. 2/4): Stuttgart, Germany (Gustav Fischer Verlag).
- Kristensen, P., Gibbard, P., Knudsen, K.L., and Ehlers, J., 2000. Last interglacial stratigraphy at Ristinge Klint, South Denmark. *Boreas*, 29(2):103–116. doi:10.1111/j.1502-3885.2000.tb01204.x
- Laj, C., and Channell, J.E.T., 2007. 5.10—geomagnetic excursions. *Treatise Geophys.*, 5:373–416. doi:10.1016/B978-044452748-6.00095-X
- Leroy, C.C., 1969. Development of simple equations for accurate and more realistic calculation of the speed of sound in seawater. *J. Acoust. Soc. Am.*, 46(1B):216–226. doi:10.1121/1.1911673
- Lever, M.A., Alperin, M., Engelen, B., Inagaki, F., Nakagawa, S., Steinsbu, B.O., Teske A., and IODP Expedition 301 Scientists, 2006. Trends in basalt and sediment core contamination during IODP Expedition 301. *Geomicrobiol. J.*, 23(7):517–530. doi:10.1080/01490450600897245
- Lougheed, B.C., 2013. Testing palaeomagnetic and ^{14}C based geochronological methods in the Baltic Sea [Ph. D. dissert.]. Lund Univ., Sweden. <https://lup.lub.lu.se/search/publication/3787514>
- Lougheed, B.C., Nilsson, A., Björck, S., Snowball, I., and Muscheler, R., in press. A deglacial palaeomagnetic master curve for Fennoscandia—providing a dating template and supporting millennial-scale geomagnetic field patterns for the past 14 ka. *Quat. Sci. Rev.*, doi:10.1016/j.quascirev.2014.03.008
- Lurcock, P.C., and Wilson, G.S., 2012. PuffinPlot: a versatile, user-friendly program for paleomagnetic analysis. *Geochem., Geophys., Geosyst.*, 13(6):Q06Z45. doi:10.1029/2012GC004098
- Marret, F., and Zonneveld, K.A.F., 2003. Atlas of modern organic-walled dinoflagellate cyst distribution. *Rev. Palaeobot. Palynol.*, 125(1–2):1–200. doi:10.1016/S0034-6667(02)00229-4
- Marsaglia, K., Milliken, K., and Doran, L., 2013. IODP smear slides digital reference for sediment analysis, Part 1: Methodology and atlas of siliciclastic and volcanogenic components. *IODP Tech. Note*, 1. doi:10.2224/iodp.tn.1.2013
- Mölder, K., and Tynni, R., 1967. Über Finnlands rezente und subfossile Diatomeen, I. *C. R. Soc. Geol. Finl.*, 39:199–217.
- Mölder, K., and Tynni, R., 1968. Über Finnlands rezente und subfossile Diatomeen, II. *Bull. Geol. Soc. Finl.*, 40:151–170.
- Mölder, K., and Tynni, R., 1969. Über Finnlands rezente und subfossile Diatomeen, III. *Bull. Geol. Soc. Finl.*, 41:235–251.
- Mölder, K., and Tynni, R., 1970. Über Finnlands rezente und subfossile Diatomeen, IV. *Bull. Geol. Soc. Finl.*, 42:129–144.
- Mölder, K., and Tynni, R., 1971. Über Finnlands rezente und subfossile Diatomeen, V. *Bull. Geol. Soc. Finl.*, 43:203–220.
- Mölder, K., and Tynni, R., 1972. Über Finnlands rezente und subfossile Diatomeen, VI. *Bull. Geol. Soc. Finl.*, 44:141–149.
- Mölder, K., and Tynni, R., 1973. Über Finnlands rezente und subfossile Diatomeen, VII. *Bull. Geol. Soc. Finl.*, 45:159–179.
- Moncrieff, A.C.M., 1989. Classification of poorly-sorted sedimentary rocks. *Sediment. Geol.*, 65(1–2):191–194. doi:10.1016/0037-0738(89)90015-8
- Morono, Y., and Inagaki, F., 2010. Automatic slide-loader fluorescent microscope for discriminative enumeration of seafloor life. *Sci. Drill.*, 9:32–36. doi:10.2204/iodp.sd.9.06.2010
- Morono, Y., Terada, T., Masui, N., and Inagaki, F., 2009. Discriminative detection and enumeration of microbial life in marine subsurface sediments. *ISME J.*, 3(5):503–511. doi:10.1038/ismej.2009.1
- Munsell Color Company, Inc., 1988. *Munsell Soil Color Charts*: Baltimore, MD (Munsell).
- Murray, J.W., and Alve, E., 2011. The distribution of agglutinated foraminifera in NW European seas: baseline data for the interpretation of fossil assemblages. *Palaeontol. Electron.*, 14(2):14A. http://palaeo-electronica.org/2011_2/248/index.html
- Muylaert, K., and Sabbe, K., 1996. The diatom genus *Thalassiosira* (Bacillariophyta) in the estuaries of the Schelde (Belgium/The Netherlands) and the Elbe (Germany). *Bot. Mar.*, 39(1–6):103–115. doi:10.1515/botm.1996.39.1-6.103
- Nehring, S., 1997. Dinoflagellate resting cysts in Recent sediments of the western Baltic as indicators for the occurrence of “non-indigenous” species in the water column. *Proc. 13th Symp. Baltic Mar. Biol.*, 79–85.
- Pillet, L., Voltski, I., Korsun, S., and Pawlowski, J., 2013. Molecular phylogeny of Elphidiidae (foraminifera). *Mar. Micropaleontol.*, 103:1–14. doi:10.1016/j.marmicro.2013.07.001
- Rasmussen, J.A., Heinberg, C., and Håkansson, E., 2005. Planktonic foraminifers, biostratigraphy and the diachronous nature of the lowermost Danian Cerithium limestone at Stevns Klint, Denmark. *Bull. Geol. Soc. Den.*, 52(2):113–131. <http://2dgg.dk/xpdf/bull52-2-113-131.pdf>
- Reinholdsson, M., Snowball, I., Zillén, L., Lenz, C., and Conley, D.J., 2013. Magnetic enhancement of Baltic Sea sapropels by greigite magnetofossils. *Earth Planet. Sci. Lett.*, 366:137–150. doi:10.1016/j.epsl.2013.01.029
- Rider, M., 2002. *The Geological Interpretation of Well Logs* (2nd ed.): Sutherland, Scotland (Rider-French Consulting Ltd.)
- Rider, M., 2006. *The Geological Interpretation of Well Logs* (2nd ed., rev. ed.): Sutherland, Scotland (Whittles).
- Rosenfeld, A., 1977. Die rezenten Ostracoden-Arten in der Ostsee. *Meyniana*, 29:11–49.
- Sabbe, K., and Vyverman, W., 1995. Taxonomy, morphology and ecology of some widespread representatives of the diatom genus *Opephora*. *Eur. J. Phycol.*, 30(4):235–249. doi:10.1080/09670269500651011

- Schlumberger, 1989. *Log Interpretation Principles/Applications*: Houston (Schlumberger Educ. Serv.), SMP-7017.
- Seeberg-Elverfeldt, J., Schlüter, M., Feseker, T., and Kölling, M., 2005. Rhizon sampling of porewaters near the sediment-water interface of aquatic systems. *Limnol. Oceanogr.: Methods*, 3(8):361–371. <http://aslo.org/lomethods/free/2005/0361.pdf>
- Seidenkrantz, M.-S., 1993. Foraminifera from the Quaternary sequence in the Anholt boring, Denmark. *Boreas*, 22(4):283–290. doi:10.1111/j.1502-3885.1993.tb00188.x
- Serra, O., 1984. *Fundamentals of Well-Log Interpretation* (Vol. 1): *The Acquisition of Logging Data*: Amsterdam (Elsevier).
- Serra, O., 1986. *Fundamentals of Well-Log Interpretation* (Vol. 2): *The Interpretation of Logging Data*. Amsterdam (Elsevier).
- Shepard, F.P., 1954. Nomenclature based on sand-silt-clay ratios. *J. Sediment. Res.*, 24(3):151–158. doi:10.1306/D4269774-2B26-11D7-8648000102C1865D
- Shipboard Scientific Party, 2003. Explanatory notes. In D'Hondt, S.L., Jørgensen, B.B., Miller, D.J., et al., *Proc. ODP, Init. Repts.*, 201: College Station, TX (Ocean Drilling Program), 1–103. doi:10.2973/odp.proc.ir.201.105.2003
- Singer, B.S., 2013. A Quaternary geomagnetic instability time scale. *Quat. Geochronol.*, 21:29–52. doi:10.1016/j.quageo.2013.10.003
- Smith, D.C., Spivack, A.J., Fisk, M.R., Haveman, S.A., and Staudigel, H., 2000a. Tracer-based estimates of drilling-induced microbial contamination of deep sea crust. *Geomicrobiol. J.*, 17(3):207–219. doi:10.1080/01490450050121170
- Smith, D.C., Spivack, A.J., Fisk, M.R., Haveman, S.A., Staudigel, H., and the Leg 185 Shipboard Scientific Party, 2000b. Methods for quantifying potential microbial contamination during deep ocean coring. *ODP Tech. Note*, 28. doi:10.2973/odp.tn.28.2000
- Snoeijs, P., 1992. Studies in the *Tabularia fasciculata* complex. *Diatom Res.*, 7(2):313–344. doi:10.1080/0269249X.1992.9705223
- Snoeijs, P., Vilbaste, S., Potapova, M., Kasperoviciene, J., and Balashova, J. (Eds.), 1993–1998. *Intercalibration and Distribution of Diatom Species in the Baltic Sea* (Vol. 1–5): Uppsala, Sweden (Opulus Press).
- Snowball, I., Zillén, L., Ojala, A., Saarinen, T., and Sandgren, P., 2007. FENNOSTACK and FENNORPIS: varved dated Holocene palaeomagnetic secular variation and relative palaeointensity stacks for Fennoscandia. *Earth Planet. Sc. Lett.*, 255(1–2):106–116. doi:10.1016/j.epsl.2006.12.009
- Sohlenius, G., 1996. Mineral magnetic properties of late Weichselian–Holocene sediments from the northwestern Baltic proper. *Boreas*, 25(2):79–88. doi:10.1111/j.1502-3885.1996.tb00837.x
- Terry, R.D., and Chilingar, G.V., 1955. Summary of “Concerning some additional aids in studying sedimentary formations,” by M. S. Shvetsov. *J. Sediment. Res.*, 25(3):229–234. <http://jsedres.geoscienceworld.org/cgi/content/abstract/25/3/229>
- Tomas, C. (Ed.), 1997. *Identifying Marine Phytoplankton*: San Diego (Academic Press). <http://www.sciencedirect.com/science/book/9780126930184>
- Tynni, R., 1975. Über Finnlands rezente und subfossile Diatomeen, VIII. *Bull.—Geol. Surv. Finl.*, 274.
- Tynni, R., 1976. Über Finnlands rezente und subfossile Diatomeen, IX. *Bull.—Geol. Surv. Finl.*, 284.
- Tynni, R., 1978. Über Finnlands rezente und subfossile Diatomeen, X. *Bull.—Geol. Surv. Finl.*, 296.
- Tynni, R., 1980. Über Finnlands rezente und subfossile Diatomeen, XI. *Bull.—Geol. Surv. Finl.*, 312.
- Viehberg, F.A., Frenzel, P., and Hoffman, G., 2008. Succession of late Pleistocene and Holocene ostracode assemblages in a transgressive environment: a study at a coastal locality of the southern Baltic Sea (Germany). *Palaeogeogr., Palaeoclimatol., Palaeoecol.*, 264(3–4):318–329. doi:10.1016/j.palaeo.2007.05.026
- Von Herzen, R., and Maxwell, A.E., 1959. The measurement of thermal conductivity of deep-sea sediments by a needle-probe method. *J. Geophys. Res.*, 64(10):1557–1563. doi:10.1029/JZ064i010p01557
- Wentworth, C.K., 1922. A scale of grade and class terms for clastic sediments. *J. Geol.*, 30(5):377–392. doi:10.1086/622910
- Whatley, R.C., 1983. Some simple procedures for enhancing the use of Ostracoda in palaeoenvironmental analysis. *Norw. Pet. Dir., Bull.*, 2:129–146.
- Witkowski, A., Lange-Bertalot, H., and Metzeltin, D., 2000. Diatom flora of marine coasts (Vol. 1). In Lange-Bertalot, H. (Ed.), *Iconographia Diatomologica* (Vol. 7): *Annotated Diatom Micrographs—Diversity—Taxonomy—Identification*: Königstein, Germany (Koeltz Scientific Books).

Publication: 20 February 2015
MS 347-102

Figure F1. Geographic locations of local names used in text. 1 = Landsort Deep, 2 = Øresund, 3 = south central Sweden, 4 = Lake Vänern, 5 = Darss, 6 = Møn, 7 = Mecklenburger Bay, 8 = Fehmar Belt, 9 = Langeland, 10 = Great Belt, 11 = Little Belt, 12 = Anholt, 13 = Blekinge archipelago, 14 = Kriegers Flak. **A.** Full map. (Continued on next page.)

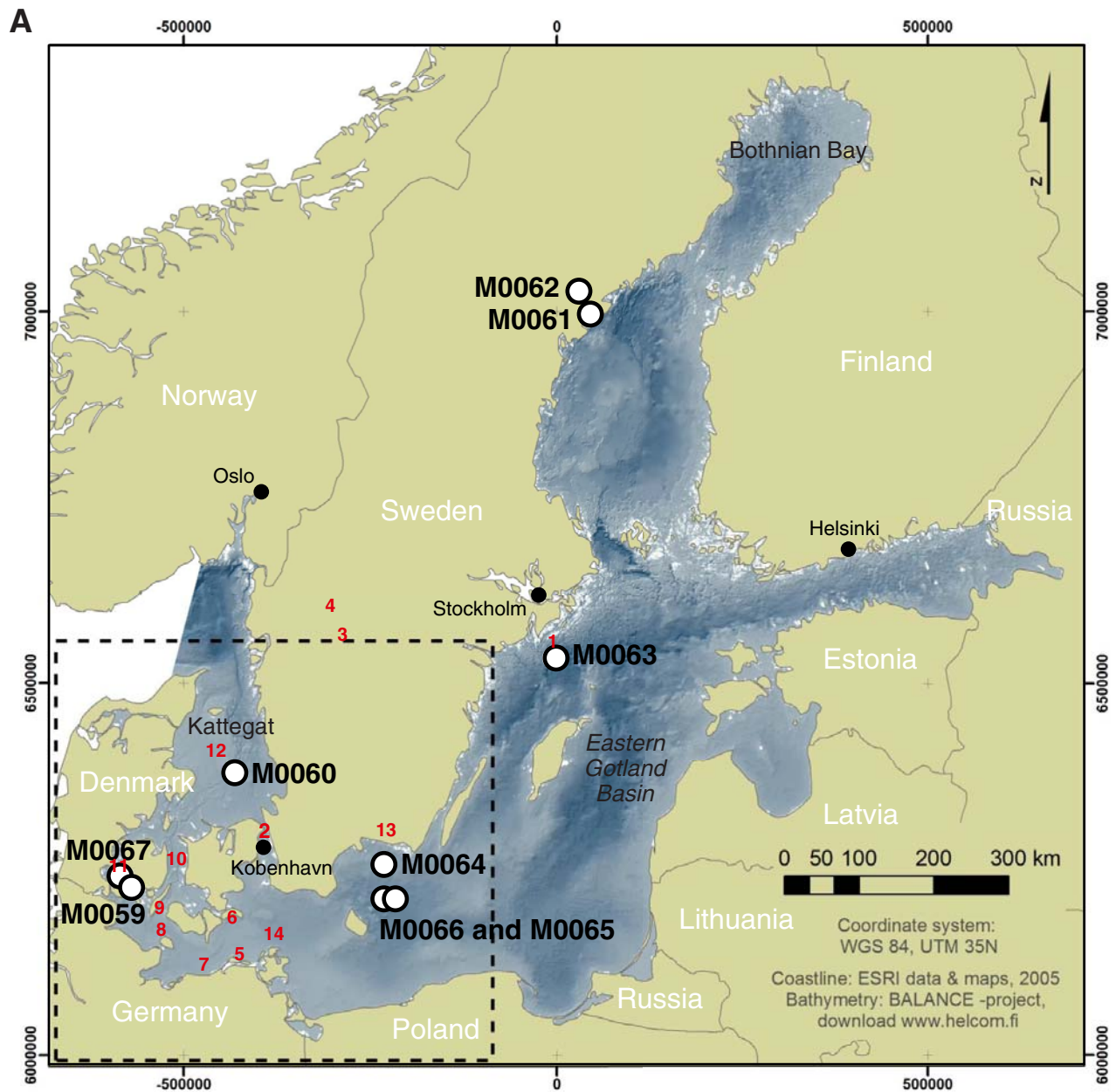


Figure F1 (continued). B. Close-up map.

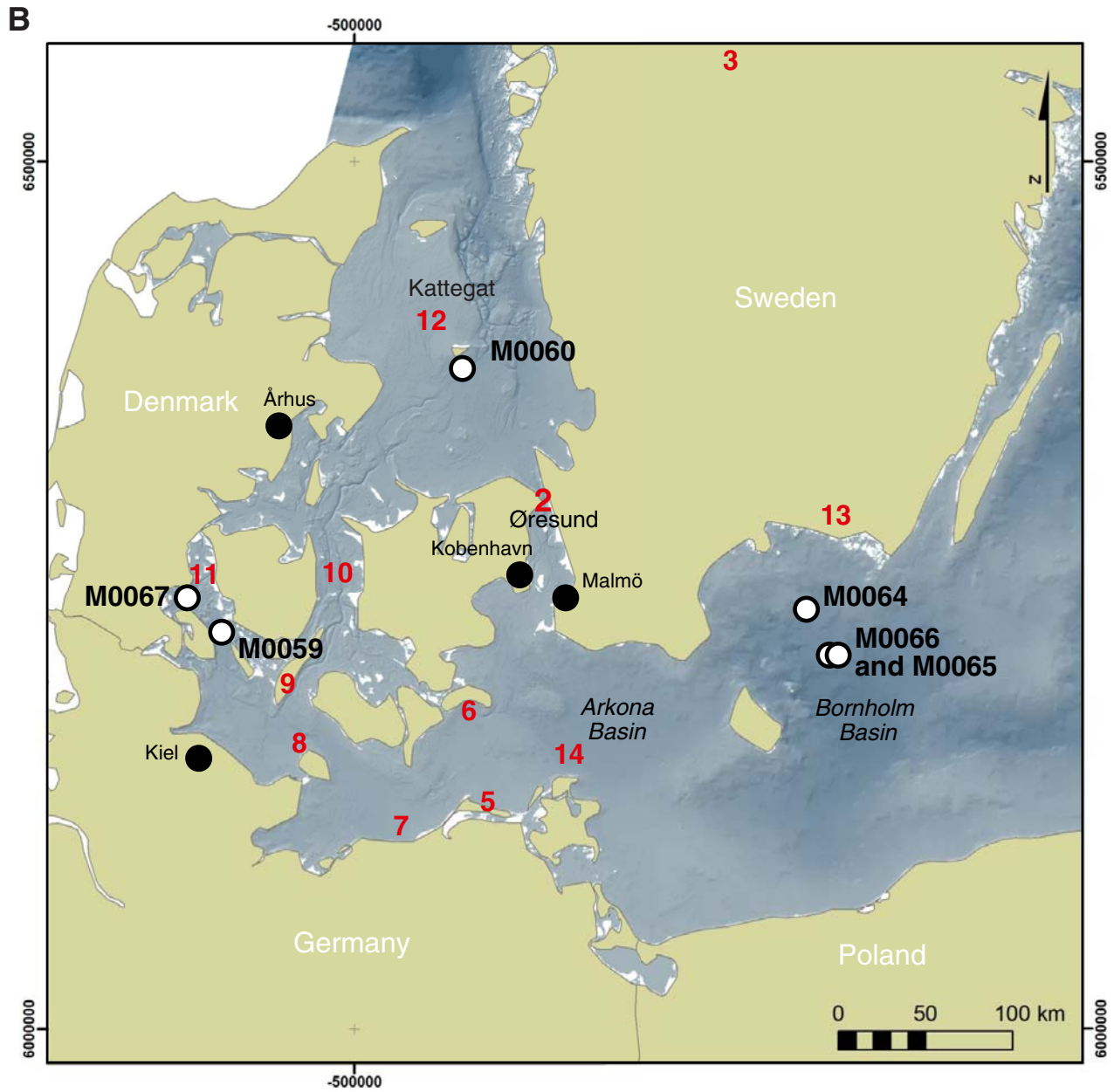


Figure F2. Schematic of hole positions around central Hole A for each site where multiple holes were drilled to form a composite recovery, Expedition 347.

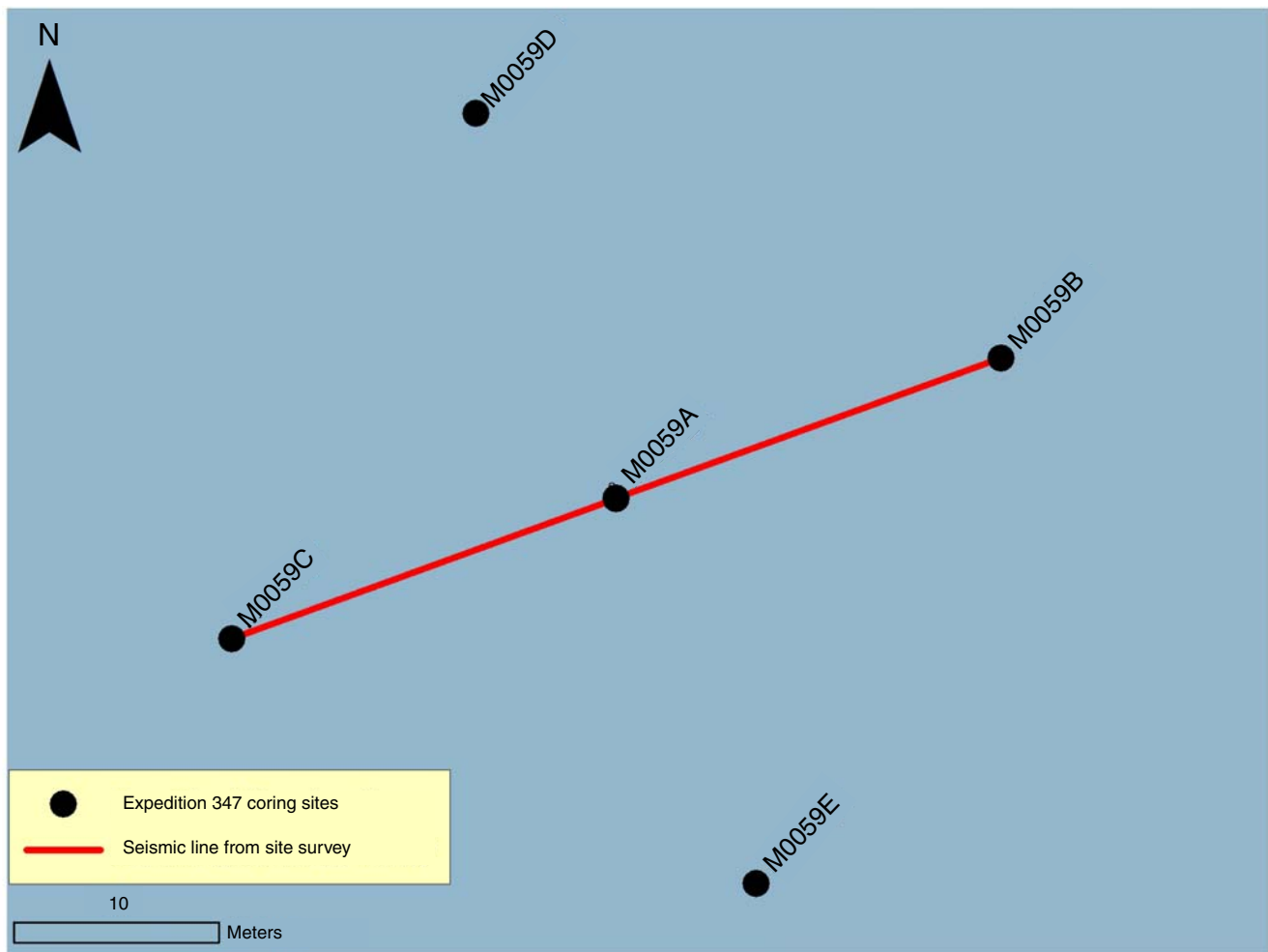


Figure F3. Close-up of primary transponder, Expedition 347. (Image courtesy of Bo Barker Jørgensen.)



Figure F4. The *Greatship Manisha* at Site M0063, Expedition 347. (Image courtesy of Carol Cotterill.)



Figure F5. Layout of the ESO mobile offices, workshops, and laboratories on the aft deck of the *Greatship Manisha*, taken from the top of the drill derrick, Expedition 347. (Image courtesy of Andy Frazer.)

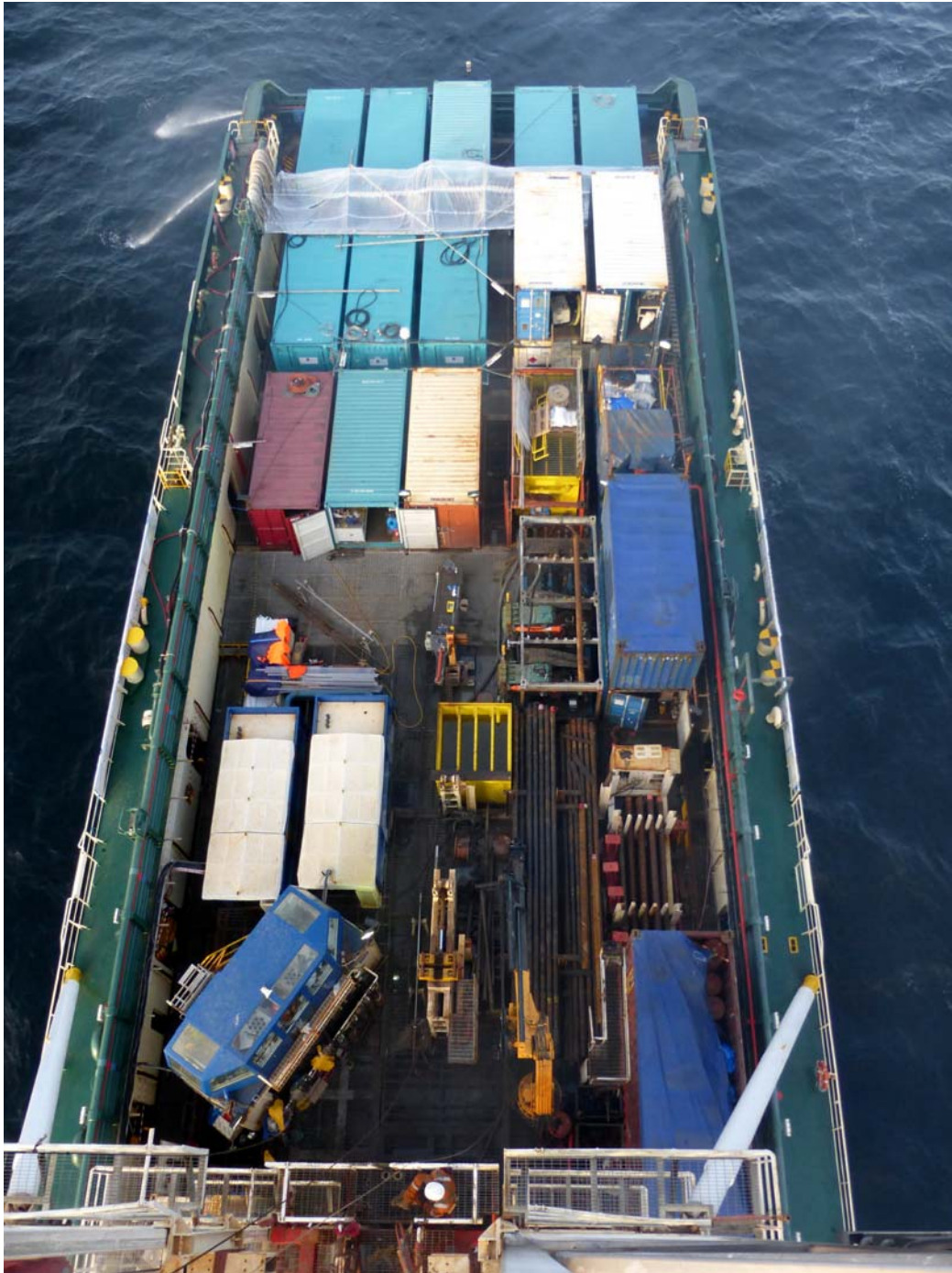


Figure F6. Geoquip GMTR 120 drilling rig, Expedition 347. (Images courtesy of Dave Smith and Carol Cotterill, respectively.) A. Overview of drilling derrick. (Continued on next page.)



Figure F6 (continued). B. Closer view showing the top drive and the heave compensation system.



Figure F7. Rumohr corer, Expedition 347. (Image courtesy of Michael Kenzler.)



Figure F8. Seabed frame used during Expedition 347. (Image courtesy of Carol Cotterill.)

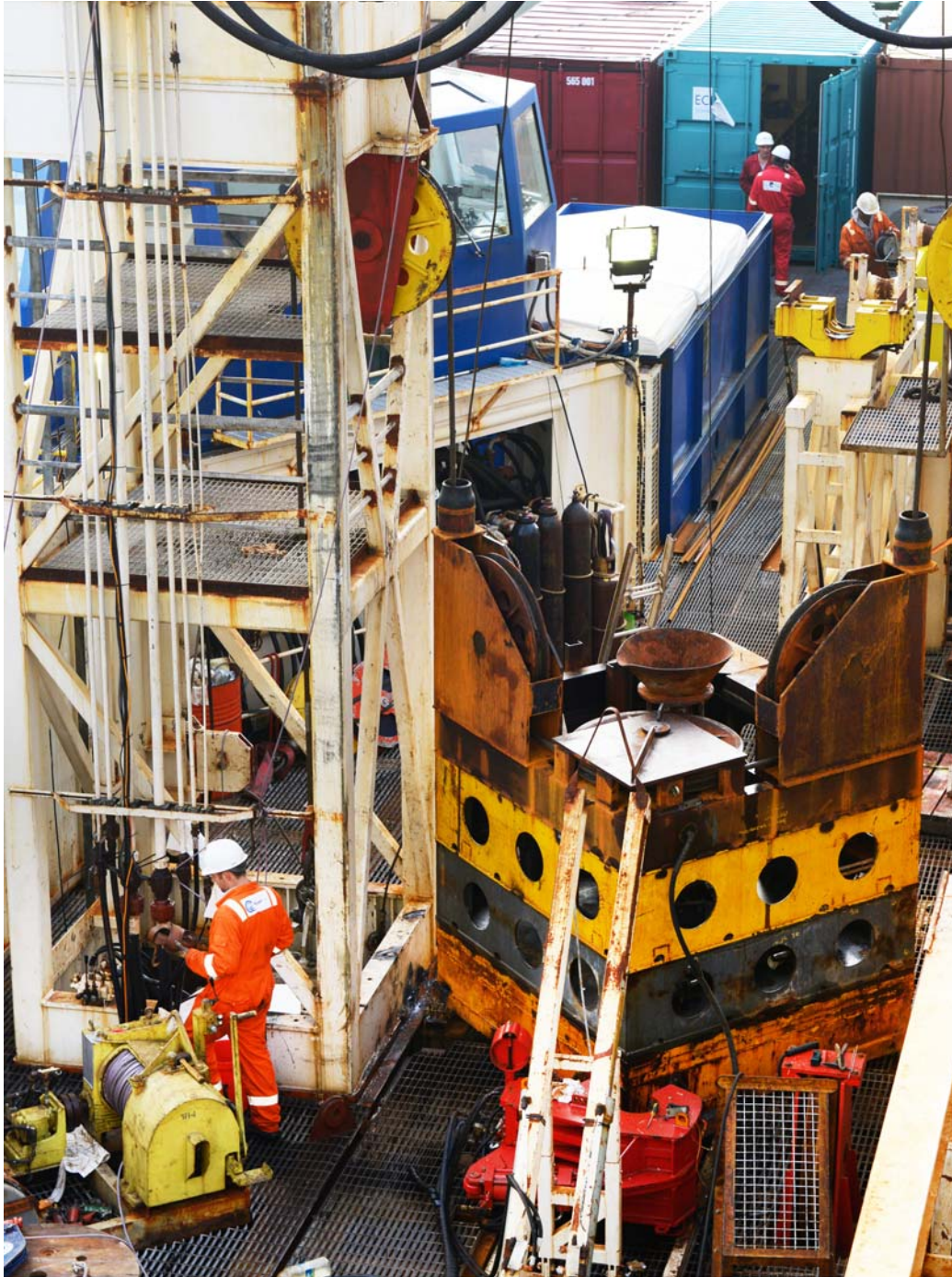


Figure F9. Seabotix LBV 150 SE Little Benthic Vehicle supplied by the BGS, Expedition 347. (Image courtesy of Michael Kenzler.)

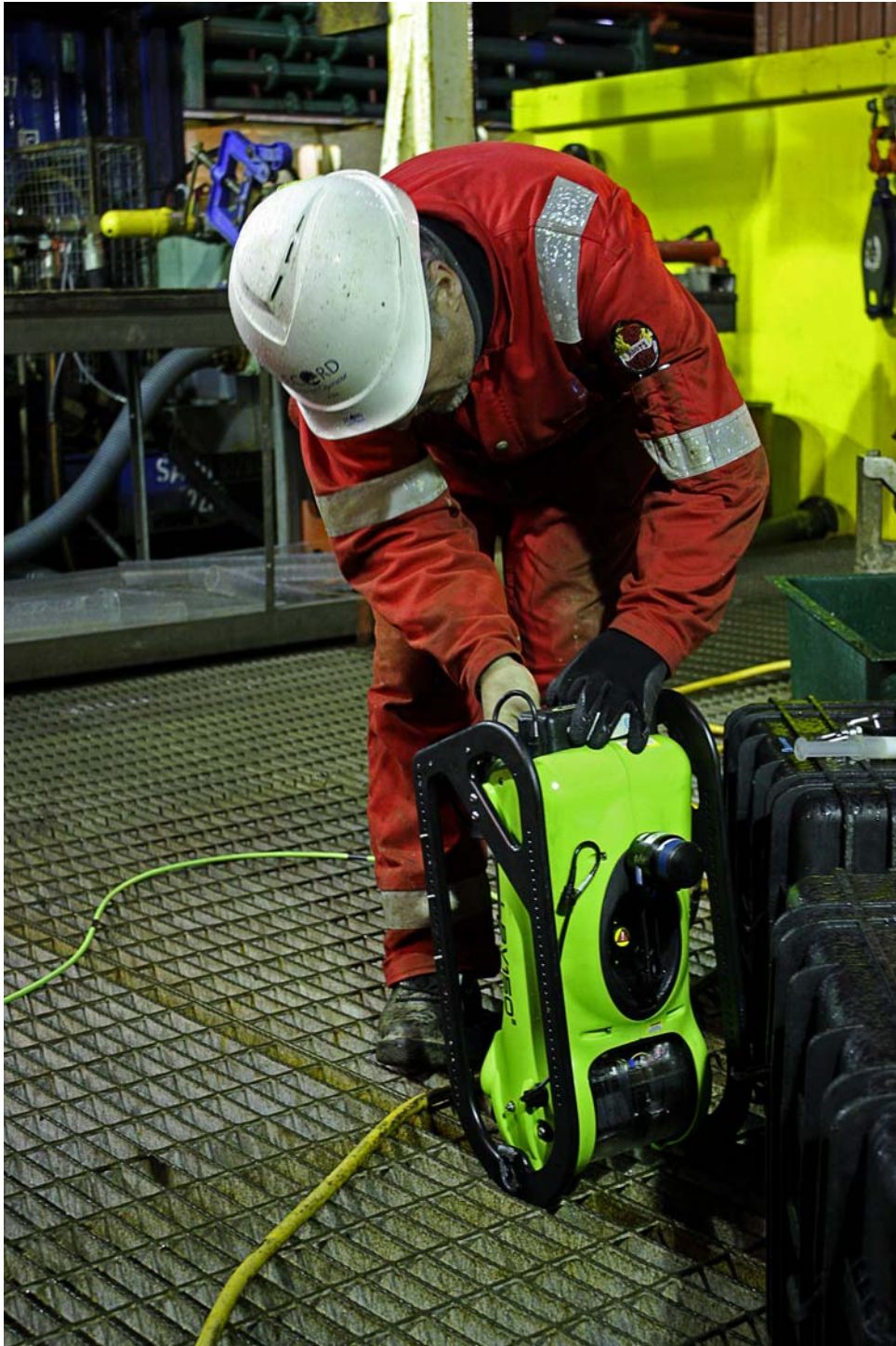


Figure F10. Schematic of IODP recovery and naming conventions, Expedition 347.

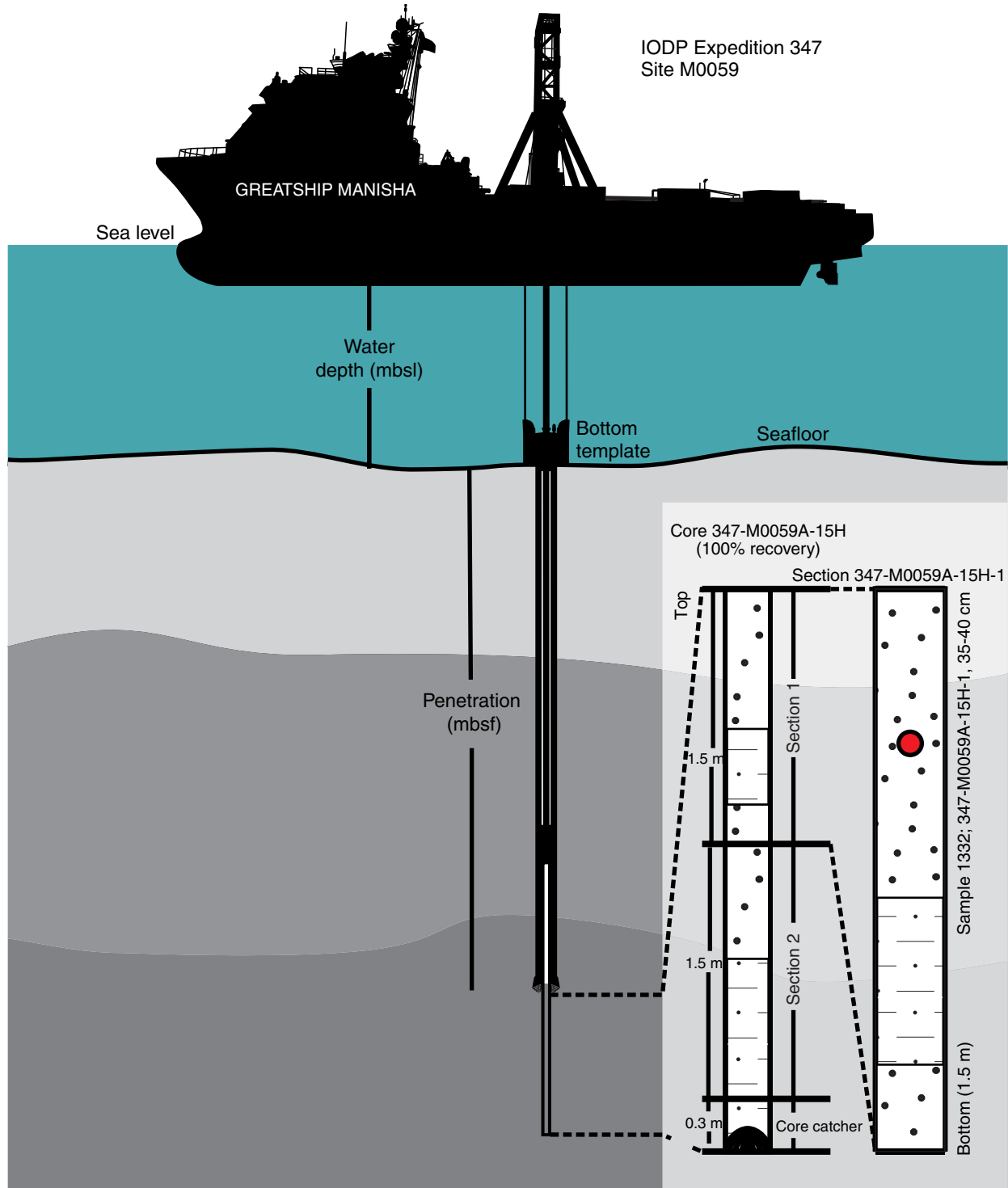


Figure F11. Core flow for the offshore phase of Expedition 347. MBIO = microbiology, IW = interstitial water, MSCL = multisensor core logger, CC = core catcher, DeepBIOS = deep biosphere IODP samples held at Kochi Core Center.

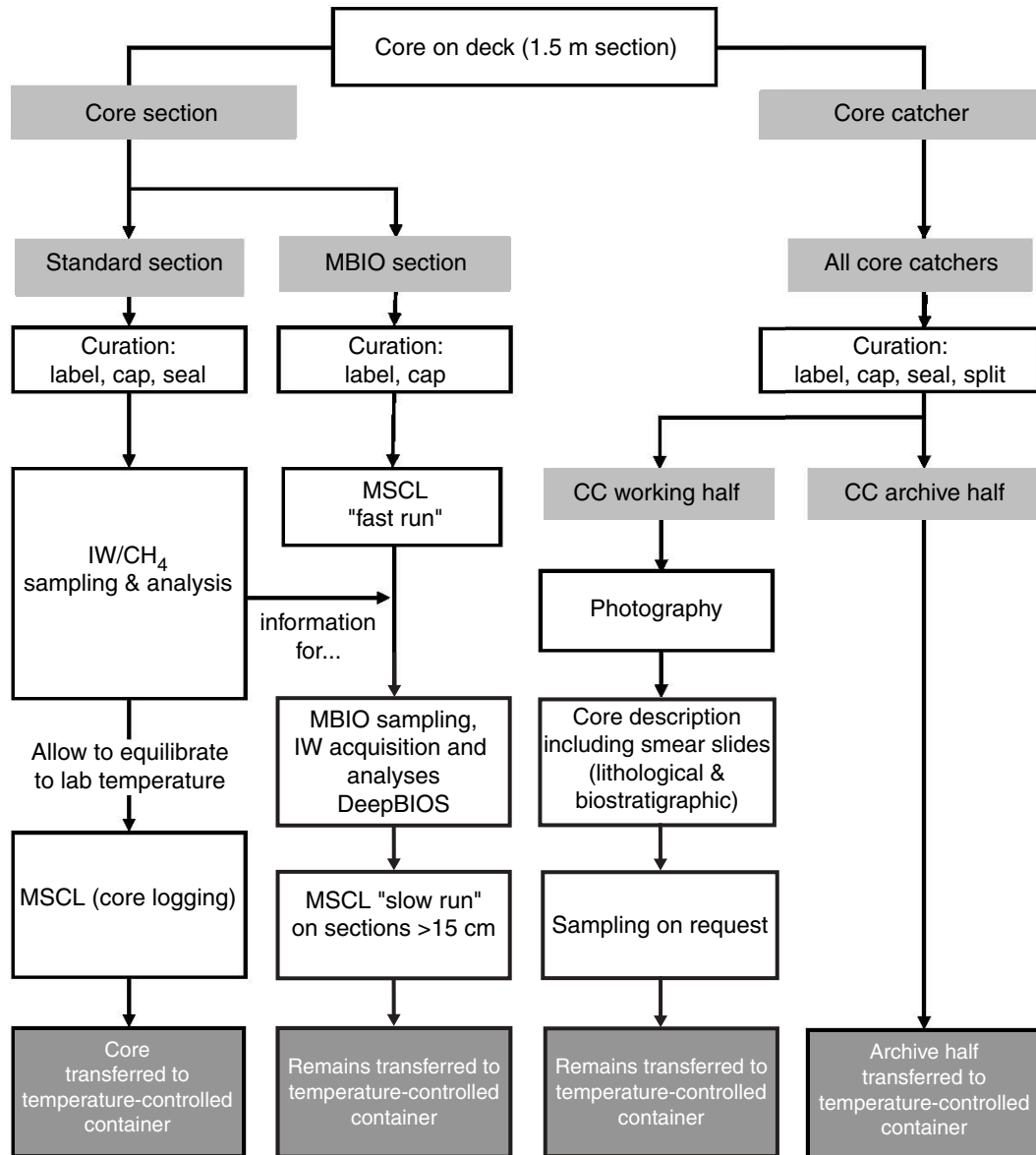


Figure F12. Core flow for the onshore phase of Expedition 347. OSP = Onshore Science Party, MSCL = multi-sensor core logger, TOC = total organic carbon, XRD = X-ray diffraction.

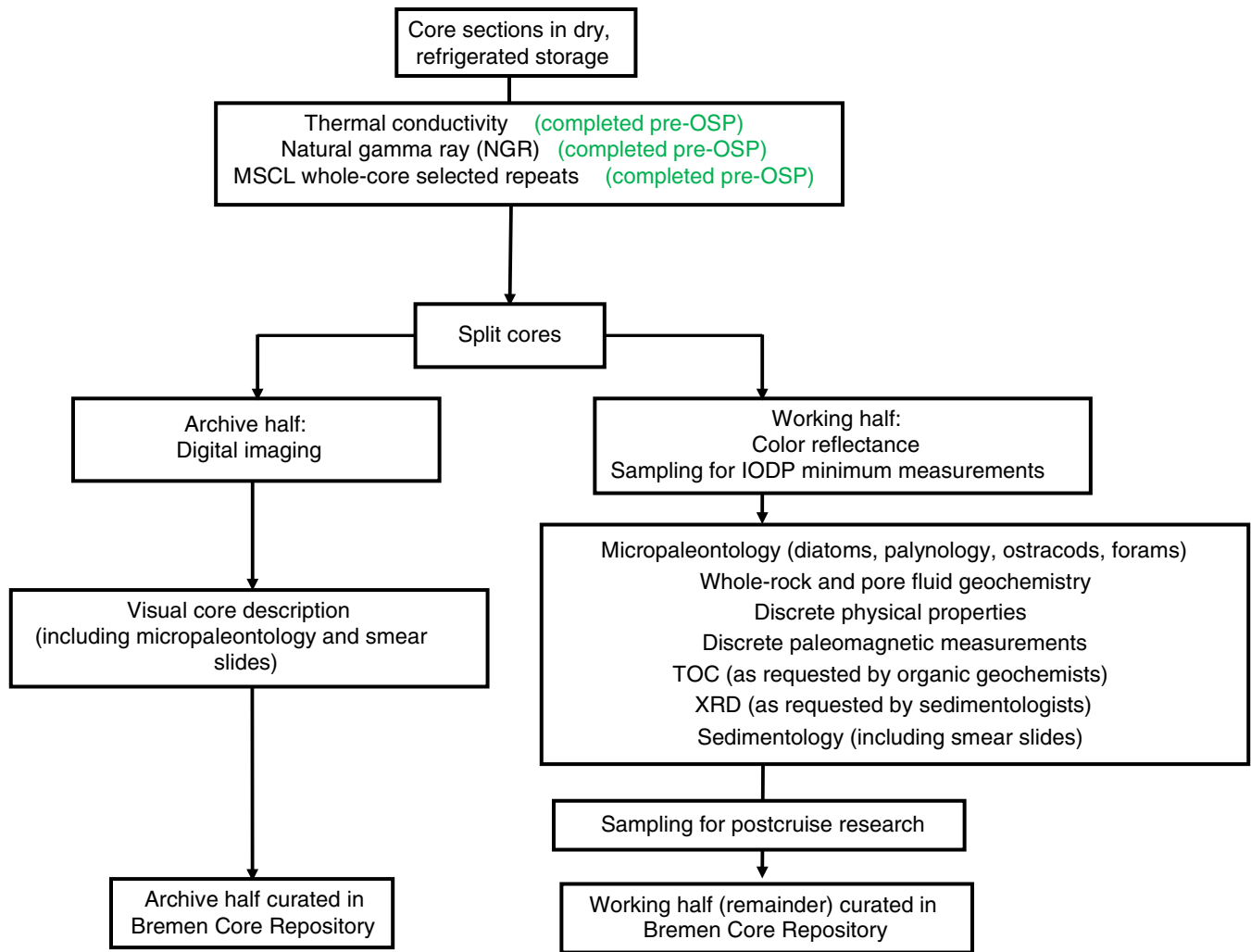


Figure F13. Example visual core description sheet, Expedition 347.

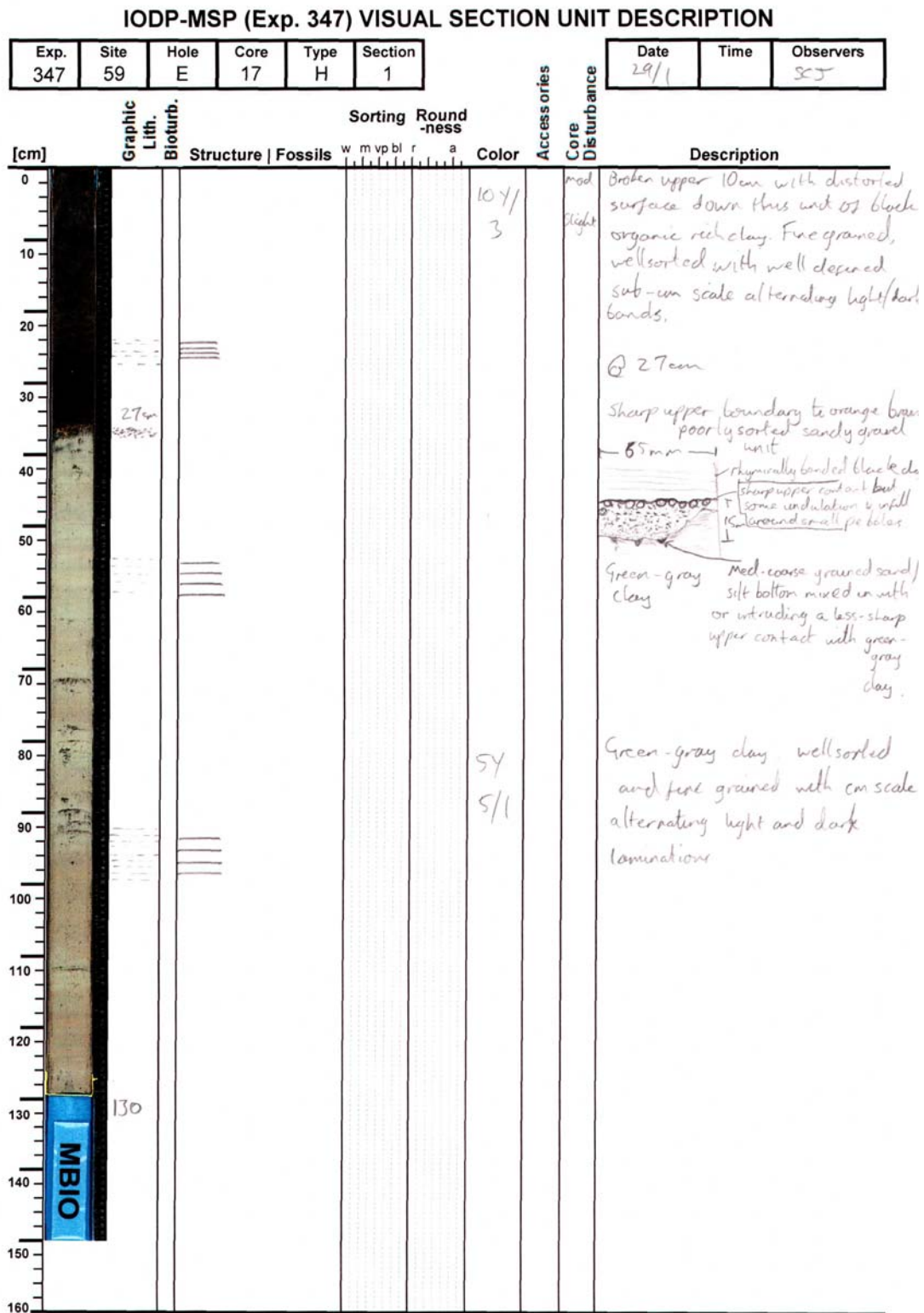
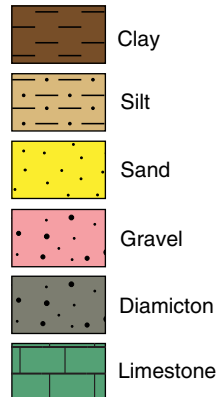


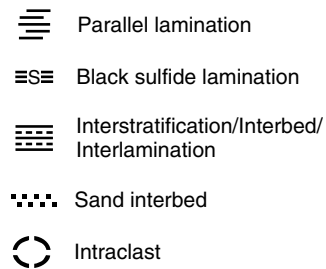
Figure F14. VCD patterns key.

Lithology

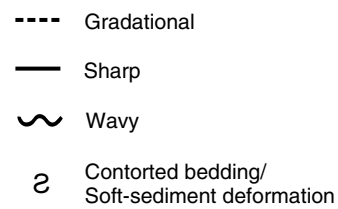
Siliciclastics



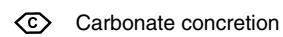
Sedimentary structures



Boundary



Diagenetic features



Macrofossils

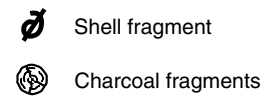


Figure F15. Lithology patterns key.

Lithology

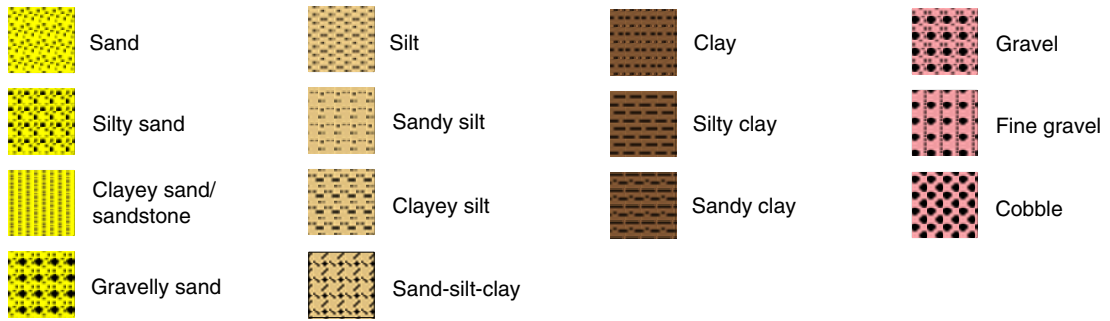


Figure F16. Wentworth classification diagram (Wentworth, 1922).

Millimeters (mm)	Micrometers (μm)	Phi (ϕ)	Wentworth size class
4096		-12.0	Boulder
256		-8.0	Cobble
64		-6.0	Pebble
4		-2.0	Granule
2.00		-1.0	Very coarse sand
1.00		0.0	Coarse sand
1/2	500	1.0	Medium sand
1/4	250	2.0	Fine sand
1/8	125	3.0	Very fine sand
1/16	63	4.0	Coarse silt
1/32	31	5.0	Medium silt
1/64	15.6	6.0	Fine silt
1/128	7.8	7.0	Very fine silt
1/256	3.9	8.0	Clay
0.00006	0.06	14.0	

Figure F17. Sediment classification diagram (Shepard, 1954).

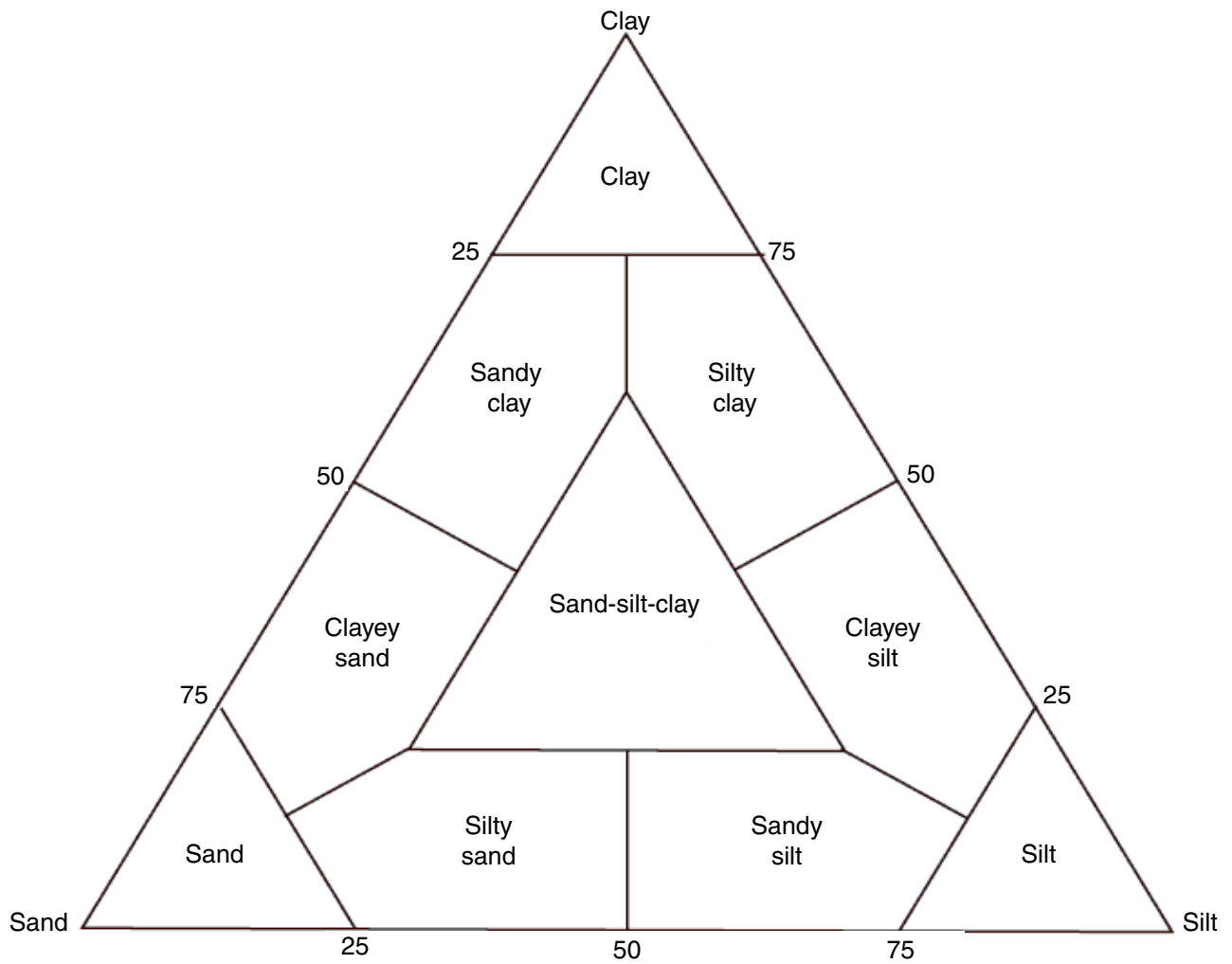


Figure F18. Modified classification scheme of poorly sorted sediments with a gravel component to facilitate the characterization of diamicts, conglomerates, and breccias, after Moncrieff (1989).

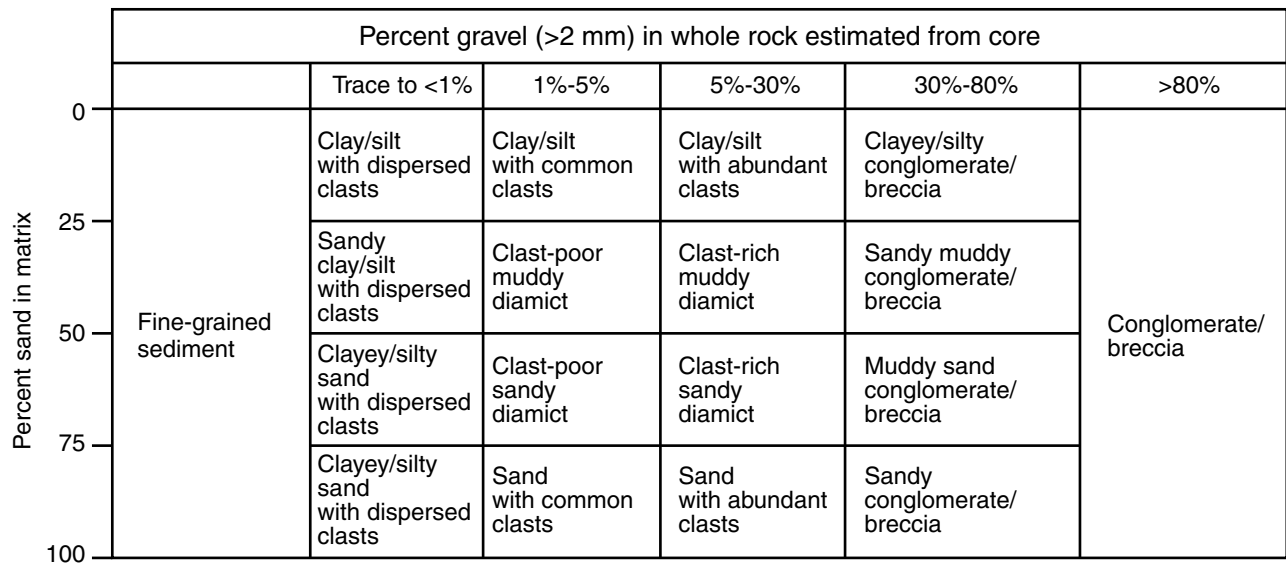


Figure F19. Graphic overview of syringe sampling scheme used when taking multiple samples from each microbiology core. Example shows the scheme for Core 347-M0059-2H, 3–6 mbsf. The overview shows in color coding the types of syringe samples taken, their position in Sections 1 or 2, the related sample requests, and the further treatment of each sample. PFC = perfluorocarbon.

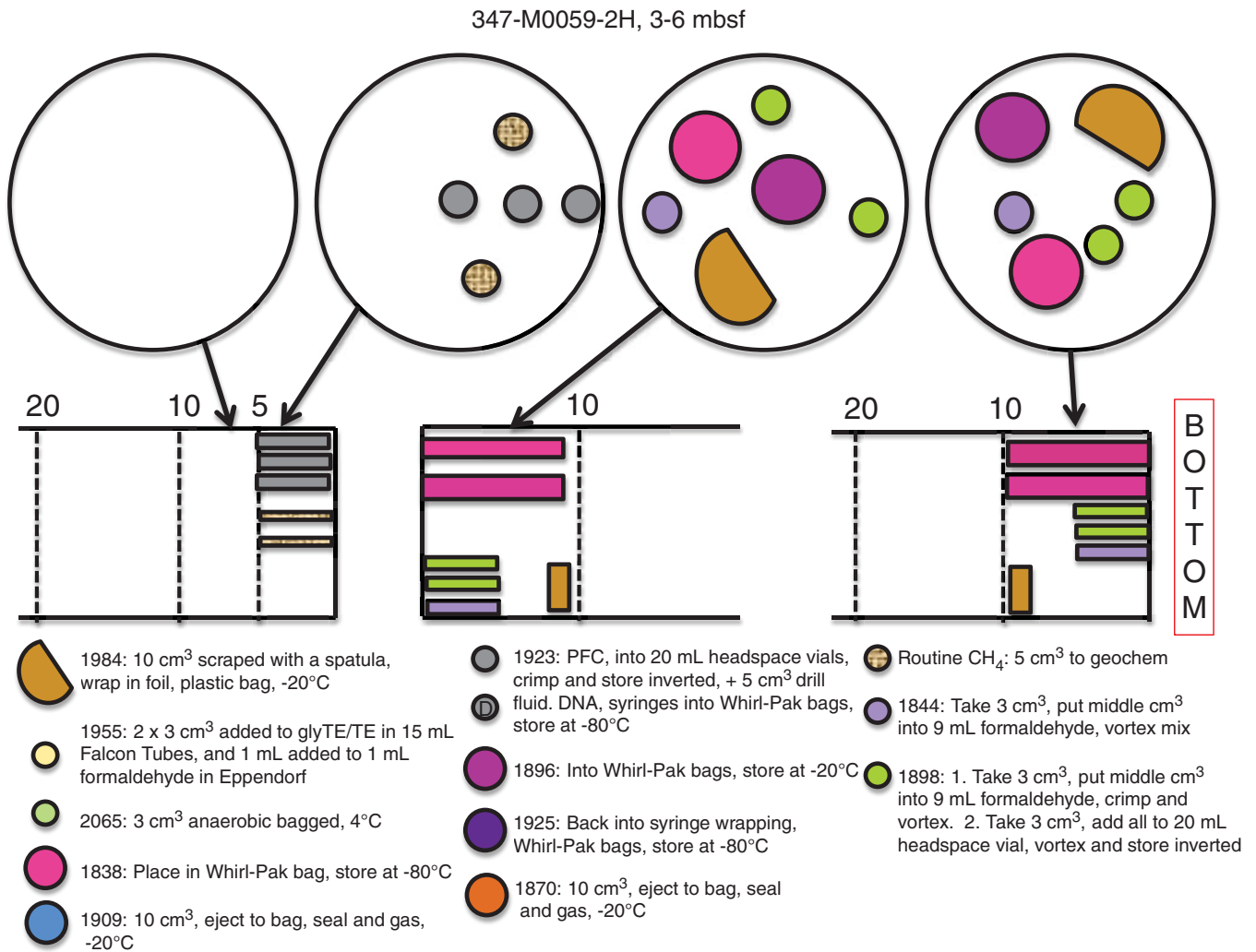


Figure F20. Graphic overview of whole-round core (WRC) sampling scheme used when cutting up microbiology cores. Example shows the scheme for Core 347-M0059-2H from 3–6 mbsf. The overview shows in color coding the length of WRC samples taken, their position in Sections 1 or 2, the related sample request, and the further subsampling and treatment of each WRC sample. The syringe samples had been taken at the section ends before cutting WRC samples (Fig. F19).

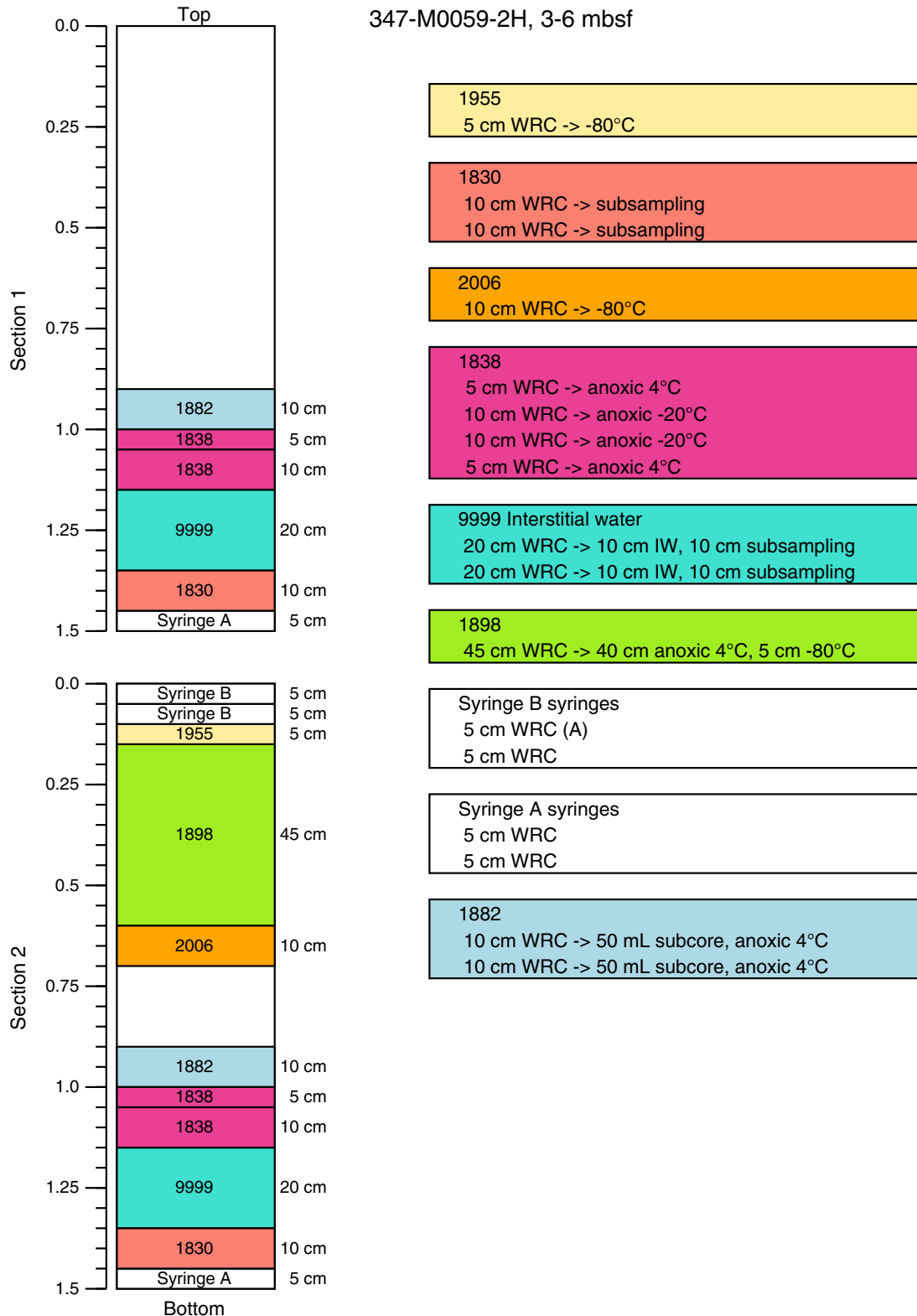


Figure F21. Color coded overview of samples taken for microbiology sample requests. To avoid mistakes, the overview was posted in hard copy both in the core reception container, where syringe sampling and WRC cutting were done, and in the refrigerated microbiology container, where the further subsampling and bagging were done.

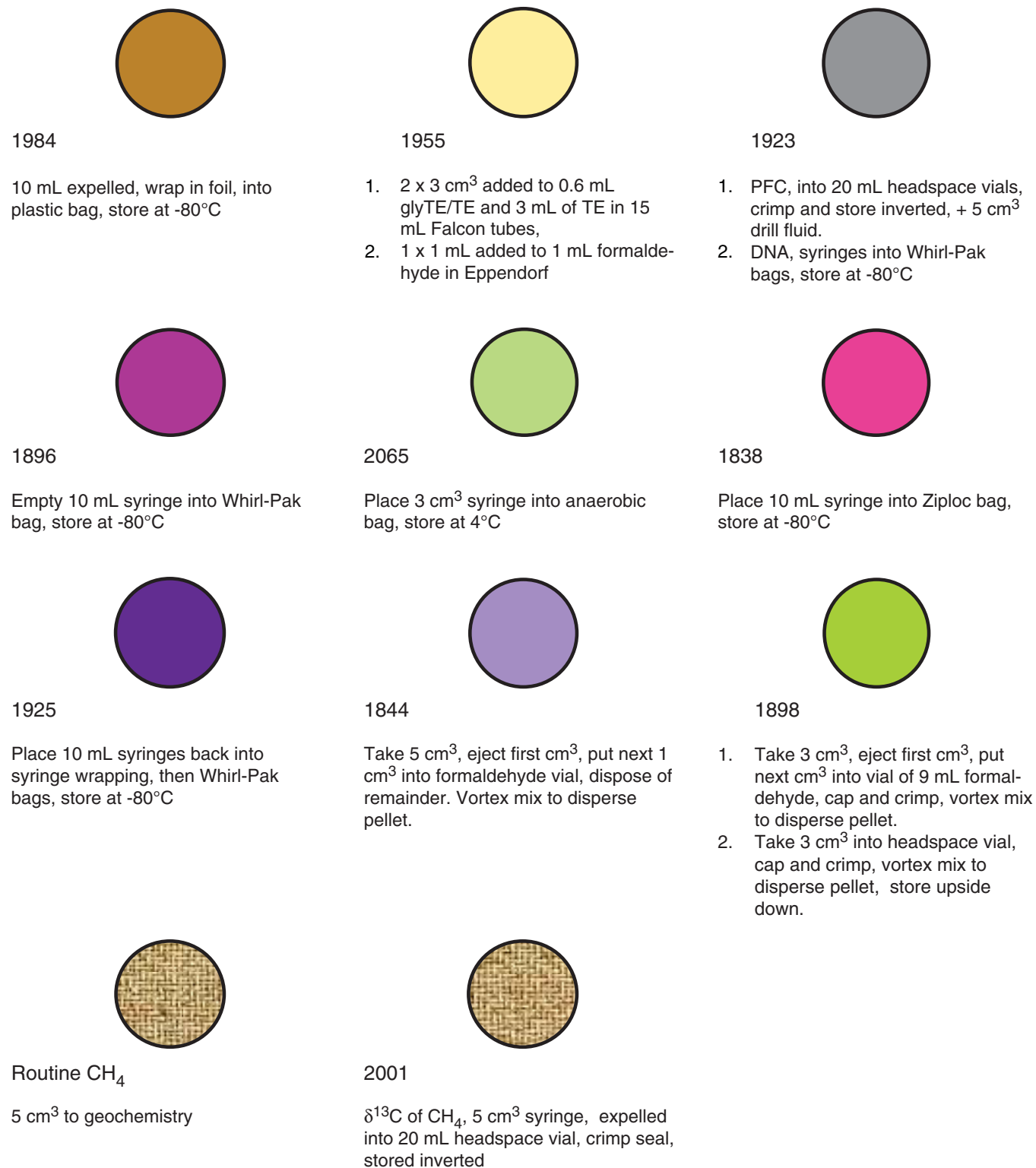


Figure F22. Wireline logging tool strings (example) used during Expedition 347. See the site chapters for tool strings deployed at each site.

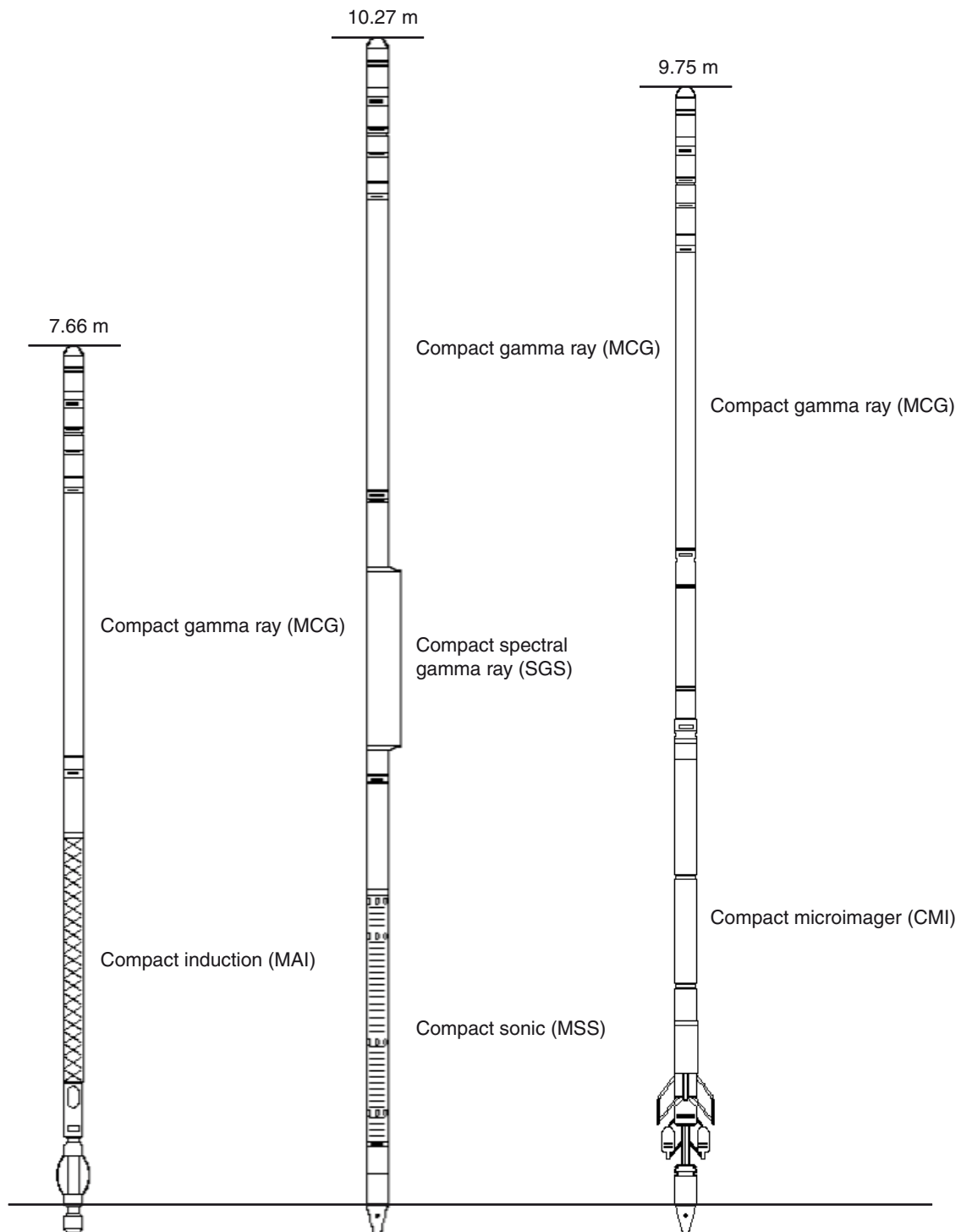


Table T1. Master species list of authorities. This table is available in an [oversized format](#).

Table T2. Trace element data available for individual coring sites.

	Rb	Mo	Ti	V	Zr
Site M0059	Y	X	X	Y	Y
Site M0060	Y	Y	X	X	X
Site M0061	X	Y	Y	Y	X
Site M0062	X	Y	Y	Y	Y
Site M0063	Y	Y	X	Y	Y
Site M0064	X	X	X	X	X
Site M0065	Y	X	X	Y	X
Site M0066	X	Y	X	X	X
Site M0067	Y	X	X	Y	X

Y = data available in site report tables. X = concentrations below detection limit or inconsistent between sites.

Table T3. MSCL sensor specifications.

Sensor	Calibration pieces used		Acceptable departure from full calibration values	Standard sampling interval (cm)	Sampling interval for M0061 and M0062 (cm)	Spatial resolution (cm)
	Full calibration	Calibration check				
Gamma density	Stepped Al/H ₂ O (6, 5, 4, 3, 2, and 0 cm Al)	Distilled water	±100 cps	2	1	1
P-wave velocity	Distilled water	Distilled water	±1 µs	2	1	1
Noncontact resistivity	Saline fluids (35, 17.5, 8.75, 3.5, 1.75, and 0.35 g/L)	17.5 g/L saline fluid	±10 mV	2	1	2–3
Magnetic susceptibility 80 mm loop	Impregnated resin	Impregnated resin	±2%–4%	2	1	2–3
Magnetic susceptibility 90 mm loop	Impregnated resin	Impregnated resin	±2%–4%	4	4	3–4

Table T4. Downhole tool specifications.

Acronym	Tool	Tool length (m)	Investigation depth (m)	Vertical resolution (m)
MCG	Weatherford Compact Gamma Ray	2.65	0.6	0.305
SGS	Weatherford Compact Spectral Gamma Ray	2.37	0.6	0.305
MSS	Weatherford Compact Sonic Sonde	3.82	0.0 762	0.29
MAI	Weatherford Compact Array Induction	3.29	0.3–1.2	0.610
CMI	Weatherford Compact Microimager	5.68	0.0254	0.0051

Specifications from Weatherford tool description brochure.

Table T5. Logged intervals.

Tools	Open-hole logged intervals m (WSF)								
	M0059B	M0059E	M0060B	M0062D	M0063A	M0064A	M0064D	M0065A	M0065C
MCG	20–72.5, 87–186.4	15–70	17.5–67	2–10.4	17.5–108.5	2–5	7.6–31	14–41	13.2–40
SGS	20–72.5	15–59	17.5–61	2–10.4	17.5–108.5	—	7.6–26.4	14–20	13.2–40
MSS	20–72.5	15–59	17.5–61	—	17.5–108.5	—	—	—	13.2–40
MAI	20–72.5, 87–186.4	15–70	17.5–67	2–10.4	17.5–108.5	2–5	7.6–31	14–41	—
CMI	—	15–59	17.5–56	—	17.5–108.5	—	—	—	13.2–40

